

THE P21-ACTIVATED KINASES CLA4 AND STE20 REGULATE VACUOLE
INHERITANCE IN *S. cerevisiae*.

By

Clinton Ron Bartholomew

Dissertation

Submitted to the Faculty of the
Graduate School of Vanderbilt University
in partial fulfillment of the requirements

for the degree of

DOCTOR OF PHILOSOPHY

in

Cell and Developmental Biology

May, 2008

Nashville, Tennessee

Approved:

Professor Christopher F.J. Hardy

Professor Kathleen L. Gould

Professor James R. Goldenring

Professor Todd R. Graham

ACKNOWLEDGEMENTS

First I like to thank my mentor, Chris Hardy. When I graduated from Brigham Young University he was gracious enough to take me under his wing and give me my first experience studying budding yeast as a technician in his lab at Washington University School of Medicine in St. Louis. After entering Washington University School of Medicine in St. Louis as a graduate student, I chose to return to his lab for my graduate work and transferred with him to Vanderbilt University School of Medicine. Chris is not only has an ingenuous and brilliant mind but I consider him a personal friend.

I would additionally like to thank Susan Wente and the members of her lab. I have thoroughly enjoyed sharing lab space with the Wente Lab members for the last several years and they have gone out of the way to make me feel a part of their lab family. I would also like to express my appreciation for their willingness to listen to countless discussions on vacuole inheritance and for their camaraderie and encouragement which each member of the lab has offered me over the last few years.

I would additionally like to express my thanks to my committee members Kathy Gould, Jim Goldenring, and Todd Graham and past committee member David Greenstein. Their encouragement and useful comments during committee meetings have been very helpful. I would also like to thank my committee members for their advice and help in choosing a postdoctoral fellowship.

Finally I would like to thank my wife for her love, support, and willingness to follow me to Nashville. She has always been supportive of me through this entire tough process and I will love her forever.

TABLE OF CONTENTS

	Page
ACKNOWLEDGEMENT	ii
LIST OF TABLES	vii
LIST OF FIGURES	viii
LIST OF ABBREVIATIONS	x
Chapter	
I. INTRODUCTION	1
Organelle inheritance	1
Budding and actin cable formation	2
Vacuole inheritance in budding yeast.....	3
Transportation of the segregation structure.....	7
Formation of the segregation structure.....	10
Resolution of the segregation structure.....	14
Coordination of vacuole inheritance with the cell cycle	16
Mitogen-activated protein kinases	17
Cellular functions of Ste20 and Cla4	20
Signal transduction.....	20
Polarized growth	23
Septin formation.....	24
Cell cycle progression.....	25
Vacuole fusion	27
Conclusions.....	27
References	29
II. BOI1 AND BOI2 REGULATE VACUOLE INHERITANCE	38
Abstract	38
Introduction.....	39
Materials and Methods	41
Results	44
Boi1 and Boi2 are inherited by the daughter cell.....	44
<i>boi1 boi2</i> cells display a daughter-specific budding delay.....	45
<i>boi1 boi2</i> cells have a vacuole inheritance defect.....	47
<i>boi1 boi2</i> daughter-specific budding delay and vacuole.....	49
inheritance defects is suppressed by <i>CLA4</i> or <i>STE20</i> deletion	

	The PH domain of Boi1 is required for vacuole inheritance	52
	Discussion	54
	References	58
III.	THE P21-ACTIVATED KINASES CLA4 AND STE20 REGULATE THE DESTRUCTION OF THE VACUOLE SPECIFIC MYOSIN RECEPTOR VAC17	63
	Abstract	63
	Introduction.....	64
	Materials and Methods	66
	Results	71
	Cells overexpressing <i>CLA4</i> have a daughter-specific.....	71
	budding delay and a vacuole inheritance defect	
	Cells overexpressing <i>STE20</i> have a vacuole inheritance defect.....	75
	<i>vac17ΔPEST</i> expression suppresses the vacuole	77
	inheritance defect of <i>CLA4</i> and <i>STE20</i> overexpressing and <i>boi1 boi2</i> cells	
	Vac17 is a phosphoprotein degraded in late-M.....	79
	PAK function is required for Vac17-ProA degradation in late-M.....	81
	<i>CLA4</i> overexpression promotes Vac17 degradation.....	81
	<i>CLA4</i> or <i>STE20</i> overexpression inhibits peroxisome	84
	but not late Golgi inheritance	
	Discussion	87
	References	92
IV.	THE P21-ACTIVATED KINASES CLA4 AND STE20 ARE	95
	REQUIRED FOR RESOLUTION OF THE VACUOLE SEGREGATION STRUCTURE	
	Abstract	95
	Introduction.....	96
	Materials and Methods	97
	Results	100
	Cell cycle progression is not required for segregation.....	100
	Structure resolution	
	Cla4 localizes to the segregation structure	100
	PAKs are required for segregation structure resolution.....	104
	Cells overexpressing <i>CLA4t</i> fail to form a daughter vacuole.....	106
	and have a partial <i>in vivo</i> fusion defect	
	Discussion	108
	References	113

V.	THE VACUOLE SEGREGATION STRUCTURE IS A SENSOR	117
	FOR REGULATING ENTRY INTO MITOSIS	
	Abstract.....	117
	Introduction	118
	Materials and Methods.....	120
	Results	123
	<i>cla4-75 ste20</i> cells fail to form a daughter vacuole and	123
	arrest at G2/M.	
	The metaphase arrest of <i>cla4-75 ste20</i> is linked to the	125
	vacuole segregation structure.	
	Deletion of <i>SWE1</i> uncouples daughter vacuole formation.....	125
	and mitotic progression.	
	Hsl1 is mislocalized in <i>cla4-75 ste20</i> and	127
	<i>cla4-75 ste20 vac8</i> cells.	
	Cdc5 through an interaction with Atg11 is a target of the	128
	vacuole segregation checkpoint.	
	Deletion of <i>ATG11</i> suppresses the metaphase arrest of	129
	<i>cla4-75 ste20</i> cells in a Cdc5 dependent manner.	
	Discussion.....	132
	References.....	135
VI.	FUTURE DIRECTIONS	137
	How do Cla4 and Ste20 promote resolution of the	137
	segregation structure?	
	How do Boi1 and Boi2 regulate Cla4 and Ste20?	139
	How do Cla4 and Ste20 regulate Vac17?.....	141
	Is PAK regulation of vacuole inheritance connected to Vac17	143
	degradation?	
	Do PtdIns(3,5)P2 levels increase during segregation structure.....	144
	formation?	
	How do PAKs regulate peroxisome inheritance?	145
	Vacuole inheritance checkpoint.....	145
	References	147

LIST OF TABLES

Table	Page
1-1 Classes of vacuole partitioning (<i>vac</i>) mutants.....	6
2-1 Strains	42
2-2 Plasmids	42
2-3 <i>boi1 boi2</i> cells have a vacuole inheritance defect dependent on <i>CLA4</i> and <i>STE20</i>	48
3-1 Strains	66
3-2 Plasmids	67
3-3 <i>vac17</i> Δ <i>PEST</i> expression suppresses the vacuole inheritance of <i>CLA4</i> or <i>STE20</i> overexpressing or <i>boi1 boi2</i> cells.	78
4-1 Strains	97
5-1 Strains	120
5-2 Plasmids	120

LIST OF FIGURES

Figure	Page
1-1 Proteins involved in transport of the vacuole into the bud.....	8
1-2 Ste20 and Cla4 are involved in signal transduction.	21
2-1 Boi1-GFP has a dynamic localization during the cell cycle and is inherited by daughter cells.	44
2-2 <i>boi1 boi2</i> and <i>vac8</i> cells have a daughter-specific delay	46
2-3 <i>boi1 boi2</i> cells have a vacuole inheritance defect.....	49
2-4 <i>boi1 boi2</i> daughter-specific budding delay and vacuole inheritance defects are suppressed by <i>CLA4</i> or <i>STE20</i> deletion.	51
2-5 The PH domain of Boi1 is required for vacuole inheritance in the absence of <i>BOI2</i> .	53
3-1 Proposed model for the bud-specific degradation of Vac17	64
3-2 Cells overexpressing <i>CLA4</i> have a daughter-specific budding delay	72
3-3 Cells overexpressing <i>CLA4</i> have a vacuole inheritance defect	74
3-4 Cells overexpressing <i>STE20</i> have a vacuole inheritance defect	76
3-5 Vac17 is a phosphoprotein and is degraded in late-M phase	80
3-6 PAK function is required for Vac17-ProA degradation in late-M and <i>CLA4</i> overexpression promotes Vac17-ProA degradation.	83
3-7 PAK overexpression inhibits peroxisome but not late Golgi..... inheritance.	85
3-8 Model for PAK priming of Vac17 for degradation.....	89
4-1 Cell cycle progression is not required for segregation structure resolution.	100
4-2 Cla4 localizes with the vacuole	101
4-3 Cla4 remains on the daughter vacuole until late-M phase	102

4-4	Cla4-GFP requires vacuole inheritance for vacuole associated punctate structure localization.	103
4-5	Cells lacking PAK function form but do not resolve segregation structures.	105
4-6	Cells overexpressing <i>CLA4t</i> fail to form a daughter vacuole and have a partial <i>in vivo</i> vacuole fusion defect.	107
5-1	<i>cla4-75 ste20</i> cells fail to form a daughter vacuole and arrest at G2/M.	123
5-2	<i>cla4-75 ste20 vac8</i> and <i>cla4-75 ste20 vac17</i> cells do not arrest.	124
5-3	Deletion of <i>SWE1</i> partially suppresses the <i>cla4-75 ste20</i> G2/M arrest but not the failure to resolve segregation structures.	126
5-4	Hsl1 is mislocalized in <i>cla4-75 ste20</i> and <i>cla4-75 ste20 vac8</i> cells.	128
5-5	Cdc5 is a target of the vacuole segregation checkpoint.	129
5-6	Model of the vacuole segregation checkpoint partial <i>in vivo</i> vacuole fusion defect.	132

LIST OF ABBREVIATIONS

α F	alpha factor
Δ	null
μ m	micrometer
μ M	micromolar
Async	asynchronous
ATP	adenosine triphosphate
C	carboxyl
CDK	Cyclin-dependent Kinase
DIC	differential contrast interference
cER	cortical endoplasmic reticulum
DAPI	4',6-diamidino-2-phenylindole
EDTA	ethylenediaminetetraacetic acid
FACS	fluorescence-activated cell sorting
FM 4-64	<i>N</i> -(3-triethylammoniumpropyl)-4-(<i>p</i> -diethylaminophenyl)-hexatrienyl) pyridinium dibromide
FRAP	fluorescence recovery after photobleaching
G1	gap 1 phase
G2	gap 2 phase
GAL	galactose
GCK	germinal center kinase
GDP	guanosine-5'-diphosphate
GEF	guanine nucleotide exchange factor

GFP	green fluorescent protein
GLU	glucose
GPCR	G-protein coupled receptor
GTP	guanosine-5'-triphosphate
HA	influenza hemagglutinin epitope
Hr.	hour
HU	hydroxyurea
IgG	immunoglobulin G
M	molar
MAPK	mitogen-activated protein kinase
MAPKK	mitogen-activated protein kinase kinase
MAPKKK	mitogen-activated protein kinase kinase kinase
MAPKKKK	mitogen-activated protein kinase kinase kinase kinase
MEN	mitotic exit network
Min.	minutes
mM	millimolar
N	amino
NZ	nocodazole
PAGE	polyacrylamide gel electrophoresis
PAK	p21-activated kinase
PBD	p21 binding domain
PCR	polymerase chain reaction
PH	pleckstrin homology

PMSF	phenylmethanesulphonylfluoride
PtdIns	phosphatidylinositol
UT	untagged
<i>vac</i>	vacuole partitioning mutant
WT	wild type

CHAPTER I

INTRODUCTION

Organelle Inheritance

Eukaryotic cells contain membrane bound compartments called organelles that perform various essential cellular functions. Organelle function is critical for proper cellular function; and each time eukaryotic cells divides they ensure that each of the progeny cells inherits a full complement of organelles.

There are two main non mutually exclusive strategies used by cells to ensure high fidelity transmission of organelles to their progeny. Stochastic inheritance requires that an organelle is present in multiple copies and evenly distributed throughout the cell. Division of the cell approximately in half by cytokinesis then ensures that both progeny contain a nearly equal amount of a multicopy organelle. The second strategy used by eukaryotic cells is an ordered process requiring the active transport of organelles to ensure equal partitioning. This second strategy is required for the accurate dispersal of low copy number organelles ¹.

My studies have focused on how the ordered process of organelle inheritance is regulated. To study the regulation of organelle inheritance I have used the genetically tractable organism *S. cerevisiae*. One advantage to studying organelle inheritance in budding yeast is that they divide asymmetrically, as opposed to symmetrically down the center. Therefore, organelles must be

actively transported into the bud to ensure that the daughter cell receives an equal share of organelles.

Budding and actin cable formation

Budding occurs through a stereotypical pattern of growth and division. Just prior to entry into S-phase polarized growth forms the nascent bud which emerges from the mother cell. This bud continues to grow throughout G2 and mitosis until cytokinesis. Cytokinesis yields a mother and a smaller daughter cell. Under nutrient rich conditions the mother cell quickly initiates another round of budding. The daughter undergoes a brief period of growth until it reaches a critical size and begins budding.

Budding yeast require the polarization of the actin cytoskeleton to establish polarity. There are three different actin structures found in budding yeast: patches, cables, and rings². Actin cables are composed of bundled actin filaments and are the primary tracks along which secretory vesicles are transported to direct polarized growth. During late G1, the Rho-like GTPase Cdc42 is activated at a predetermined cortical site. Active GTP bound Cdc42 activates the formins Bni1 and Bnr1. Actin cables are then formed by the actin-nucleating activity of formins and the actin binding protein profilin³⁻⁶. Secretory vesicles are transported along actin cables by the processive myosin V motor, Myo2.

Actin cables, which are almost exclusively localized along the cortex of the cell, are dynamic structures and undergo spatial rearrangements during the cell

cycle. During late G1, actin cables are polarized to the nascent bud site. While the bud is growing actin cables are polarized within the bud. Finally, as cells exit mitosis the actin cytoskeleton polarizes towards the mother bud neck in preparation for cytokinesis ⁷.

Vacuole inheritance in budding yeast

My research has focused on the regulation of vacuole inheritance in budding yeast. The yeast vacuole is a membrane bound organelle that is often considered analogous to the mammalian lysosome because of its acidification and the hydrolase activities that are localized to the vacuole. The vacuole is also the terminal degradative compartment of the endocytic pathway. In addition to its degradative capacity, the vacuole serves as a storage site for amino acids and polyphosphate ⁸. Additionally, the vacuole plays a role in regulating cytoplasmic pH and in modulating water and ion concentration within the cell ⁸⁻¹¹.

Vacuoles can be observed in living cells by at least three different methods. First, differential interference contrast (DIC) microscopy is used to examine vacuole morphology and partitioning; however, unambiguous identification of the vacuole can often be difficult with this method ¹². Second, *ade2* mutant cells accumulate amino-imidazole ribotide polymers within the vacuole that are fluorescent and allow vacuole visualization by fluorescence microscopy ^{13 14}. Third, vacuoles can be visualized by pulse-chase of cells with the fluorescent dye *N*-(3-triethylammoniumpropyl)-4-(*p*-diethylaminophenyl)-hexatrienyl) pyridinium dibromide (FM 4-64). FM 4-64 is imported into cells by

endocytosis and accumulates specifically on the vacuole membrane. FM 4-64 staining has several advantages in comparison to other methods. Specifically, FM 4-64 staining of the vacuole is quick, strain background independent, and the membrane localization of FM 4-64, as opposed to luminal accumulation of amino-imidazole ribotide polymers, allows for unencumbered visualization of organelle structure especially when differentiating clusters of small vacuoles¹⁵.

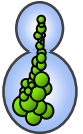
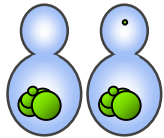
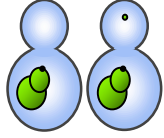
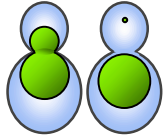
On average wild type yeast cells contain 1-3 large vacuole lobes¹⁶. These vacuole lobes are dynamic and undergo continuous fission and fusion¹⁷. Early experiments designed to visualize the vacuole showed that a portion of the vacuole forms a tubular and vesicular structure, termed the “segregation structure”, that is partitioned into the bud to found the daughter vacuole^{13, 18}. This high fidelity partitioning of vacuole material from the mother into the bud prompted the search for mutants defective for vacuole partitioning.

Two large-scale methods have been developed to search for vacuole partitioning (*vac*) mutants. The yeast vacuole contains many proteinases and these proteinases are transported to the vacuole as inactive precursors that must be cleaved for activation. One of these proteinases, carboxypeptidase Y, is activated by a proteinase cascade consisting of proteinase A cleaving and activating proteinase B, which in turn cleaves and activates carboxypeptidase Y. A simple plate assay exists to measure carboxypeptidase Y activity. To screen for vacuole inheritance mutants, cells are mutagenized and proteinase A is produced for a short period of time under the control of the *GAL* promoter in a *pep4* (proteinase A gene) mutant. This leads to proteinase B and subsequent

carboxypeptidase Y cleavage and activation. Proteinase A transcription is then squelched by the addition of glucose. Daughter cells that inherit vacuolar material from their mothers maintain carboxypeptidase Y activity for up to 20 generations due to transmission of activated proteinase B from mother into daughter cells. However, *vac* mutants have to make a vacuole *de novo* and all of their proteinase B is therefore inactive. Screening mutants for loss of carboxypeptidase Y after proteinase A was shut off by glucose has revealed multiple *vac* mutants¹⁹⁻²¹.

FM 4-64 has also been used to screen for *vac* mutants. After FM 4-64 pulsing cells, FM 4-64 accumulates on the vacuole membrane. Each cell division approximately half the mother's FM 4-64 stained vacuole membrane is partitioned to the daughter. Mother cells that fail to partition vacuole material to the daughter will maintain high levels of FM 4-64 fluorescent membrane after several divisions and daughters will have very little or no stained vacuole membrane. To screen for *vac* mutants, mutagenized cells are FM 4-64 stained and sorted by FACS to isolate highly fluorescent and very low fluorescent cells. Isolates then are subjected to secondary screens to confirm that mutants are legitimate *vac* mutants^{22, 23}.

Table 1-1. Classes of vacuole partitioning (*vac*) mutants

	WT	Gene	Corresponding gene product
Class I mutants			
	Normal vacuole morphology, often multilobed.	<i>act1</i>	Actin ²⁴
	<i>pfy1</i>	Profilin ²⁴	
	<i>myo2</i>	Myo2, class V myosin ²⁴	
	<i>vac8</i>	Vac8, vacuole membrane protein binds Vac17 ²⁵	
	<i>vac9</i>	Unknown ²⁵	
	<i>vac10</i>	Unknown ²⁵	
	<i>vac16</i>	Unknown ²⁶	
	<i>vac17</i>	Vac17, vacuole specific Myo2 receptor ^{20, 27}	
	<i>vac19</i>	Unknown ²⁶	
Class II mutants			
	Enlarged vacuole, often the vacuole is positioned towards bud.	<i>vac5</i>	Pho80 ²⁸
	<i>vac6</i>	Unknown ¹⁹	
	<i>vac11</i>	Unknown ²⁵	
	<i>vac12</i>	Unknown ²⁵	
	<i>vps3</i>	Vps3, subunit of CORVET tethering complex ¹⁸	
	<i>pep12/vps6</i>	Syntaxin, t-SNARE	
	<i>vps8</i>	Vps8, subunit of CORVET tethering complex	
	<i>vps9</i>	Vps9, GEF for Vps21	
	<i>pep7/vps19/vac1</i>	Pep7, Vps21 effector	
	<i>vps21/ypt51</i>	Vps21, Rab	
	<i>vps45</i>	Vps45, Sec1-like	
Class III mutants			
	Highly enlarged vacuole membrane fission defects.	<i>fab1</i>	Fab1, PtdIns(3)P 5-Kinase ^{29, 30}
	<i>vac7</i>	Vac7, regulator of Fab1 ³¹	
	<i>vac14</i>	Vac14, regulator of Fab1 ¹⁰	
	<i>fig4</i>	Fig4, PtdIns 5' phosphatase ¹⁰	
	<i>atg18</i>	PtdIns(3,5)P2 binding protein ³²	
	<i>vps15</i>	Vps15, activator of Vps34 ³³	
	<i>vps34</i>	Vps34, PtdIns 3-Kinase ³⁴	

Based on vacuole morphology all of the presently known *vac* mutants can be divided into one of three different classes (Table 1-1)²². Class I vacuole partitioning mutants have normally sized vacuoles but often contain multiple vacuole lobes. To date, each of the class I *vac* mutants, for which the corresponding gene has been identified, identifies a part of the physical machinery necessary for transport of the segregation structure into the bud. Class II mutants display a moderately enlarged vacuole, normal vacuole

morphology, and a portion of the vacuole is often positioned towards the bud. Class II *vac* mutants include a number of vacuole protein sorting (*vps*) mutants which fail to transport carboxypeptidase Y to the vacuole. The mechanism by which class II mutants abrogate vacuole inheritance is not known¹⁴. Class III mutants have a greatly enlarged vacuole which is defective for vacuole fission. All of the known class III mutants identify proteins required for the production of, or that bind to PtdIns(3,5)P₂.

Transport of the segregation structure

Vesicle transport requires both a track along which a vesicle must travel and a motor protein to physically transport the vesicle. Eukaryotic cells have three main cytoskeletal tracks: actin filaments, microtubules, and intermediate filaments. In mammalian cells, organelle transport commonly utilizes microtubules³⁵. However, microtubules are not necessary for vacuole inheritance as cell treated with the microtubule depolymerizing drug nocodazole (NZ) partition vacuoles normally³⁶. Instead, budding yeast transport the vacuole along polarized actin cables²⁴. Multiple actin mutants are defective for vacuole inheritance. In particular *act1-ΔDSE*, which eliminates three NH₂-terminal amino acids, shows no observable cytoskeletal defects except a vacuole inheritance defect. Importantly, the three NH₂-terminal amino acids form a portion of the myosin binding site and other actin mutants in the actin-myosin binding site also show vacuole inheritance defects^{24, 37}. Immunofluorescence also shows the segregation structure is juxtaposed along actin cables²⁴.

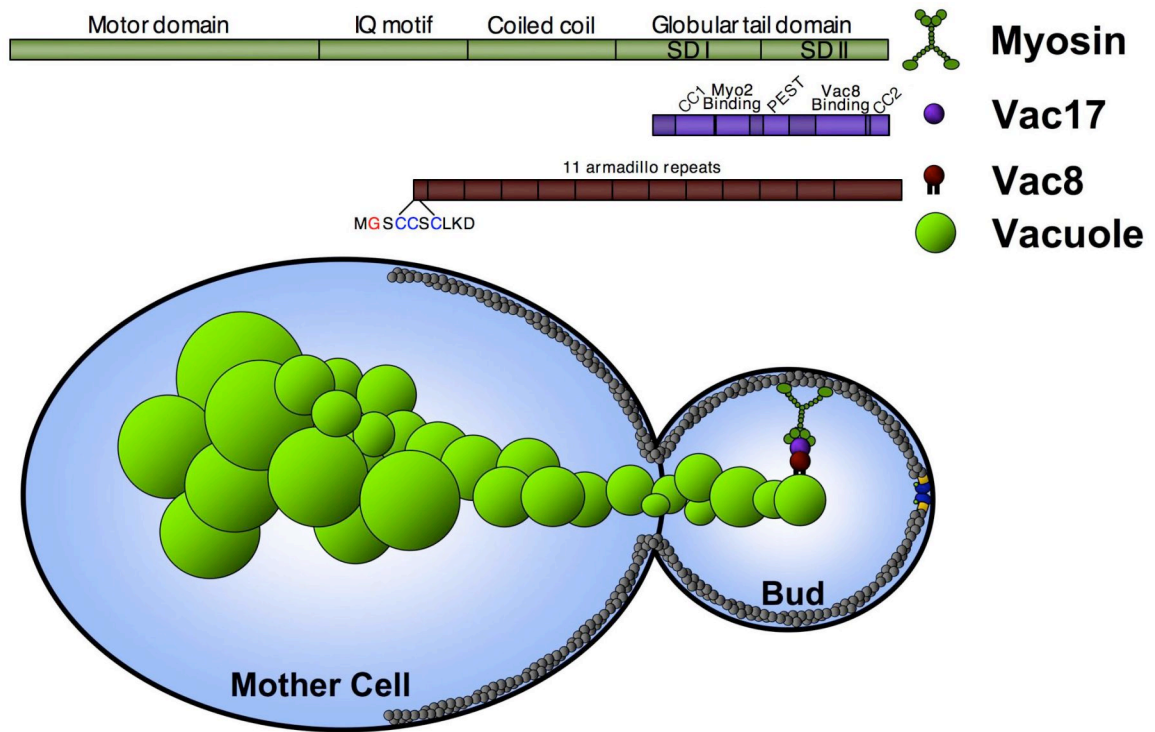


Figure 1-1. Proteins involved in transport of the vacuole into the bud. (Details in the text)

Myosin V motors are composed of two heavy chains that dimerize to form a processive two-headed molecular motor with a large step size³⁸. Budding yeast contain two myosin V motors, Myo2 and Myo4, which travel along actin cables. Myo4 is not involved in vacuole partitioning. Multiple lines of evidence show that Myo2 is the motor protein that transports the vacuole into the bud. First, temperature sensitive alleles of *MYO2* when grown at the restrictive temperature disrupt vacuole movement into the bud²⁴. Second, Myo2 localizes to punctate structure on the vacuole and is enriched at the tip of the segregation structure oriented towards the bud²⁴. Third, mutations in *MYO2*, which specifically abrogate the Myo2-Vacuole interaction, have been isolated^{21, 23}.

Further analysis of the Myo2 globular tail domain, that is known to bind cargo, has revealed it to be composed of two subdomains, SDI and SDII. SDI and SDII dimerize *in vitro* and *in vivo* and this dimerization is required for cargo binding. SDI and SDII bind different cargo. SDI binds to the vacuole-specific myosin receptor Vac17 (described below). Mutants in *MYO2* that disrupt vacuole inheritance all map to SDI. SDII binds to secretory vesicles³⁹⁻⁴¹.

Attachment of Myo2 to the vacuole is accomplished through the vacuole transport complex consisting of Myo2-Vac17-Vac8. Vac8 is both myristoylated and palmitoylated on residues at the NH₂-terminus, and these modifications are necessary for Vac8 localization to the vacuole^{25, 42-45}. Vac8 plays many roles in the cell, including roles in caffeine resistance, homotypic vacuole fusion, nucleus-vacuole junction (NVJ) formation, cytoplasm to vacuole transport (CVT), and vacuole inheritance^{11, 25, 42, 43, 46-49}. Vac8 contains eleven armadillo repeat domains. Armadillo repeats are known to mediate protein-protein interaction and Vac8 is known to bind at least nine different receptors⁴⁹. Vac8 is enriched on three different subdomains of the vacuole associating with the NVJ, sites of homotypic vacuole fusion, and domains that act in vacuole transport⁴⁴.

The Vac8 receptor protein Vac17 connects Vac8 to Myo2 and is the final member of the vacuole transport complex. Vac17 binds directly to both Myo2 and Vac8 through separable protein domains^{20, 27}. Vac17 production and degradation play key roles in the spatial and temporal regulation of vacuole inheritance. *VAC17* mRNA levels oscillate with the cell cycle and increase as cells begin budding^{50, 51}. Concordantly Vac17 levels increase during early budding. Vac17

contains a region abundant in proline (P), glutamic acid (E), serine (S), and threonine (E) known as a PEST sequence which acts as a signal for rapid turnover. Intriguingly, turnover of Vac17 is spatially dependent and requires transport of Vac17 into the bud. The vacuole inheritance mutants *vac8* and *myo2-2* fail to degrade Vac17 and Vac17 accumulates to high levels²⁰. Examination of the timing of Vac17 degradation shows that it is normally degraded prior to cytokinesis. The spatial and temporal regulation of Vac17 is necessary to ensure that the vacuole is not transported back to the mother-bud neck when the actin cytoskeleton concentrates at the mother-bud neck in preparation for cytokinesis. When Vac17 missing the PEST sequence (*vac17 Δ PEST*) is expressed in cells, *Vac17 Δ PEST* localizes to the vacuole but is not degraded. Furthermore, both the mother and daughter vacuole are transported to the mother-bud neck²⁰.

Vac17 is degraded in a bud-specific manner, but how this is achieved remains unknown. One model posits that factors specifically localized to or activated in the bud promote Vac17 degradation¹⁴. Thus Vac17 does not come into contact with these factors until Vac17 enters the bud. The identity of these factors remains unknown.

Formation of the segregation structure

Isolation of the class III *vac* mutants shed light on the machinery necessary for forming the segregation structure. Like wild type yeast, class III *vac* mutants transport a portion of the vacuole into the bud. Unlike wild type cells the

class III mutants usually contain an enlarged single lobed vacuole. During inheritance the vacuole is transported into the bud, but the vacuole is commonly seen as one enlarged contiguous vacuole stretched from the mother into the bud that is constricted at the neck, forming what looks like an “open-figure-eight” (Table 1-1) ^{29, 30}. The enlarged vacuole and the persistence of the vacuole in the neck of the most severe class III *vac* mutant, *fab1*, adversely affects spindle positioning leading to aploid and binucleate cells ²⁹. Proteins identified by the class III *vac* mutants have been proposed to form the tubules and vesicles making up the segregation structure, allowing vacuolar material to pass easily through the confined space of the mother bud neck ^{14, 26}.

Cloning of the class III *vac* mutants helped elucidate the mechanism of segregation structure formation (Table 1-1). Each of the class III *vac* mutants are in genes that code for proteins that produce, regulate the production of, or bind to PtdIns(3,5)P₂. Vps15 binds to and activates the sole PtdIns 3'-Kinase in yeast, Vps34, and PtdIns(3)P is required as a precursor for PtdIns(3,5)P₂ production ^{33, 34, 52, 53}. Fab1 is the sole PtdIns(3) 5-kinase in yeast ⁵⁴ and it is positively regulated by Vac7 and Vac14 ^{10, 31}.

Importantly PtdIns(3,5)P₂ production has physiological effects on vacuole morphology. PtdIns(3,5)P₂ levels are 18-28 fold lower than PtdIns(3)P, PtdIns(4)P, and PtdIns(4,5)P₂ under normal physiological conditions but rapidly rise 20-fold after hyperosmotic stress ¹⁰. Concomitant with the rise in PtdIns(3,5)P₂ levels the vacuole fissions to form multiple small lobes. The fissioning of the vacuole is linked to the production of PtdIns(3,5)P₂; and *fab1*

and *vac14* mutants do not fission under hyperosmotic conditions^{10, 31}. The rapid fissioning of the vacuole may mitigate problems caused by the rapid efflux of water out of the cell under hyperosmotic conditions by releasing water from the vacuole. A sphere with a given diameter can produce four spheres with a total of half the volume¹⁰. Under hyposmotic conditions the vacuole undergoes fusion and *vac8* mutants are defective for hyposmotic induced homotypic vacuole fusion¹¹.

How does PtdIns(3,5)P₂ promote the fissioning of the vacuole? Fission of the vacuole requires, at least in part, the recruitment of PtdIns(3,5)P₂ effector proteins. One effector, Atg18, binds directly to PtdIns(3,5)P₂ and *atg18* mutants display an enlarged vacuole phenotype like all known class III *vac* mutants^{32, 55}. Atg18 was originally isolated in a screen for mutants defective in autophagy. However, PtdIns(3,5)P₂ does not appear necessary for autophagy as *fab1* mutants are not defective for autophagy³². Cells lacking *ATG18* additionally have a 5-10 fold higher levels of PtdIns(3,5)P₂ under normal physiological conditions while retaining an enlarged vacuole³². Atg18 and other fission machinery (Fab1 and Vac14) localize to punctate structures on the vacuole. In a small number of cells FM 4-64 stained vesicles bud from the Atg18-GFP punctate structures and Atg18-GFP containing vacuoles travel into the bud and fuse with what is presumably the daughter vacuole. This is especially intriguing as Atg18 binds Vac17 by 2-hybrid and coimmunoprecipitation⁵⁵. Thus it has been proposed that Atg18 serves a nonessential role in facilitating the formation of the segregation structure by promoting vesicle fission⁵⁵.

Inhibition of vacuole fusion also plays a role in maintaining vacuole fragmentation after exposure to hyperosmotic conditions and in forming the segregation structure. The yeast casein kinase, Yck3, negatively regulates homotypic vacuole fusion by inhibiting the tethering of vacuoles. Inhibition of homotypic vacuole fusion is essential to maintain vacuole fragmentation after PtdIns(3,5)P₂ levels have returned to normal after hyperosmotic shock⁵⁶. Inhibition of vacuole fusion is also important for the efficient partitioning of the vacuole into the bud. Mutant *yck3* cells have a moderate vacuole inheritance defect, reduced daughter vacuole size in cells inheriting vacuole material from the mother, and tubular and vesicular segregation structures were not observed in the mutant⁵⁶. These data combined lead to the current model for segregation structure formation which proposes that vacuole fission is required to form the vesicles and tubules that compose the segregation structure⁵⁷.

Despite the added clarity that recent experiments have shed on how the segregation structure is formed, many unanswered questions exist about the process and several key experiments to test the model remain undone. One of the major roadblocks to analyzing vacuole partitioning revolves around the transience of segregation structures. Based on the rate of vacuole movement and the distance of travel, segregation structures can be around for as little as 30 seconds during the cell cycle¹⁴. During this 30 seconds a complex set of reactions has been proposed to occur, including the production of PtdIns(3,5)P₂¹⁴, the recruitment PtdIns(3,5)P₂ binding proteins, segregation structure formation^{32, 55, 58, 59}, transport of the segregation structure into the bud, and resolution of

the segregation structure (discussed below). The transient nature of the segregation structure and the impossibility of reliably synchronizing a population with intact segregation structures have made testing if PtdIns(3,5)P₂ levels transiently rise during segregation structure formation difficult. Visualization and quantification of Atg18, or other potential PtdIns(3,5)P₂ effectors, on segregation structures is also difficult or impossible due to the transience of the segregation structure. Identification of mutants defective for resolving the segregation, therefore extending the amount of time the segregation structure persists, could potentially be useful to further study these problems.

Resolution of the segregation structure

Once formed, the segregation structure is transported into the bud. Upon entry into the bud the segregation structure is resolved to form a discrete mother and daughter vacuole. Over the years various strides have been made in forming a model for how the segregation structure is resolved.

Together the experimental data suggests that the segregation structure is resolved by the fusion of tubular and vesicular structures in the bud. The data that support this model are reviewed below. (1) Formation of the vacuole segregation structure requires PtdIns(3,5)P₂ production on the vacuole which promotes fission of the vacuole, suggesting that the opposing process fusion is required for resolution^{10, 30, 31, 60-62}. (2) Examination of labeled vacuoles by microscopy showed transport of vesicular structures from the mother into the daughter and fusion of these vesicles to form a larger daughter vacuole⁶³. (3)

Studies on vacuoles in semi-permeabilized cells show the formation of tubular and vesicular structures followed by vacuole fusion ⁶³⁻⁶⁶. (4) Resolution of segregation structure in zygotes involves vacuole fusion and merging of vacuole contents ⁶⁷. (5) Formation of the segregation structure is promoted by Yck3 which maintains fragmentation through inhibition of homotypic vacuole fusion ⁵⁶.

Together these data suggest a model in which the vesicles and tubules composing the segregation structure are formed by fission machinery and resolved by fusion of the tubules and vesicles in the bud. A non-exclusive alternate model suggests that both formation and resolution of the segregation structure is accomplished by fission of the tubules to form the daughter vacuole. However, this possibility has not been rigorously tested and is solely supported by the observation that class III *vac* mutant often have vacuoles which span the mother bud neck ⁵⁷. Missing from these models of segregation resolution, is a mechanism for not only promoting, but insuring, that the segregation structure is only resolved after arriving in the bud. As was proposed for Vac17 degradation ¹⁴, there may be proteins localized specifically to the bud which promote vacuole fusion (or fission) to resolve the segregation structure as it enters the bud. However, as with the daughter-specific degradation of Vac17, potential daughter localized proteins that promote resolution of the segregation structure after it has entered the bud have not been identified.

Coordination of vacuole inheritance with the cell cycle

Cells must coordinate organelle inheritance with other cell cycle driven events including mitosis and cytokinesis. This coordination ensures that each time an eukaryotic cell divides, each of the progeny receives an accurate copy of each of the chromosomes and a full complement of organelles. Checkpoints can delay cell cycle progression in response to a failure to complete earlier events through transduction of a negative signal to the cell cycle machinery^{68, 69}. Recent evidence has shown that checkpoints exist to ensure the faithful propagation of organelles to each progeny cell.

In mammalian cells the Golgi apparatus is composed of 4-8 cisternae anchored at pericentriolar region of the cell. During prophase this Golgi ribbon fragments into smaller vesicles and tubules that are subsequently dispersed during metaphase³⁵. Failure to fragment the Golgi activates the Golgi mitotic checkpoint and delays cells at G2/M⁷⁰.

Organelle partitioning checkpoints are not exclusive to mammalian cells. In budding yeast the cortical endoplasmic reticulum (cER) is transported along actin cables by the myosin V family motor Myo4 into the bud where it becomes anchored at the tip of the bud and expands to fill the bud³⁵. Cells lacking proteins required for cER inheritance also delay in G2/M. This cER inheritance checkpoint requires the morphogenesis checkpoint proteins which acts to delay the cell cycle by negatively regulating the cyclin B-CDK complex essential for mitotic progression⁷¹.

Checkpoints may also be required to ensure that segregation structure resolution occurs prior to mitosis. Budding yeast have a relatively narrow neck through which both the segregation structure and the nucleus must pass. Early studies noted that segregation structures are oriented towards the emerging bud early in the cell cycle and inheritance was completed prior to nuclear division^{12, 13, 36}. This opens the possibility that budding yeast monitor and delay cell cycle progression until segregation structures are resolved, thus clearing the neck for karyokinesis. How segregation structure resolution is coordinated with the cell cycle is unknown⁵⁷.

Currently there are two known checkpoints that delay mitotic progression in response to failure to complete organelle inheritance: the Golgi mitotic checkpoint and the cER inheritance checkpoint. Mitogen-activated protein kinases regulate (MAPKs) regulate the inheritance of both of these organelles. In mammalian cells the Golgi mitotic checkpoint delays cells in G2/M⁷⁰. While the mechanism for this checkpoint has not been fully elucidated, inhibition of MAP kinases involved in Golgi fragmentation results in checkpoint activation^{72, 73}. cER inheritance is also regulated by a MAP kinase pathway⁷⁴.

Mitogen-activated protein kinases

The Ste20 group kinases are regulators of mitogen-activated protein kinase (MAPK) cascades and are divided into two main groups the p21-activated kinases (PAKs) and the germinal center kinases (GCKs)⁷⁵. My studies have

focused on the role of PAKs in regulating vacuole inheritance. Yeast contain two main p21-activated kinases, the founding member of the family, Ste20, and Cla4.

Ste20 and Cla4 contain multiple domains and share similar domain structures. Both Ste20 and Cla4 have a kinase domain towards the C-terminus of the protein. There are multiple known targets of the PAKs in budding yeast. Both Ste20 and Cla4 are known to phosphorylate the myosin-I isoforms Myo3 and Myo5^{76, 77}. Ste20 phosphorylates the MAPKKK Ste11⁷⁸. Cla4 has several known targets including the Cdc42 guanine nucleotide exchange factor (GEF) Cdc24^{79, 80}, septins⁸¹, Swe1^{82, 83}, and Lte1⁸⁴⁻⁸⁶. Despite the increasing data about Ste20 and Cla4 substrates, it must be noted that a complete catalog of substrates for either kinase remains undetermined and the data on the redundancy of Ste20 and Cla4 substrates remains elusive.

Ste20 and Cla4 activity is carefully controlled by both positive and negative regulation. Regions in the N-terminal halves of the PAKs interact with the kinase domain in the C-terminal half of the PAKs leading to autoinhibition. This model is supported by genetic and structural data on Ste20, Cla4, and other PAKs⁸⁷⁻⁸⁹. Autoinhibition is relieved when PAKs bind to activated GTP bound Cdc42 through the p21 binding domain (PBD) located within the N-terminal half of the protein⁸⁹⁻⁹¹. In budding yeast the adaptor protein Bem1 facilitates the interactions between Cdc42 and the PAKs. Bem1 is a multidomain protein and it binds both Cdc42 and Cdc24⁹²⁻⁹⁵. Bem1 contains two SH3 domains and the second SH3 domain interacts with proline rich domains in Ste20 and Cla4^{79, 80, 96}. The adaptor protein Bem1 thus brings together Cdc42 with its GEF leading to

Cdc42 activation. Activated Cdc42's interaction with Ste20 and Cla4 relieves PAK autoinhibition and activates the PAKs. Cla4 activity is also cell cycle regulated and peaks near mitosis⁸⁸.

Both Cla4 and Ste20 localize to sites of polarized growth^{87, 97-99}. To ensure that Ste20 and Cla4 localize to regions where potential targets reside, both proteins contain domains necessary and sufficient to bind phosphatidylinositides. Cla4 contains a pleckstrin homology (PH) domain. PH domains are known to vary in their specificity for different phosphatidylinositides¹⁰⁰. *In vitro* analysis by protein-lipid overlay analysis demonstrates that Cla4's PH domain binds to PtdIns(3)P, PtdIns(3,5)P₂, PtdIns(4)P, and PtdIns(5)P. Surface plasmon resonance showed strong binding to both PtdIns(4,5)P₂ and PtdIns(3,5)P₂. *In vivo* analysis finds that Cla4-GFP localization to the plasma membrane requires PtdIns(4)P but not PtdIns(4,5)P₂^{100, 101}. Functional analysis of Cla4 mutants unable to bind phosphatidylinositides shows that phosphatidylinositide binding acts in conjunction with Cdc42 localization and activation to promote Cla4 activity¹⁰¹. Ste20 also binds to phosphatidylinositides using a basic-rich (BR) domain, but the phosphatidylinositide specificity of the Ste20's BR domain has not been tested. Like the PH domain in Cla4, the BR domain in Ste20 acts in conjunction with the PBD to both localize and activate Ste20¹⁰².

Ste20 was originally isolated in a screen for suppressors of a dominant negative mutant of the β -subunit of a heterotrimeric G-protein coupled receptor,

Ste4, involved in mating¹⁰³. Ste4 binds to Ste20 through a noncatalytic region in the extreme C-terminus of Ste20¹⁰⁴.

Cellular functions of Ste20 and Cla4

Ste20 and Cla4 are not only similar in their domain structure but they also share many overlapping functions. However, they also perform nonoverlapping functions. In budding yeast PAKs are known to play roles in signal transduction involved in mating, filamentous growth, and in responding to osmotic stress. Additionally, they promote polarized growth, septin formation, and cell cycle progression.

Signal transduction

Signal transduction networks are necessary for cells to respond to external signals and to coordinate intracellular changes with the extracellular environment. In budding yeast the best studied of these signal transduction networks is the pathway required for mating. Haploid yeast excrete peptide pheromones which bind to cell-surface receptors on yeast of the opposite mating type. Pheromone binding causes G1 cell cycle arrest and polarized growth towards a partner cell of the opposite mating type. Once the two cells come into contact they fuse to form a diploid cell. A G-protein coupled receptor (GPCR) activated MAPK cascade is required to coordinate the process of mating. This kinase cascade requires the MAPKKKK Ste20, a MAPKKK Ste11, a MAPKK Ste7, and two MAPKs Fus3 and Kss1 which are all connected by the scaffolding

protein Ste5¹⁰⁵. Ste20 directly interacts with Ste4, the β -subunit of the GPCR¹⁰⁴. After binding Ste4, Ste20 directly phosphorylates Ste11, relieving its autoinhibition and thus promoting Ste7 phosphorylation⁷⁸. The scaffolding protein Ste5 also binds to Bem1 allowing for the efficient activation of Ste20 by GTP-Cdc42¹⁰⁶. Cla4 is not known to bind to Ste4. However, genetic and biochemical data suggest that Cla4 does participate in the mating type pathway – though probably by negatively regulating it¹⁰⁷.

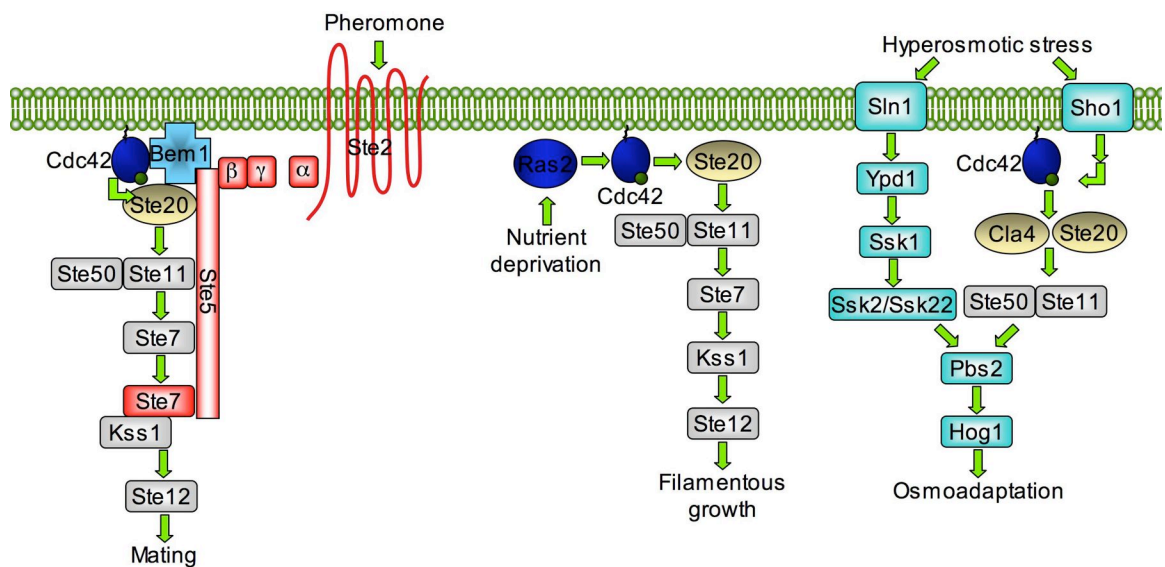


Figure 1-2. Ste20 and Cla4 are involved in signal transduction. (Details in the text)

Although less understood than the mating type cascade, Ste20 also plays key roles in regulating filamentous growth (also called invasive growth in haploid cells and pseudohyphal growth development in diploid) under nutrient deprivation conditions. The filamentous growth MAPK cascade causes cells to become elongated and fail to separate after division causing cells to penetrate into the agar. The filamentous growth MAPK cascade consists of Ste20 (MAPK) →

Ste11 (MAPKKK) → Ste7 (MAPKK) → Kss1 (MAPK) ¹⁰⁸. Unlike in the mating type cascade, Fus3 is not activated, the scaffolding protein Ste5 is not used, and Cdc42 is activated by Ras2 ¹⁰⁵. Thus Ste20 plays key roles in regulating both mating and filamentous growth.

In response to hyperosmotic stress, vacuoles fragment immediately to accommodate osmotic changes. Prolonged hyperosmotic change requires long-term cellular adaptations to the new environment. In response to hyperosmotic shock cells arrest and begin producing the compatible solute glycerol ¹⁰⁹. Budding yeast contain two putative osmosensors, Sln1 and Sho1. Sln1 and Sho1 activate different branches of the pathway but both culminate in the activation of the same MAPK cascade consisting of Pbs2 (MAPKK) → Hog1 (MAPK). The Sho1 branch of the pathway requires Ste11 (MAPKKK) activation of Pbs2. Both Ste20 and Cla4 play roles in activating Ste11 in response to hyperosmotic stress as assayed in a reporter strain ¹¹⁰. Further evidence supporting a role for Cla4 in hyperosmotic stress response is found in the early findings that cells lacking *CLA4* are normally elongated and this elongation is suppressed by growth under hyperosmotic conditions but not in the absence of either *PBS2* or *HOG1* ⁹¹. Intriguingly hyperosmotic stress can cause cells to arrest in G1 or delay in G2. This G2 delay requires the Hog1 dependent phosphorylation of the Nim1-related protein kinase in yeast Hsl1 (discussed further below) ¹¹¹.

Polarized Growth

Polarized growth requires the activation of Cdc42 by Cdc24 and temperature sensitive *cdc42* and *cdc24* mutants arrest as large unbudded cells at the restrictive temperature^{112, 113}. Cdc24 is normally localized to the nucleus during G1 and is exported into the cytoplasm at bud emergence^{114, 115}. Cdc24 is initially localized to the site of bud emergence by proteins that mark the presumptive bud site¹¹⁶. Stabilization of Cdc24 at the site of polarized growth is accomplished by interactions with the adaptor protein Bem1^{93, 117}. Cla4 and Ste20 interact with Bem1, and Cla4 (and possibly Ste20) phosphorylates Cdc24. The effect of Cdc24 phosphorylation, however, is an unresolved issue with separate groups reporting contradictory results. Gulli *et al.* find that phosphorylation of Cdc24 by Cla4 causes Cdc24 to dissociate from Bem1⁷⁹. In contrast Bose *et al.* find that phosphorylation of Cdc24 by Cla4 causes a stabilization of the Cdc24-Bem1 interaction⁸⁰. Therefore, Cla4 regulates polarized growth by regulating Cdc24 localization, though the consequences of this regulation are disputed.

Ste20 and Cla4 also indirectly regulate actin branching. Neither Ste20 nor Cla4 are necessary for the polarization of actin cables required for bud emergence^{91, 118, 119}. However, Ste20 and Cla4 are involved in promoting actin polymerization through the Arp2/3 complex. Cdc42 activates Arp2/3 dependent branching through a defined pathway. Cdc42 activates the Wiskott-Aldrich syndrome protein (Las17) bound to the WASP-interacting protein (Vrp1)¹²⁰⁻¹²⁴ and Las17/Vrp1 activates the Arp2/3 complex to promote actin polymerization³.

¹²⁵. Ste20 and Cla4 phosphorylate the type I myosins, Myo3 and Myo5 ^{76, 77, 126}. In turn, phosphorylated Myo3 and Myo5 activate the Las17/Vrp1 complex ^{126, 127}. Through modulating Arp2/3 mediated branching it has been proposed that the PAKs regulate the actin cytoskeleton in *S. cerevisiae* and other organisms ¹²⁸.

Septin Formation

Septins are evolutionarily conserved GTP-binding proteins that form hetero-oligomeric filaments. In budding yeast these septin filaments form at the mother bud neck where they act as a scaffold on which other proteins assemble ¹²⁹. In G1 cells, septins are localized to the nascent bud site but are highly mobile and fluid as judged by fluorescence recovery after photobleaching (FRAP) but they quickly reorganize to form a protein collar concomitant with bud emergence ^{130, 131}. During cytokinesis the septin collar splits into two rings.

A role for PAKs in septin organization was recognized in early studies. In cells lacking both Ste20 and Cla4 activity the mother bud neck appears particularly wide and the septin Cdc3 is mislocalized ⁹¹. PAKs appear to promote reorganization of the septins leading to their immobilization and in both *cdc42* and *cla4* mutant cells septins remain more dynamic throughout budding ¹³⁰⁻¹³². Cla4 directly phosphorylates the septins Cdc3, Cdc10, and Cdc11, and removal of the Cla4 phosphorylation site on Cdc10 causes septin organization defects ⁸¹. Ste20 also plays a role in regulating septin formation. Evidence supporting this conclusion include the findings that Cdc10 has residual phosphorylation in a *cla4* mutant, Ste20 phosphorylates Cdc10 *in vitro*, and septins mislocalize to a greater

extent in cells lacking both *CLA4* and *STE20* than in cells lacking either PAK individually^{81, 91}.

Cell Cycle Progression

Each time budding yeast reproduce, bud formation must be coordinated with organelle partitioning and mitotic progression. In the event of a failure to properly form a bud, checkpoints ensure that mitotic progression is delayed until a bud is formed. The checkpoint linking bud formation with cell cycle progression is called the morphogenesis checkpoint and it delays cells in G2¹³³. The morphogenesis checkpoint is thought to monitor proper bud formation by monitoring proper formation of the septin collar. In response to a failure to properly form the septin scaffold, cells delay or arrest at G2. To delay cell cycle progression the morphogenesis checkpoint modulates the localization and stability of the Wee1 kinase in budding yeast, Swe1. Swe1 is a dual specificity kinase that prevents cell cycle progression by phosphorylating the mitosis-promoting cyclin B/CDK complex on a conserved tyrosine residue¹³⁴. When septin rings are properly formed at the mother-bud neck the Nim1-family protein kinase Hsl1 recruits the protein methyltransferase Hsl7 to the mother bud neck. Hsl7 interacts directly with Swe1 and recruits Swe1 to the mother bud neck where it is negatively regulated¹³⁵⁻¹⁴⁰.

Multiple lines of evidence show that Cla4 and Ste20 regulate Swe1. Failure to negatively regulate Swe1 leads to cells with elongated buds. The Cdc42 mutant *cdc42*^{V44A} has elongated buds. This elongated bud phenotype is

suppressed by deletion of *SWE1* or by overexpression of *CLA4* or *STE20*¹⁴¹. Cells lacking both Cla4 and Ste20 activity arrest in G2 in a *SWE1* dependent manner^{91, 118, 119}. Cells lacking *CLA4* are elongated and this elongation is suppressed by *SWE1* deletion¹³⁵. Finally, Cla4 is targeted to the mother bud neck and directly phosphorylates Swe1^{82, 83}. In this way PAKs act to promote cell cycle progression through G2. The yeast Polo-like kinase, Cdc5, also interacts with Swe1 and phosphorylates Swe1 to promote cell cycle progression^{82, 83, 142}.

In addition to promoting progression into mitosis PAKs act to promote mitotic exit. In budding yeast mitotic exit is driven by the protein phosphatase Cdc14 that acts to reverse CDK phosphorylation events. From the beginning of the cell cycle until metaphase, Cdc14 is kept inactive within the nucleolus. In order to promote mitotic exit, sustained Cdc14 release from the nucleolus requires a network of proteins called the MEN (mitotic exit network). The MEN consists of the GTPase Tem1; its putative GEF Lte1; a two-component GTPase activating protein (GAP) Bub2/Bfa1; the protein kinases Cdc5, Cdc15, Dbf2; a Dbf2 associated factor Mob1, and a scaffold protein Nud1¹⁴³. The GTPase Tem1 is localized to the spindle pole body entering the bud. Once transported into the bud Tem1 comes into contact with and probably activated by Lte1 localized at bud cortex. Cla4 phosphorylates Lte1 regulating its initial localization and binding to the bud cortex⁸⁴⁻⁸⁶. Ste20 is not necessary for Lte1 phosphorylation or localization but is synthetically lethal with *lte1*. The *ste20 lte1* synthetic lethality combined with other genetic and molecular biological data show that Cla4 and Ste20 act in parallel pathways to promote mitotic exit^{84, 119}.

Vacuole Fusion

The yeast vacuole is a dynamic structure and constantly undergoes fusion and fission. Fusion of separate lobes of the vacuole requires a multistep process. First vacuoles are primed for fusion by the ATP dependent activation of fusion factors. Second, vacuoles are reversibly tethered together. Next unpaired SNAREs assemble into a *trans*-complexes leading to docking. Finally, lipid bilayer mixing and fusion of vacuoles occurs ¹⁴⁴. Both Cdc42 and actin polymerization are required for the docking stage of vacuole fusion ^{122, 124, 145, 146}. *In vitro* and *in vivo* studies show that inhibition of actin branching by inhibiting either Las17 or the Arp2/3 complex inhibits docking ¹²². Importantly, Cla4 and Ste20 both indirectly activate Las17 by phosphorylating Myo3 and Myo5 ^{76, 77, 126, 127}. Therefore, PAKs may play a role in vacuole fusion. In further support of a role for PAKs in vacuole fusion, Cla4 localizes to purified vacuole and *cla4* mutants have fragmented vacuoles ^{16, 122}. Additionally, the Cla4 and Ste20 interacting protein Bem1 promotes vacuole fusion ^{147, 148}.

Conclusions

Cla4 and Ste20 play many roles in regulating various biological processes in *S. cerevisiae*. In the chapters that follow I will present data showing that Cla4 and Ste20 act to regulate vacuole inheritance. In chapter two I identify a novel class I *vac* mutant. Boi1 and Boi2 are functionally redundant proteins that interact with Bem1. Mutant *boi1 boi2* cells display a class I *vac* defect which is

suppressible by deletion of *CLA4* or *STE20*. Unlike all other known class I vac mutants which are part of the physical machinery transporting the segregation structure into the bud, Boi1 and Boi2 play no known structural role in inheritance and may instead be regulators of vacuole inheritance.

In chapter three I address an open question in the vacuole inheritance field of how Vac17 is degraded in a spatially dependent fashion. It has been previously hypothesized that bud-specific degradation of Vac17 is promoted by bud localized factors. However, the identity of these factors was not known. In chapter three I show that Cla4 and Ste20, which localize specifically to the bud, are required for Vac17 degradation. I also show that *CLA4* and *STE20* overexpression causes a vacuole inheritance defect that is suppressed by non-degradable Vac17.

In chapter four I address the question of how the segregation structure is resolved. I show that Cla4 localizes to the segregation structure just prior to segregation structure resolution placing it in the right time and place to resolve the segregation structure. I additionally show that PAKs are required for daughter vacuole formation.

Checkpoints delay cell cycle progression in response to a failure to complete earlier events through transduction of a negative signal to the cell cycle machinery. Vacuole inheritance is finished before mitosis occurs. In chapter five I present data supporting a novel vacuole inheritance checkpoint. Together this data advances our understanding of how vacuole inheritance is regulated in a spatially dependent manner and how it is coordinated with cell cycle progression.

References

1. Warren, G. & Wickner, W. Organelle inheritance. *Cell* **84**, 395-400 (1996).
2. Moseley, J.B. & Goode, B.L. The yeast actin cytoskeleton: from cellular function to biochemical mechanism. *Microbiol Mol Biol Rev* **70**, 605-45 (2006).
3. Evangelista, M., Pruyne, D., Amberg, D.C., Boone, C. & Bretscher, A. Formins direct Arp2/3-independent actin filament assembly to polarize cell growth in yeast. *Nat Cell Biol* **4**, 260-9 (2002).
4. Sagot, I., Klee, S.K. & Pellman, D. Yeast formins regulate cell polarity by controlling the assembly of actin cables. *Nat Cell Biol* **4**, 42-50 (2002).
5. Pruyne, D. et al. Role of formins in actin assembly: nucleation and barbed-end association. *Science* **297**, 612-5 (2002).
6. Sagot, I., Rodal, A.A., Moseley, J., Goode, B.L. & Pellman, D. An actin nucleation mechanism mediated by Bni1 and profilin. *Nat Cell Biol* **4**, 626-31 (2002).
7. Amberg, D.C. Three-dimensional imaging of the yeast actin cytoskeleton through the budding cell cycle. *Mol Biol Cell* **9**, 3259-62 (1998).
8. Klionsky, D.J., Herman, P.K. & Emr, S.D. The fungal vacuole: composition, function, and biogenesis. *Microbiol Rev* **54**, 266-92 (1990).
9. Dove, S.K. et al. Osmotic stress activates phosphatidylinositol-3,5-bisphosphate synthesis. *Nature* **390**, 187-92 (1997).
10. Bonangelino, C.J. et al. Osmotic stress-induced increase of phosphatidylinositol 3,5-bisphosphate requires Vac14p, an activator of the lipid kinase Fab1p. *J Cell Biol* **156**, 1015-28 (2002).
11. Wang, Y.X., Kauffman, E.J., Duex, J.E. & Weisman, L.S. Fusion of docked membranes requires the armadillo repeat protein Vac8p. *J Biol Chem* **276**, 35133-40 (2001).
12. Jones, H.D., Schliwa, M. & Drubin, D.G. Video microscopy of organelle inheritance and motility in budding yeast. *Cell Motil Cytoskeleton* **25**, 129-42 (1993).
13. Weisman, L.S., Bacallao, R. & Wickner, W. Multiple methods of visualizing the yeast vacuole permit evaluation of its morphology and inheritance during the cell cycle. *J Cell Biol* **105**, 1539-47 (1987).
14. Weisman, L.S. Yeast vacuole inheritance and dynamics. *Annu Rev Genet* **37**, 435-60 (2003).
15. Vida, T.A. & Emr, S.D. A new vital stain for visualizing vacuolar membrane dynamics and endocytosis in yeast. *J Cell Biol* **128**, 779-92 (1995).
16. Seeley, E.S., Kato, M., Margolis, N., Wickner, W. & Eitzen, G. Genomic analysis of homotypic vacuole fusion. *Mol Biol Cell* **13**, 782-94 (2002).
17. Wickner, W. Yeast vacuoles and membrane fusion pathways. *Embo J* **21**, 1241-7 (2002).
18. Raymond, C.K., O'Hara, P.J., Eichinger, G., Rothman, J.H. & Stevens, T.H. Molecular analysis of the yeast VPS3 gene and the role of its product

- in vacuolar protein sorting and vacuolar segregation during the cell cycle. *J Cell Biol* **111**, 877-92 (1990).
19. Gomes de Mesquita, D.S., van den Hazel, H.B., Bouwman, J. & Woldringh, C.L. Characterization of new vacuolar segregation mutants, isolated by screening for loss of proteinase B self-activation. *Eur J Cell Biol* **71**, 237-47 (1996).
 20. Tang, F. et al. Regulated degradation of a class V myosin receptor directs movement of the yeast vacuole. *Nature* (2003).
 21. Catlett, N.L., Duex, J.E., Tang, F. & Weisman, L.S. Two distinct regions in a yeast myosin-V tail domain are required for the movement of different cargoes. *J Cell Biol* **150**, 513-26 (2000).
 22. Wang, Y.X. et al. Multiple classes of yeast mutants are defective in vacuole partitioning yet target vacuole proteins correctly. *Mol Biol Cell* **7**, 1375-89 (1996).
 23. Catlett, N.L. & Weisman, L.S. The terminal tail region of a yeast myosin-V mediates its attachment to vacuole membranes and sites of polarized growth. *Proc Natl Acad Sci U S A* **95**, 14799-804 (1998).
 24. Hill, K.L., Catlett, N.L. & Weisman, L.S. Actin and myosin function in directed vacuole movement during cell division in *Saccharomyces cerevisiae*. *J Cell Biol* **135**, 1535-49 (1996).
 25. Wang, Y.X., Catlett, N.L. & Weisman, L.S. Vac8p, a vacuolar protein with armadillo repeats, functions in both vacuole inheritance and protein targeting from the cytoplasm to vacuole. *J Cell Biol* **140**, 1063-74 (1998).
 26. Catlett, N.L. & Weisman, L.S. Divide and multiply: organelle partitioning in yeast. *Curr Opin Cell Biol* **12**, 509-16 (2000).
 27. Ishikawa, K. et al. Identification of an organelle-specific myosin V receptor. *J Cell Biol* **160**, 887-97 (2003).
 28. Nicolson, T.A., Weisman, L.S., Payne, G.S. & Wickner, W.T. A truncated form of the Pho80 cyclin redirects the Pho85 kinase to disrupt vacuole inheritance in *S. cerevisiae*. *J Cell Biol* **130**, 835-45 (1995).
 29. Yamamoto, A. et al. Novel PI(4)P 5-kinase homologue, Fab1p, essential for normal vacuole function and morphology in yeast. *Mol Biol Cell* **6**, 525-39 (1995).
 30. Bonangelino, C.J., Catlett, N.L. & Weisman, L.S. Vac7p, a novel vacuolar protein, is required for normal vacuole inheritance and morphology. *Mol Cell Biol* **17**, 6847-58 (1997).
 31. Gary, J.D., Wurmser, A.E., Bonangelino, C.J., Weisman, L.S. & Emr, S.D. Fab1p is essential for PtdIns(3)P 5-kinase activity and the maintenance of vacuolar size and membrane homeostasis. *J Cell Biol* **143**, 65-79 (1998).
 32. Dove, S.K. et al. Svp1p defines a family of phosphatidylinositol 3,5-bisphosphate effectors. *Embo J* **23**, 1922-33 (2004).
 33. Herman, P.K., Stack, J.H., DeModena, J.A. & Emr, S.D. A novel protein kinase homolog essential for protein sorting to the yeast lysosome-like vacuole. *Cell* **64**, 425-37 (1991).

34. Herman, P.K. & Emr, S.D. Characterization of VPS34, a gene required for vacuolar protein sorting and vacuole segregation in *Saccharomyces cerevisiae*. *Mol Cell Biol* **10**, 6742-54 (1990).
35. Lowe, M. & Barr, F.A. Inheritance and biogenesis of organelles in the secretory pathway. *Nat Rev Mol Cell Biol* **8**, 429-39 (2007).
36. Gomes de Mesquita, D.S., ten Hoopen, R. & Woldringh, C.L. Vacuolar segregation to the bud of *Saccharomyces cerevisiae*: an analysis of morphology and timing in the cell cycle. *J Gen Microbiol* **137 (Pt 10)**, 2447-54 (1991).
37. Sutoh, K. Identification of myosin-binding sites on the actin sequence. *Biochemistry* **21**, 3654-61 (1982).
38. Desnos, C. et al. Myosin va mediates docking of secretory granules at the plasma membrane. *J Neurosci* **27**, 10636-45 (2007).
39. Pashkova, N., Catlett, N.L., Novak, J.L. & Weisman, L.S. A point mutation in the cargo-binding domain of myosin V affects its interaction with multiple cargoes. *Eukaryot Cell* **4**, 787-98 (2005).
40. Pashkova, N. et al. Myosin V attachment to cargo requires the tight association of two functional subdomains. *J Cell Biol* **168**, 359-64 (2005).
41. Pashkova, N., Jin, Y., Ramaswamy, S. & Weisman, L.S. Structural basis for myosin V discrimination between distinct cargoes. *Embo J* (2006).
42. Pan, X. & Goldfarb, D.S. YEB3/VAC8 encodes a myristylated armadillo protein of the *Saccharomyces cerevisiae* vacuolar membrane that functions in vacuole fusion and inheritance. *J Cell Sci* **111 (Pt 15)**, 2137-47 (1998).
43. Fleckenstein, D., Rohde, M., Klionsky, D.J. & Rudiger, M. Yel013p (Vac8p), an armadillo repeat protein related to plakoglobin and importin alpha is associated with the yeast vacuole membrane. *J Cell Sci* **111 (Pt 20)**, 3109-18 (1998).
44. Peng, Y., Tang, F. & Weisman, L.S. Palmitoylation plays a role in targeting Vac8p to specific membrane subdomains. *Traffic* **7**, 1378-87 (2006).
45. Subramanian, K. et al. Palmitoylation determines the function of Vac8 at the yeast vacuole. *J Cell Sci* **119**, 2477-85 (2006).
46. Pan, X. et al. Nucleus-vacuole junctions in *Saccharomyces cerevisiae* are formed through the direct interaction of Vac8p with Nvj1p. *Mol Biol Cell* **11**, 2445-57 (2000).
47. Scott, S.V. et al. Apg13p and Vac8p are part of a complex of phosphoproteins that are required for cytoplasm to vacuole targeting. *J Biol Chem* **275**, 25840-9 (2000).
48. Veit, M., Laage, R., Dietrich, L., Wang, L. & Ungermann, C. Vac8p release from the SNARE complex and its palmitoylation are coupled and essential for vacuole fusion. *Embo J* **20**, 3145-55 (2001).
49. Tang, F., Peng, Y., Nau, J.J., Kauffman, E.J. & Weisman, L.S. Vac8p, an armadillo repeat protein, coordinates vacuole inheritance with multiple vacuolar processes. *Traffic* **7**, 1368-77 (2006).

50. Spellman, P.T. et al. Comprehensive identification of cell cycle-regulated genes of the yeast *Saccharomyces cerevisiae* by microarray hybridization. *Mol Biol Cell* **9**, 3273-97 (1998).
51. Zhu, G. et al. Two yeast forkhead genes regulate the cell cycle and pseudohyphal growth. *Nature* **406**, 90-4 (2000).
52. Schu, P.V. et al. Phosphatidylinositol 3-kinase encoded by yeast VPS34 gene essential for protein sorting. *Science* **260**, 88-91 (1993).
53. Stack, J.H., Herman, P.K., Schu, P.V. & Emr, S.D. A membrane-associated complex containing the Vps15 protein kinase and the Vps34 PI 3-kinase is essential for protein sorting to the yeast lysosome-like vacuole. *Embo J* **12**, 2195-204 (1993).
54. Cooke, F.T. et al. The stress-activated phosphatidylinositol 3-phosphate 5-kinase Fab1p is essential for vacuole function in *S. cerevisiae*. *Curr Biol* **8**, 1219-22 (1998).
55. Efe, J.A., Botelho, R.J. & Emr, S.D. Atg18 regulates organelle morphology and fab1 kinase activity independent of its membrane recruitment by phosphatidylinositol 3,5-bisphosphate. *Mol Biol Cell* **18**, 4232-44 (2007).
56. LaGrassa, T.J. & Ungermann, C. The vacuolar kinase Yck3 maintains organelle fragmentation by regulating the HOPS tethering complex. *J Cell Biol* **168**, 401-14 (2005).
57. Weisman, L.S. Organelles on the move: insights from yeast vacuole inheritance. *Nat Rev Mol Cell Biol* **7**, 243-52 (2006).
58. Ito, T. et al. A comprehensive two-hybrid analysis to explore the yeast protein interactome. *Proc Natl Acad Sci U S A* **98**, 4569-74 (2001).
59. Georgakopoulos, T. et al. Functional analysis of the *Saccharomyces cerevisiae* YFR021w/YGR223c/YPL100w ORF family suggests relations to mitochondrial/peroxisomal functions and amino acid signalling pathways. *Yeast* **18**, 1155-71 (2001).
60. Efe, J.A., Botelho, R.J. & Emr, S.D. The Fab1 phosphatidylinositol kinase pathway in the regulation of vacuole morphology. *Curr Opin Cell Biol* **17**, 402-8 (2005).
61. Rudge, S.A., Anderson, D.M. & Emr, S.D. Vacuole size control: regulation of PtdIns(3,5)P₂ levels by the vacuole-associated Vac14-Fig4 complex, a PtdIns(3,5)P₂-specific phosphatase. *Mol Biol Cell* **15**, 24-36 (2004).
62. Gary, J.D. et al. Regulation of Fab1 phosphatidylinositol 3-phosphate 5-kinase pathway by Vac7 protein and Fig4, a polyphosphoinositide phosphatase family member. *Mol Biol Cell* **13**, 1238-51 (2002).
63. Conradt, B., Shaw, J., Vida, T., Emr, S. & Wickner, W. In vitro reactions of vacuole inheritance in *Saccharomyces cerevisiae*. *J Cell Biol* **119**, 1469-79 (1992).
64. Haas, A., Conradt, B. & Wickner, W. G-protein ligands inhibit in vitro reactions of vacuole inheritance. *J Cell Biol* **126**, 87-97 (1994).
65. Haas, A. & Wickner, W. Organelle inheritance in a test tube: the yeast vacuole. *Seminars in Cell & Developmental Biology* **7**, 517-24 (1996).
66. Xu, Z. & Wickner, W. Thioredoxin is required for vacuole inheritance in *Saccharomyces cerevisiae*. *J Cell Biol* **132**, 787-94 (1996).

67. Weisman, L.S. & Wickner, W. Intervacuole exchange in the yeast zygote: a new pathway in organelle communication. *Science* **241**, 589-91 (1988).
68. Hartwell, L.H. & Weinert, T.A. Checkpoints: Controls That Ensure the Order of Cell Cycle Events. *Science* **246**, 629-634 (1989).
69. Elledge, S.J. Cell cycle checkpoints: preventing an identity crisis. *Science* **274**, 1664-72 (1996).
70. Sutterlin, C., Hsu, P., Mallabiabarrena, A. & Malhotra, V. Fragmentation and dispersal of the pericentriolar Golgi complex is required for entry into mitosis in mammalian cells. *Cell* **109**, 359-69 (2002).
71. Loewen, C.J., Young, B.P., Tavassoli, S. & Levine, T.P. Inheritance of cortical ER in yeast is required for normal septin organization. *J Cell Biol* **179**, 467-83 (2007).
72. Feinstein, T.N. & Linstedt, A.D. Mitogen-activated protein kinase kinase 1-dependent Golgi unlinking occurs in G2 phase and promotes the G2/M cell cycle transition. *Mol Biol Cell* **18**, 594-604 (2007).
73. Shaul, Y.D. & Seger, R. ERK1c regulates Golgi fragmentation during mitosis. *J Cell Biol* **172**, 885-97 (2006).
74. Du, Y., Walker, L., Novick, P. & Ferro-Novick, S. Ptc1p regulates cortical ER inheritance via Slf2p. *Embo J* **25**, 4413-22 (2006).
75. Dan, I., Watanabe, N.M. & Kusumi, A. The Ste20 group kinases as regulators of MAP kinase cascades. *Trends Cell Biol* **11**, 220-30 (2001).
76. Wu, C., Lytvyn, V., Thomas, D.Y. & Leberer, E. The phosphorylation site for Ste20p-like protein kinases is essential for the function of myosin-I in yeast. *J Biol Chem* **272**, 30623-6 (1997).
77. Wu, C. et al. Activation of myosin-I by members of the Ste20p protein kinase family. *J Biol Chem* **271**, 31787-90 (1996).
78. Drogen, F. et al. Phosphorylation of the MEKK Ste11p by the PAK-like kinase Ste20p is required for MAP kinase signaling in vivo. *Curr Biol* **10**, 630-9 (2000).
79. Gulli, M.P. et al. Phosphorylation of the Cdc42 exchange factor Cdc24 by the PAK-like kinase Cla4 may regulate polarized growth in yeast. *Mol Cell* **6**, 1155-67 (2000).
80. Bose, I. et al. Assembly of scaffold-mediated complexes containing Cdc42p, the exchange factor Cdc24p, and the effector Cla4p required for cell cycle-regulated phosphorylation of Cdc24p. *J Biol Chem* **276**, 7176-86 (2001).
81. Versele, M. & Thorner, J. Septin collar formation in budding yeast requires GTP binding and direct phosphorylation by the PAK, Cla4. *J Cell Biol* **164**, 701-15 (2004).
82. Sakchaisri, K. et al. Coupling morphogenesis to mitotic entry. *Proc Natl Acad Sci U S A* **101**, 4124-9 (2004).
83. Asano, S. et al. Concerted mechanism of Swe1/Wee1 regulation by multiple kinases in budding yeast. *Embo J* **24**, 2194-204 (2005).
84. Hofken, T. & Schiebel, E. A role for cell polarity proteins in mitotic exit. *Embo J* **21**, 4851-62 (2002).

85. Seshan, A., Bardin, A.J. & Amon, A. Control of Ite1 localization by cell polarity determinants and cdc14. *Curr Biol* **12**, 2098-110 (2002).
86. Seshan, A. & Amon, A. Ras and the Rho effector Cla4 collaborate to target and anchor Ite1 at the bud cortex. *Cell Cycle* **4**, 940-6 (2005).
87. Lamson, R.E., Winters, M.J. & Pryciak, P.M. Cdc42 regulation of kinase activity and signaling by the yeast p21-activated kinase Ste20. *Mol Cell Biol* **22**, 2939-51 (2002).
88. Benton, B.K., Tinkelenberg, A., Gonzalez, I. & Cross, F.R. Cla4p, a *Saccharomyces cerevisiae* Cdc42p-activated kinase involved in cytokinesis, is activated at mitosis. *Mol Cell Biol* **17**, 5067-76 (1997).
89. Bokoch, G.M. Biology of the p21-Activated Kinases. *Annu Rev Biochem* (2003).
90. Simon, M.N. et al. Role for the Rho-family GTPase Cdc42 in yeast mating-pheromone signal pathway. *Nature* **376**, 702-5 (1995).
91. Cvrckova, F., De Virgilio, C., Manser, E., Pringle, J.R. & Nasmyth, K. Ste20-like protein kinases are required for normal localization of cell growth and for cytokinesis in budding yeast. *Genes Dev* **9**, 1817-30 (1995).
92. Leeuw, T. et al. Pheromone response in yeast: association of Bem1p with proteins of the MAP kinase cascade and actin. *Science* **270**, 1210-3 (1995).
93. Peterson, J. et al. Interactions between the bud emergence proteins Bem1p and Bem2p and Rho-type GTPases in yeast. *J Cell Biol* **127**, 1395-406 (1994).
94. Ito, T., Matsui, Y., Ago, T., Ota, K. & Sumimoto, H. Novel modular domain PB1 recognizes PC motif to mediate functional protein-protein interactions. *Embo J* **20**, 3938-46 (2001).
95. Yamaguchi, Y., Ota, K. & Ito, T. A novel Cdc42-interacting domain of the yeast polarity establishment protein Bem1. Implications for modulation of mating pheromone signaling. *J Biol Chem* **282**, 29-38 (2007).
96. Winters, M.J. & Pryciak, P.M. Interaction with the SH3 domain protein Bem1 regulates signaling by the *Saccharomyces cerevisiae* p21-activated kinase Ste20. *Mol Cell Biol* **25**, 2177-90 (2005).
97. Holly, S.P. & Blumer, K.J. PAK-family kinases regulate cell and actin polarization throughout the cell cycle of *Saccharomyces cerevisiae*. *J Cell Biol* **147**, 845-56 (1999).
98. Huh, W.K. et al. Global analysis of protein localization in budding yeast. *Nature* **425**, 686-91 (2003).
99. Peter, M., Neiman, A.M., Park, H.O., van Lohuizen, M. & Herskowitz, I. Functional analysis of the interaction between the small GTP binding protein Cdc42 and the Ste20 protein kinase in yeast. *Embo J* **15**, 7046-59 (1996).
100. Yu, J.W. et al. Genome-wide analysis of membrane targeting by *S. cerevisiae* pleckstrin homology domains. *Mol Cell* **13**, 677-88 (2004).
101. Wild, A.C., Yu, J.W., Lemmon, M.A. & Blumer, K.J. The p21-activated protein kinase-related kinase Cla4 is a coincidence detector of signaling

- by Cdc42 and phosphatidylinositol 4-phosphate. *J Biol Chem* **279**, 17101-10 (2004).
102. Takahashi, S. & Pryciak, P.M. Identification of novel membrane-binding domains in multiple yeast Cdc42 effectors. *Mol Biol Cell* **18**, 4945-56 (2007).
 103. Leberer, E., Dignard, D., Marcus, D., Thomas, D.Y. & Whiteway, M. The protein kinase homologue Ste20p is required to link the yeast pheromone response G-protein beta gamma subunits to downstream signalling components. *Embo J* **11**, 4815-24 (1992).
 104. Leeuw, T. et al. Interaction of a G-protein beta-subunit with a conserved sequence in Ste20/PAK family protein kinases. *Nature* **391**, 191-5 (1998).
 105. Elion, E.A. Pheromone response, mating and cell biology. *Curr Opin Microbiol* **3**, 573-81 (2000).
 106. Lyons, D.M., Mahanty, S.K., Choi, K.Y., Manandhar, M. & Elion, E.A. The SH3-domain protein Bem1 coordinates mitogen-activated protein kinase cascade activation with cell cycle control in *Saccharomyces cerevisiae*. *Mol Cell Biol* **16**, 4095-106 (1996).
 107. Heinrich, M., Kohler, T. & Mosch, H.U. Role of Cdc42-Cla4 interaction in the pheromone response of *Saccharomyces cerevisiae*. *Eukaryot Cell* **6**, 317-27 (2007).
 108. Rua, D., Tobe, B.T. & Kron, S.J. Cell cycle control of yeast filamentous growth. *Curr Opin Microbiol* **4**, 720-7 (2001).
 109. Hohmann, S., Krantz, M. & Nordlander, B. Yeast osmoregulation. *Methods Enzymol* **428**, 29-45 (2007).
 110. Tatebayashi, K. et al. Adaptor functions of Cdc42, Ste50, and Sho1 in the yeast osmoregulatory HOG MAPK pathway. *Embo J* **25**, 3033-44 (2006).
 111. Clotet, J. et al. Phosphorylation of Hsl1 by Hog1 leads to a G2 arrest essential for cell survival at high osmolarity. *Embo J* **25**, 2338-46 (2006).
 112. Adams, A.E., Johnson, D.I., Longnecker, R.M., Sloat, B.F. & Pringle, J.R. CDC42 and CDC43, two additional genes involved in budding and the establishment of cell polarity in the yeast *Saccharomyces cerevisiae*. *J Cell Biol* **111**, 131-42 (1990).
 113. Sloat, B.F. & Pringle, J.R. A mutant of yeast defective in cellular morphogenesis. *Science* **200**, 1171-3 (1978).
 114. Nern, A. & Arkowitz, R.A. Nucleocytoplasmic shuttling of the Cdc42p exchange factor Cdc24p. *J Cell Biol* **148**, 1115-22 (2000).
 115. Shimada, Y., Gulli, M.P. & Peter, M. Nuclear sequestration of the exchange factor Cdc24 by Far1 regulates cell polarity during yeast mating. *Nat Cell Biol* **2**, 117-24 (2000).
 116. Gulli, M.P. & Peter, M. Temporal and spatial regulation of Rho-type guanine-nucleotide exchange factors: the yeast perspective. *Genes Dev* **15**, 365-79 (2001).
 117. Butty, A.C. et al. A positive feedback loop stabilizes the guanine-nucleotide exchange factor Cdc24 at sites of polarization. *Embo J* **21**, 1565-76 (2002).

118. Weiss, E.L., Bishop, A.C., Shokat, K.M. & Drubin, D.G. Chemical genetic analysis of the budding-yeast p21-activated kinase Cla4p. *Nat Cell Biol* **2**, 677-85 (2000).
119. Chiroli, E. et al. Budding yeast PAK kinases regulate mitotic exit by two different mechanisms. *J Cell Biol* **160**, 857-74 (2003).
120. Tedrick, K., Trischuk, T., Lehner, R. & Eitzen, G. Enhanced membrane fusion in sterol-enriched vacuoles bypasses the Vrp1p requirement. *Mol Biol Cell* **15**, 4609-21 (2004).
121. Isgandarova, S. et al. Stimulation of actin polymerization by vacuoles via Cdc42p-dependent signaling. *J Biol Chem* **282**, 30466-75 (2007).
122. Eitzen, G., Wang, L., Thorngren, N. & Wickner, W. Remodeling of organelle-bound actin is required for yeast vacuole fusion. *J Cell Biol* **158**, 669-79 (2002).
123. Eitzen, G., Will, E., Gallwitz, D., Haas, A. & Wickner, W. Sequential action of two GTPases to promote vacuole docking and fusion. *Embo J* **19**, 6713-20 (2000).
124. Muller, O., Johnson, D.I. & Mayer, A. Cdc42p functions at the docking stage of yeast vacuole membrane fusion. *Embo J* **20**, 5657-65 (2001).
125. Winter, D., Lechler, T. & Li, R. Activation of the yeast Arp2/3 complex by Bee1p, a WASP-family protein. *Curr Biol* **9**, 501-4 (1999).
126. Lechler, T., Shevchenko, A. & Li, R. Direct involvement of yeast type I myosins in Cdc42-dependent actin polymerization. *J Cell Biol* **148**, 363-73 (2000).
127. Evangelista, M. et al. A role for myosin-I in actin assembly through interactions with Vrp1p, Bee1p, and the Arp2/3 complex. *J Cell Biol* **148**, 353-62 (2000).
128. Hofmann, C., Shepelev, M. & Chernoff, J. The genetics of Pak. *J Cell Sci* **117**, 4343-54 (2004).
129. Versele, M. & Thorner, J. Some assembly required: yeast septins provide the instruction manual. *Trends Cell Biol* **15**, 414-24 (2005).
130. Caviston, J.P., Longtine, M., Pringle, J.R. & Bi, E. The role of Cdc42p GTPase-activating proteins in assembly of the septin ring in yeast. *Mol Biol Cell* **14**, 4051-66 (2003).
131. Dobbelaere, J., Gentry, M.S., Hallberg, R.L. & Barral, Y. Phosphorylation-dependent regulation of septin dynamics during the cell cycle. *Dev Cell* **4**, 345-57 (2003).
132. Kadota, J., Yamamoto, T., Yoshiuchi, S., Bi, E. & Tanaka, K. Septin ring assembly requires concerted action of polarisome components, a PAK kinase Cla4p, and the actin cytoskeleton in *Saccharomyces cerevisiae*. *Mol Biol Cell* **15**, 5329-45 (2004).
133. Keaton, M.A. & Lew, D.J. Eavesdropping on the cytoskeleton: progress and controversy in the yeast morphogenesis checkpoint. *Curr Opin Microbiol* **9**, 540-6 (2006).
134. Booher, R.N., Deshaies, R.J. & Kirschner, M.W. Properties of *Saccharomyces cerevisiae* wee1 and its differential regulation of p34CDC28 in response to G1 and G2 cyclins. *Embo J* **12**, 3417-26 (1993).

135. Longtine, M.S. et al. Septin-dependent assembly of a cell cycle-regulatory module in *Saccharomyces cerevisiae*. *Mol Cell Biol* **20**, 4049-61 (2000).
136. Shulewitz, M.J., Inouye, C.J. & Thorner, J. Hsl7 localizes to a septin ring and serves as an adapter in a regulatory pathway that relieves tyrosine phosphorylation of Cdc28 protein kinase in *Saccharomyces cerevisiae*. *Mol Cell Biol* **19**, 7123-37 (1999).
137. McMillan, J.N. et al. The morphogenesis checkpoint in *Saccharomyces cerevisiae*: cell cycle control of Swe1p degradation by Hsl1p and Hsl7p. *Mol Cell Biol* **19**, 6929-39 (1999).
138. Barral, Y., Parra, M., Bidlingmaier, S. & Snyder, M. Nim1-related kinases coordinate cell cycle progression with the organization of the peripheral cytoskeleton in yeast. *Genes Dev* **13**, 176-87 (1999).
139. Cid, V.J., Shulewitz, M.J., McDonald, K.L. & Thorner, J. Dynamic localization of the Swe1 regulator Hsl7 during the *Saccharomyces cerevisiae* cell cycle. *Mol Biol Cell* **12**, 1645-69 (2001).
140. Lew, D.J. The morphogenesis checkpoint: how yeast cells watch their figures. *Curr Opin Cell Biol* **15**, 648-53 (2003).
141. Richman, T.J., Sawyer, M.M. & Johnson, D.I. The Cdc42p GTPase is involved in a G2/M morphogenetic checkpoint regulating the apical-isotropic switch and nuclear division in yeast. *J Biol Chem* **274**, 16861-70 (1999).
142. Bartholomew, C.R., Woo, S.H., Chung, Y.S., Jones, C. & Hardy, C.F. Cdc5 interacts with the Wee1 kinase in budding yeast. *Mol Cell Biol* **21**, 4949-59 (2001).
143. Stegmeier, F. & Amon, A. Closing mitosis: the functions of the Cdc14 phosphatase and its regulation. *Annu Rev Genet* **38**, 203-32 (2004).
144. Ostrowicz, C.W., Meiringer, C.T. & Ungermann, C. Yeast vacuole fusion: a model system for eukaryotic endomembrane dynamics. *Autophagy* **4**, 5-19 (2008).
145. Eitzen, G., Thorngren, N. & Wickner, W. Rho1p and Cdc42p act after Ypt7p to regulate vacuole docking. *Embo J* **20**, 5650-6 (2001).
146. Eitzen, G. Actin remodeling to facilitate membrane fusion. *Biochim Biophys Acta* **1641**, 175-81 (2003).
147. Han, B.K. et al. Bem1p, a scaffold signaling protein, mediates cyclin-dependent control of vacuolar homeostasis in *Saccharomyces cerevisiae*. *Genes Dev* **19**, 2606-18 (2005).
148. Xu, H. & Wickner, W. Bem1p is a positive regulator of the homotypic fusion of yeast vacuoles. *J Biol Chem* **281**, 27158-66 (2006).

CHAPTER II

BOI1 AND BOI2 REGULATE VACUOLE INHERITANCE.

Abstract

Each time eukaryotic cells divide, they ensure that each of the progeny cells receives a full complement of organelles. The budding yeast vacuole (lysosome) fissions to form a tubular-vesicular structure called the “segregation structure” which is transported along actin cables by myosin into the bud. Upon entering the bud the segregation structure is resolved, probably by fusion of the tubules and vesicles, to form a discrete daughter vacuole. The machinery ensuring the resolution of the segregation structure in a spatially dependent manner, specifically in the bud, has not been identified. Boi1 and Boi2 are a pair of functionally redundant proteins that localize to the bud cortex. *boi1 boi2* mutant cells were found to be defective for vacuole inheritance. The *boi1 boi2* vacuole inheritance defect was dependent on the presence of the p21-activated kinases, Cla4 and Ste20. These results suggested a model in which Boi1 and Boi2 negatively regulate Cla4 and Ste20 insuring they are only active in the bud where they potentially act as daughter-specific factors to provide spatial regulation of vacuole inheritance.

Introduction

Under normal physiological conditions the yeast vacuole is a low-copy number organelle containing on average 1-3 lobes and requires ordered transport to ensure its inheritance by the daughter cell ¹. At the time of bud emergence, proteins necessary for PtdIns(3,5)P₂ production are required to form the tubular and vesicular structure called the segregation structure ^{2, 3}. Transport of the segregation structure into the bud requires attachment of the vacuole to the myosin V motor Myo2 ⁴⁻⁶. Attachment between the vacuole and myosin requires the vacuole-specific Myo2 receptor Vac17. Vac17 binds both Myo2 and Vac8 directly and is degraded after transport into the bud thus providing directionality to the transport process ^{7, 8}. Vac8 is myristoylated and palmitoylated and is inserted into the vacuole membrane ^{9, 10}. Once attached to myosin, vacuoles, like most of the organelles in budding yeast, are transported into the bud along polarized actin cables ¹¹⁻¹⁶. Upon entering the bud, the segregation structure is resolved, probably by fusion of the tubules and vesicles, to form the daughter vacuole ¹⁷⁻²¹.

While the machinery necessary for the formation and transport of the segregation structure has been identified, the machinery regulating segregation structure resolution in a spatially dependent manner has not been identified. The fusion of tubules and vesicles leading to the formation of a separate daughter vacuole does not take place until after entering the bud. What restricts fusion to the bud? How Vac17 is degraded in a bud-specific manner is unknown. It has

been hypothesized that the bud specific degradation of Vac17 is promoted by factors specifically localized to the bud ²². However, these factors have not been identified. Similarly, I hypothesized that factors promoting vacuole fusion were specifically localized to the bud, thus creating spatial regulation of segregation structure resolution. In support of this hypothesis I identified Boi1 and Boi2 as factors localized to the bud. Double mutant *boi1 boi2* cells have a vacuole inheritance defect. The *boi1 boi2* vacuole inheritance defect was dependent on the p21-activated kinases Cla4 and Ste20.

Vacuole inheritance requires transport along polarized actin cables. Actin cable formation requires the Rho-like GTPase Cdc42 activated by the guanine nucleotide exchange factor (GEF) Cdc24 ^{23, 24}. Cdc24 is brought into contact with Cdc42 by its direct interaction with the scaffolding protein Bem1 ^{25, 26}. Bem1 also binds the p21-activated kinases Cla4 and Ste20 through Bem1's second SH3 domain ²⁷⁻³⁰. Cla4 and Ste20 are activated by Cdc42 and act as Cdc42 effectors ³⁰⁻³⁴. However, neither Cla4 nor Ste20 are required for polarization of the actin cytoskeleton, but they do promote septin organization ^{31, 35-37}.

Boi1 and Boi2 are a pair of functionally redundant proteins which also bind Bem1 on the second SH3 domain ³⁸⁻⁴⁰ and which show multiple direct and indirect protein-protein interactions with Cla4 and Ste20 ^{38, 40-42}. Cells deleted for both *BOI1* and *BOI2* grow slowly, have poor viability, and populations of *boi1 boi2* cells contain a high percentage of unbudded cells ^{38, 40}. A spontaneously faster growing *boi1 boi2* strain was isolated to further investigate the roles of Boi1 and Boi2 in living cells, as has been done previously ^{40, 43}.

Materials and Methods

Plasmid and Strain Construction

Yeast strains and sources are listed in Table 2-1. Yeast strains were constructed by genetic crosses followed by tetrad dissection or by transformation using the lithium acetate method ⁴⁴. *GFP* and the adjacent *HIS3* marker were amplified by PCR and integrated to generate *BOI1-GFP* and *BOI2-GFP* as described ^{45, 46}. Plasmid sources and construction methods are listed in Table 2-2 and DNA manipulations were performed as described ⁴⁷.

Microscopy

Digital images were taken with a 100X objective on an Olympus microscope. NIH image 1.62 (written by Wayne Rasband) was used for image acquisition. Cells were visualized by fluorescence and differential interference contrast microscopy (DIC). Within each experiment, all images were collected and scaled identically. Images were processed with Photoshop 9.0 software (Adobe). Video microscopy was performed with mid-log phase cells placed on a drop of 2% agarose in YPD flattened by an uncoated glass slide as described ⁴⁸. Cells were visualized every three to five minutes. Small, medium, and large budded cells were grouped into size categories as described ⁴⁹. Scale bar = 2.5 mm throughout all figures.

Table 2-1. Strains

Strain	Genotype	Source
BY4741	<i>MATa his3D1 leu2D0 met15D0 ura3D0</i> (S288c)	⁵⁰
Y _{CH} 463	<i>MATα BOI2-GFP-HIS3 his3 leu2 ura3</i> (S288c)	This Study
Y _{CH} 928	<i>MATα BOI1-GFP-HIS3 his3 leu2 ura3</i> (S288c)	This Study
Y _{CH} 1043	<i>MATa boi1::kanMX4 his3D1 leu2D0 met15D0 ura3D0</i> (S288c)	⁵¹
Y _{CH} 1220	<i>MATa boi1::kanMX4 boi2::URA3</i> (S288c)	This Study
Y _{CH} 1342	<i>MATa boi1::LEU2 boi2::URA3 cla4::LEU2</i> (S288c)	This Study
Y _{CH} 1478	<i>MATa vac8::kanMX4 his3D1 leu2D0 met15D0 ura3D0</i> (S288c)	⁵¹
Y _{CH} 1511	<i>MATa ste20::kanMX4 his3D1 leu2D0 met15D0 ura3D0</i> (S288c)	⁵¹
Y _{CH} 1642	<i>MATa cla4::kanMX4 his3D1 leu2D0 met15D0 ura3D0</i> (S288c)	⁵¹
Y _{CH} 1872	<i>MATa boi1::LEU2 boi2::URA3 ste20::KanMX4</i> (S288c)	This Study
Y _{CH} 1959	<i>MATa boi1::kanMX4 his3D1 leu2D0 met15D0 ura3D0</i> (S288c)	⁵¹
Y _{CH} 3576	<i>MATa pRS414-pBOI1-BOI1 boi1::kanMX4 boi2::URA3</i> (S288c)	This Study
Y _{CH} 3578	<i>MATa pRS414-pBOI1-boi1-W53K boi1::kanMX4 boi2::URA3</i> (S288c)	This Study
Y _{CH} 3580	<i>MATa pRS414-pBOI1-boi1-P7A7 boi1::kanMX4 boi2::URA3</i> (S288c)	This Study
Y _{CH} 3582	<i>MATa pRS414-pBOI1-boi1-K795A,R797A boi1::kanMX4 boi2::URA3</i> (S288c)	This Study
Y _{CH} 3584	<i>MATa pRS414-pBOI1-boi1-D5-733 boi1::kanMX4 boi2::URA3</i> (S288c)	This Study

Table 2-2. Plasmids

Plasmids	Description	Source
pCH1542	<i>pRS414-pBOI1-BOI1</i> . Made by insertion of a 4.5 kB <i>BamHI-Sall</i> fragment of pPB939 ⁵² into the <i>BamHI-Sall</i> site of pRS414 ⁵³ .	This Study
pCH1543	<i>pRS414-pBOI1-boi1-W53K</i> . Made by insertion of a 4.5 kB <i>BamHI-Sall</i> fragment of pPB952 ⁵² into the <i>BamHI-Sall</i> site of pRS414 ⁵³ .	This Study
pCH1544	<i>pRS414-pBOI1-boi1-P7A7</i> . Made by insertion of a 4.5 kB <i>BamHI-Sall</i> fragment of pPB954 ⁵² into the <i>BamHI-Sall</i> site of pRS414 ⁵³ .	This Study
pCH1545	<i>pRS414-pBOI1-boi1-K795A,R797A</i> . Made by insertion of a 4.5 kB <i>BamHI-Sall</i> fragment of pPB967 ⁵² into the <i>BamHI-Sall</i> site of pRS414 ⁵³ .	This Study
pCH1546	<i>pRS414-pBOI1-boi1D5-733</i> . Made by insertion of a 4.5 kB <i>BamHI-Sall</i> fragment of pPB1004 ⁵² into the <i>BamHI-Sall</i> site of pRS414 ⁵³ .	This Study

***In vivo* labeling of vacuoles**

To visualize vacuoles, yeast cells were concentrated and incubated for 1 hour with N-(3-triethylammoniumpropyl)-4(6(4(diethylamino)phenyl)hexatrienyl)pyridium dibromide (FM 4-64; Molecular Probes) at a final concentration of 16.5 μM ⁵⁴. Cells were then washed with appropriate media and grown for ≥ 3 hours before being viewed by fluorescence microscopy.

Other methods

YP media containing 1% yeast extract and 2% Bacto Peptone was used with addition of glucose (YPD) as a carbon source at 2% final concentration. Alternately, strains with plasmids were grown on synthetic media (SC) lacking tryptophan to maintain plasmids.

Results

Boi1 and Boi2 are inherited by the daughter cell

To determine Boi1 and Boi2 localization, *BOI1-GFP* cells and *BOI2-GFP* cells were visualized by fluorescence microscopy. Boi1-GFP and Boi2-GFP had identical localization patterns (data not shown) and only Boi2-GFP localization is presented (Figure 2-1). Boi2-GFP localized to the (I) mother-bud neck prior to separation. (II-III) Boi2-GFP then localizes to the nascent bud site of mother cells and to the cortex of buds but remained on the daughter after cell separation. (IV-VI) Boi2-GFP localized to the nascent bud site and the cortex of the bud in daughter cells and a small amount of Boi2-GFP remained at what is presumably the birth scar where it gradually disappeared as the new bud grew. These findings have been corroborated by other researchers⁵⁵. However, the daughter-specific inheritance of Boi1 and Boi2 has not been previously reported.

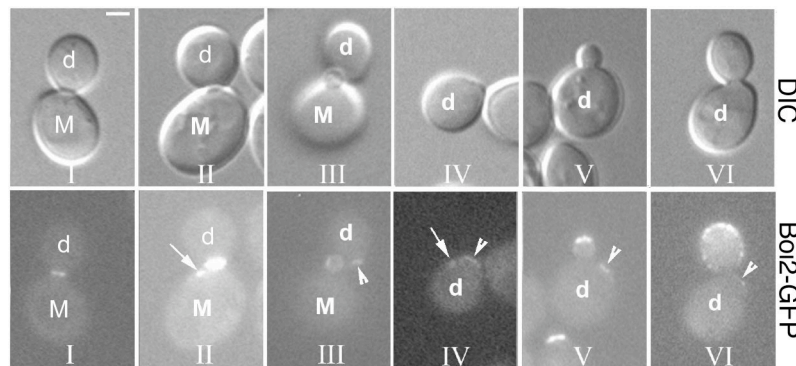


Figure 2-1. Boi2-GFP has a dynamic localization during the cell cycle and is inherited by daughter cells.

Boi2-GFP (Y_{CH463}) localization was visualized by fluorescence microscopy and representative images are shown. Arrows indicate Boi2-GFP localization to nascent bud sites and arrowheads indicate Boi2-GFP inheritance. Pedigree analysis: M (mother) d (daughter).

***boi1 boi2* mutant cells display a daughter-specific budding delay**

The daughter-specific inheritance of Boi1 and Boi2 led me to reexamine previous phenotypes of *boi1 boi2* mutant cells. Asynchronous cultures of *boi1 boi2* cells, in addition to other phenotypes, display a high proportion of unbudded cells^{38, 40}. After confirming this result (data not shown) I hypothesized that in the absence of *BOI1* and *BOI2*, daughter cells were delayed for budding and this might account for the high proportion of unbudded cells.

To test this hypothesis wild type and *boi1 boi2* cells were observed by time-lapse video microscopy. Cell division led to the production of a larger mother and a smaller daughter cell. After cell separation, wild type mother cells, which have already reached a critical size, almost immediately rebudded. However, smaller daughter cells were delayed for bud emergence an average of 42 minutes while they grew to a critical size (Figure 2-2A,C). The *boi1 boi2* mutant mother cells budded with similar kinetics to wild type mother cells. In contrast the *boi1 boi2* daughter cells were greatly delayed for bud emergence and were delayed on average 88 minutes longer than wild type daughter cells (Figure 2-2A,C). This daughter-specific budding delay suggested that there was some difference between *boi1 boi2* mother and daughter cells that led to the daughter-specific budding delay.

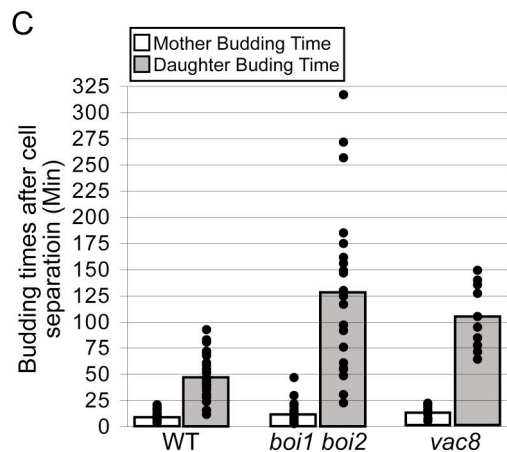
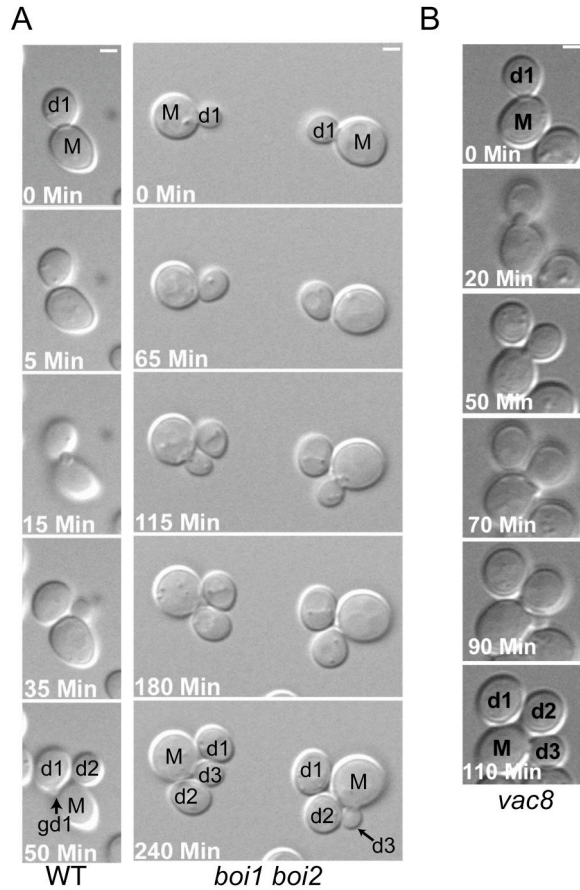


Figure 2-2. *boi1 boi2* and *vac8* cells have a daughter-specific budding delay.

(A-B) Wild type (BY4741), *boi1 boi2* (Y_{CH}1220), and *vac8* (Y_{CH}1478) cells were grown to early log phase and examined by video microscopy and pedigree analysis was performed. (C) The budding time, defined as the interval in minutes between cell separation and subsequent bud emergence for mother (light bar) and daughter (dark bar) cells, was determined. Black dots represent independent bud emergence events. Pedigree analysis: M (mother), d1-3 (primary - tertiary daughters) and gd1 (primary granddaughter).

***boi1 boi2* cells have a vacuole inheritance defect**

It has been previously shown that cells which fail to inherit a vacuole are delayed for bud emergence until daughter cells form a vacuole *de novo* and thus exhibit a daughter-specific budding delay ⁵⁶. I therefore hypothesized that vacuole inheritance mutants, when examined by time-lapse video microscopy, should have similar delays in daughter, but not mother, budding times after cell separation.

To test this hypothesis I examined a Class I vacuole inheritance mutant *vac8*. Vac8 contains 11 armadillo repeats serving in protein-protein interactions and is both myristoylated and multiply palmitoylated allowing its insertion into the vacuole membrane. At the vacuole membrane it interacts with the vacuole specific myosin receptor Vac17 enabling transport of vacuolar material into the bud ⁷⁻⁹. Examination of *vac8* mutants revealed that, similar to *boi1 boi2* mutants, *vac8* mutants have a daughter-specific budding delay and on average are delayed 65 minutes longer than wild type daughter cells (Figure 2-2B,C).

Because *vac8* cells have a daughter-specific budding delay and daughter cells bud with similar kinetics to *boi1 boi2*, I hypothesized that, like *vac8* mutants, *boi1 boi2* cells had a vacuole inheritance defect. Vacuole inheritance can be visualized by pulse chase experiment using the fluorescent dye FM 4-64 which accumulates specifically on the vacuole membrane. FM 4-64 stained vacuoles can be seen to form segregation structures which transport vacuolar material into the bud, and cells which fail to inherit a vacuole have daughter cells devoid of FM 4-64 stained vacuole membranes ⁵⁴. Pulse chase experiments were performed to

determine if *boi1 boi2* cells had a vacuole inheritance defect. Wild type and *boi1* or *boi2* single mutants formed segregation structures and 100% of large budded cells contained FM 4-64 stained vacuoles (Table 2-3). In contrast, segregation structures were only very infrequently observed in *boi1 boi2* cells and only 13% of large budded cells contained FM 4-64 stained vacuole material. Additionally, *boi1 boi2* vacuoles were frequently multilobed (Figure 2-3A).

Table 2-3. *boi1 boi2* cells have a vacuole inheritance defect dependent on *CLA4* and *STE20*.

Genotype	Vacuole Inheritance of Large Budded Cells
Wild type	100%
<i>boi1</i>	100%
<i>boi2</i>	100%
<i>ste20</i>	100%
<i>cla4</i>	100%
<i>boi1 boi2</i>	13%
<i>boi1 boi2 ste20</i>	100%
<i>boi1 boi2 cla4</i>	100%

Other yeast organelles have been reported to have cortical anchors within the bud that ensure organelle retention. Organelles in cells lacking these cortical anchors are not retained within the bud and are subsequently transported back into the mother^{57, 58}. Because *Boi1* and *Boi2* are cortically localized they could potentially be cortical anchors within the bud, and the vacuole inheritance defect I saw was solely due to a failure to retain the daughter vacuole. To assess this possibility time-lapse video microscopy was performed on FM 4-64 stained *boi1 boi2* cells and cells were examined every 5 minutes. Over the time course of the experiment vacuole inheritance structures did not form and FM 4-64 stained vacuole materials were never observed in buds (Figure 2-3C). Thus it is unlikely that *Boi1* and *Boi2* are acting, at least solely, as cortical anchors.

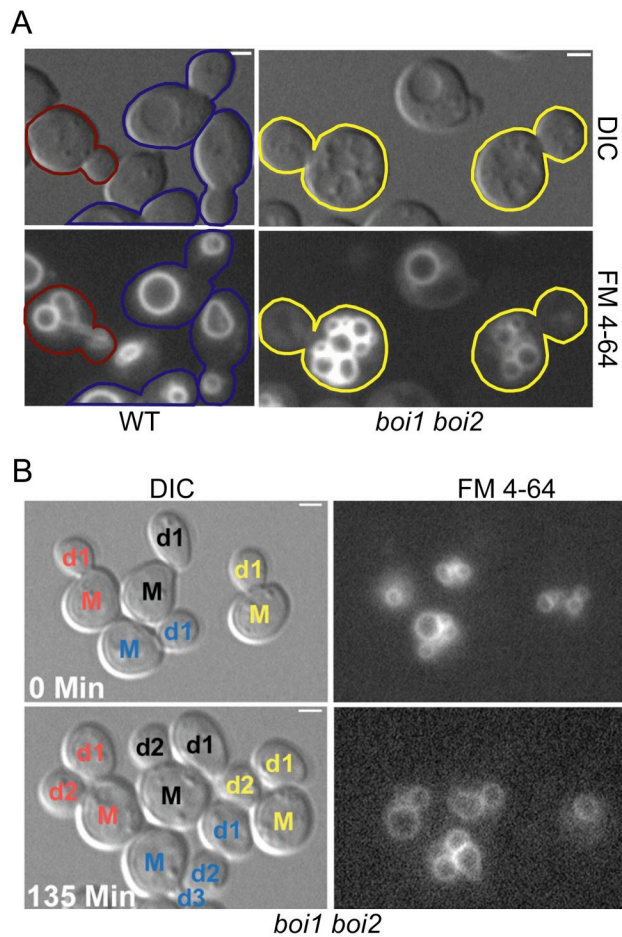


Figure 2-3. *boi1 boi2* cells have a vacuole inheritance defect.

(A) Wild type (BY4741) and *boi1 boi2* (Y_{CH}1220) strains were FM 4-64 labeled with the vacuole specific dye FM 4-64 and then observed by fluorescence microscopy. (B) Pedigree analysis was performed by video microscopy of FM 4-64 stained *boi1 boi2* (Y_{CH}1220) cells and DIC and fluorescent images are shown. Pedigree analysis: M (mother), d1-3 (primary - tertiary daughters). Min (minutes). Cell Outline Color Code, Red: bud contains segregation structure; Blue: bud has inherited vacuole material from mother cell; Yellow: medium or large bud lacking inherited vacuole material from mother cell.

***boi1 boi2* daughter-specific budding and vacuole inheritance defects are suppressed by *CLA4* or *STE20* deletion**

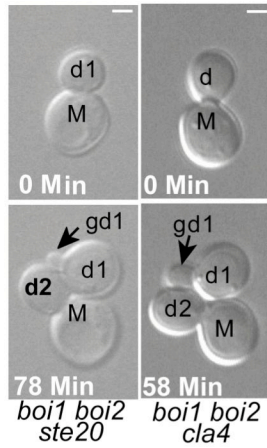
Because Boi1 and Boi2 are not known to have a catalytic function, I hypothesized that Boi1 and Boi2 effects on vacuole transport might be indirect through an interacting protein. Boi1 and Boi2 have multiple direct and indirect protein-protein interactions with the p21-activated kinases Ste20 and Cla4 in

budding yeast^{38, 40-42}. I hypothesized that Boi1 and Boi2 might negatively regulate Cla4 and or Ste20, and that in the absence of *BOI1* and *BOI2*, that Ste20 and Cla4 were overactive, or were active somewhere in the cell that they were not usually active, and therefore the PAKs were responsible for the vacuole inheritance defect.

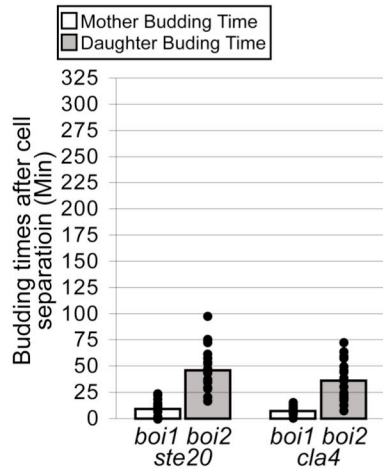
To test this model I determined if the deletion of *STE20* or *CLA4* suppressed the *boi1 boi2* daughter-specific budding delay and/or vacuole inheritance defects. Time-lapse video microscopy was performed on *boi1 boi2 ste20* and *boi1 boi2 cla4* cells (Figure 2-4A) and the elapsed time between cell separation and mother and daughter budding events was determined (Figure 2-4B). The deletion of either *STE20* or *CLA4* fully suppressed the *boi1 boi2* daughter-specific budding delay.

In addition I determined if the deletion of *STE20* or *CLA4* suppressed the *boi1 boi2* vacuole inheritance defect. Mutant *boi1 boi2 ste20* and *boi1 boi2 cla4* cells were FM 4-64 stained and examined by fluorescence microscopy. Segregation structures were common in these strains (Figure 2-4C) and 100% of large budded cells contained a daughter vacuole (Table 2-3). As expected *ste20* and *cla4* cells did not have a vacuole inheritance defects (Table 2-3). Thus I conclude that *CLA4* and *STE20* are required for the *boi1 boi2* daughter-specific budding delay and vacuole inheritance defect.

A



B



C

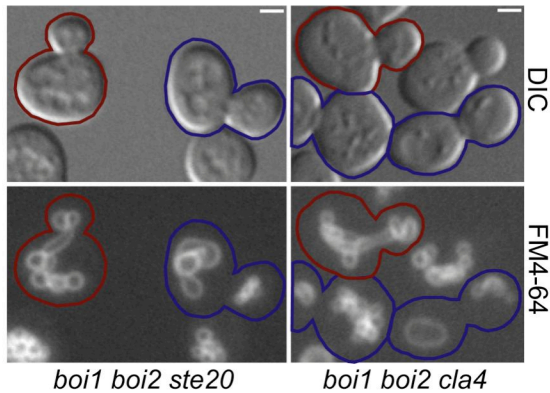


Figure 2-4. *boi1 boi2* daughter-specific budding delay and vacuole inheritance defects are suppressed by *CLA4* or *STE20* deletion.

(A-B) *boi1 boi2 ste20* (Y_{CH}1872) and *boi1 boi2 cla4* (Y_{CH}1342) cells were grown to early log phase and examined by video microscopy. The average budding time, defined as the interval in minutes between cell separation and subsequent bud emergence for mother (light bar) and daughter (dark bar) cells, was determined. Black dots represent independent bud emergence events. (C) Strains in A were FM 4-64 labeled with the vacuole specific dye FM 4-64 and then observed by fluorescence microscopy. Pedigree analysis: M (mother), d1-2 (primary - secondary daughters) and gd1 (primary granddaughter). Min. (minutes). Cell Outline Color Code, Red: bud contains segregation structure; Blue: bud has inherited vacuole material from mother cell; Yellow: medium or large bud lacking inherited vacuole material from mother cell.

The PH domain of Boi1 is required for vacuole inheritance

Finally, in hopes of further elucidating how Boi1 and Boi2 regulated vacuole inheritance, I determined what portion of Boi1 was necessary for vacuole inheritance. Boi1 and Boi2 contain an SH3 domain, a proline-rich domain, and a PH domain. To determine the region necessary for vacuole inheritance *boi1 boi2* cells were transformed with plasmids containing full length *BOI1* (*pBOI1*), *BOI1* with a specific mutation in the coding sequence for the SH3 domain which coding for a conserved tryptophan codon (*pboi1-W53K*), *BOI1* with mutations in seven of the nine prolines in the proline-rich domain changed to alanines (*pboi1-P7A7*), *BOI1* containing only the coding sequence for the PH domain and the C-terminus of the protein (*pboi1D5-733*), and full length *BOI1* with mutations in the PH domain coding sequence which disrupt the PH domain of other PH domain containing proteins^{40, 55}.

Vacuole inheritance was examined by FM 4-64 straining. Cells transformed with plasmids contained wild type *BOI1*, *BOI1* with SH3 domain or proline-rich domains mutations, and the PH domain alone all inherited vacuoles (Figure 2-5). In contrast, cells transformed with a *BOI1* containing plasmids with mutations affecting the PH domain alone were not able to restore vacuole inheritance. Taken together this data suggests that the SH3 and proline-rich domains of Boi1 are not required for vacuole inheritance, but an active PH domain is required for vacuole inheritance in cells lacking *BOI2*.

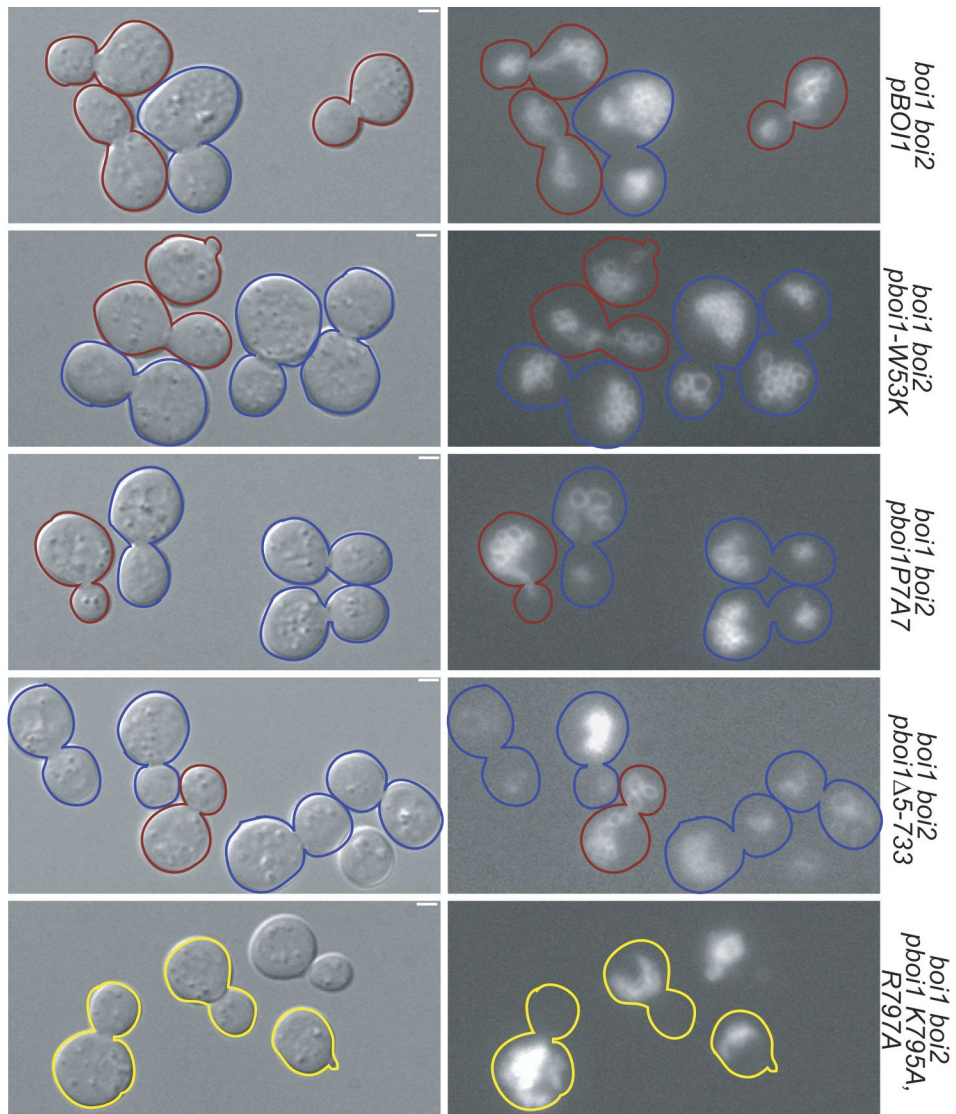


Figure 2-5. The PH domain of Boi1 is required for vacuole inheritance in the absence of *BOI2*.

Asynchronous cultures of FM 4-64 stained *boi1 boi2 pBOI1* (Y_{CH}3576), *boi1 boi2 pboi1-W53K* (Y_{CH}3578), *boi1 boi2 pboi1-P7A7* (Y_{CH}3580), *boi1 boi2 pboi1-D5-733* (Y_{CH}3584), and *boi1 boi2 pboi1-K795A,R797A* (Y_{CH}3582) were examined by fluorescence microscopy, and representative pictures are shown. Cell Outline Color Code, Red: bud contains segregation structure; Blue: bud has inherited vacuole material from mother cell; Yellow: medium or large bud lacking inherited vacuole material from mother cell.

Discussion

I here report that *boi1 boi2* mutants display a vacuole partitioning defect. Previously vacuole partitioning mutants have been classified into three classes based on vacuole morphology and transport. Class I mutants contain multilobed vacuoles and fail to form a segregation structure or transport any vacuole material into the bud. Class II mutants have moderately enlarged vacuoles and often have a node on the vacuole oriented towards the bud. Class III mutants fail to form lobes, contain a single highly enlarged vacuole and fail to form a segregation structure; but they do partition a portion of the vacuole into the daughter. Based on its vacuole morphology and failure to inherit I propose that *boi1 boi2* is a Class I *vac* mutant.

All of Class I *vac* mutants for which the corresponding gene has been identified identify components of the physical machinery necessary for transport of the vacuole into the bud, such as actin, profillin, and the vacuole transport complex (Myo2, Vac8, and Vac17). Currently there are no known Class I mutants identified that regulate the transport process. I propose Boi1 and Boi2 as the first Class I vacuole partitioning mutants that play a role in regulating vacuole inheritance. In support of this proposal I found that deletion of *CLA4* or *STE20* suppressed both the daughter-specific budding delay and the vacuole partitioning defect of *boi1 boi2* cells. Therefore, it is unlikely that, like other Class I *vac* mutant, Boi1 and Boi2 are part of the physical machinery necessary for vacuole inheritance.

How do Boi1 and Boi2 regulate vacuole inheritance? Boi1 and Boi2 show multiple direct and indirect interactions with Cla4 and Ste20 as assayed by either two-hybrid or coimmunoprecipitation^{38, 40-42}. Cla4 and Ste20 are autoinhibitory and only become active by binding activated GTP-Cdc42^{31, 33, 59-61}. Cla4 and Ste20 activation is facilitated by binding of the proline-rich domain in Cla4 and Ste20 to the second SH3 domain of the adaptor protein Bem1²⁸⁻³⁰. Bem1 also binds to Cdc42 and its GEF Cdc24, thus bringing together GTP-Cdc42 with its effectors Cla4 and Ste20⁶²⁻⁶⁵. Importantly Boi1 and Boi2 also bind to the second SH3 domain of Bem1³⁸⁻⁴⁰ and therefore could potentially negatively regulate Cla4 and Ste20 by competitive inhibition of PAKs for access to Bem1. In this model the vacuole inheritance defect in *boi1 boi2* cells would be caused by overactive PAKs in the bud. I do not favor such a model since *boi1 boi2* cells expressing plasmid born *BOI1* lacking the proline-rich domain necessary for Bem1 binding do not exhibit a vacuole inheritance defect (Figure 2-5).

While *boi1 boi2 pboi1-P7A7* cells did not have a vacuole inheritance defect, I found that *boi1 boi2* cells with *boi1* covered by a plasmid expressing *BOI1* with a mutation in the PH domain or *BOI1* containing only the PH domain and the C-terminus of the protein did not suppress and suppressed respectively the *boi1 boi2* vacuole inheritance defect (Figure 2-5). How does the PH domain alone act to regulate vacuole inheritance? PH domains bind phosphatidylinositides and are the 11th most common domain in the human genome. Studies examining the PH domain of all 33 proteins in yeast showed that most PH domains, including the PH domains of Boi1 and Boi2, have little

specificity towards different phosphatidylinositide species and usually bound with very low affinity⁶⁶. However, a growing number of examples indicate that PH domains also bind to activated small GTPases and specifically to Rho type GTPases, of which Cdc42 is a member⁶⁷⁻⁷². In support of this possibility, Bender *et al.* show that the PH domain of Boi1 interacts with GTP but not GDP bound Cdc42. Additionally, the overexpression of the PH domain and C-terminus of Boi1 inhibits bud emergence and this defect is suppressed by co-overexpression of *CDC42*⁴⁰. Thus Boi1 and Boi2 may negatively regulate PAKs by directly interacting with Cdc42 and either negatively regulating Cdc42 or more likely restricting access to Cdc42.

Formation of the tubular and vesicular segregation structure requires PtdIns(3,5)P₂. Cells defective for PtdIns(3,5)P₂ production have one contiguous vacuole stretched from the mother into the bud that is constricted at the neck^{2,73}. PtdIns(3,5)P₂ is produced in response to hyperosmotic shock and leads to vacuole fission, thus leading researchers to hypothesize that the segregation structure is formed using the fission machinery^{3, 5, 22}. In addition to fission, efficient segregation structure formation also requires the inhibition of fusion²¹.

How then might deletion of *Boi1* and *Boi2* prevent segregation structure formation? Cdc42 and Bem1 localize to the vacuole and promote homotypic vacuole fusion *in vitro* and *in vivo*⁷⁴⁻⁷⁷. Cla4 is found on isolated vacuoles and *cla4* mutants have a vacuole fusion defect *in vivo*^{1, 78}. Therefore, I suggest that Boi1 and Boi2 negatively regulate Cla4 and Ste20 by restricting access of PAKs to Cdc42. In *boi1 boi2* cells residual Cla4 and Ste20 in the mother cell may bind

Cdc24 on the vacuole promoting vacuole fusion thus inhibiting vacuole segregation structure formation. Deletion of either *CLA4* or *STE20* suppresses the *boi1 boi2* vacuole inheritance defect. This suggests that Cla4 and Ste20 are required for vacuole fusion and that Cla4 and Ste20 likely have an additive or synergistic affect on vacuole fusion.

References

1. Seeley, E.S., Kato, M., Margolis, N., Wickner, W. & Eitzen, G. Genomic analysis of homotypic vacuole fusion. *Mol Biol Cell* **13**, 782-94 (2002).
2. Bonangelino, C.J., Catlett, N.L. & Weisman, L.S. Vac7p, a novel vacuolar protein, is required for normal vacuole inheritance and morphology. *Mol Cell Biol* **17**, 6847-58 (1997).
3. Bonangelino, C.J. et al. Osmotic stress-induced increase of phosphatidylinositol 3,5-bisphosphate requires Vac14p, an activator of the lipid kinase Fab1p. *J Cell Biol* **156**, 1015-28 (2002).
4. Catlett, N.L. & Weisman, L.S. The terminal tail region of a yeast myosin-V mediates its attachment to vacuole membranes and sites of polarized growth. *Proc Natl Acad Sci U S A* **95**, 14799-804 (1998).
5. Catlett, N.L. & Weisman, L.S. Divide and multiply: organelle partitioning in yeast. *Curr Opin Cell Biol* **12**, 509-16 (2000).
6. Hill, K.L., Catlett, N.L. & Weisman, L.S. Actin and myosin function in directed vacuole movement during cell division in *Saccharomyces cerevisiae*. *J Cell Biol* **135**, 1535-49 (1996).
7. Tang, F. et al. Regulated degradation of a class V myosin receptor directs movement of the yeast vacuole. *Nature* (2003).
8. Ishikawa, K. et al. Identification of an organelle-specific myosin V receptor. *J Cell Biol* **160**, 887-97 (2003).
9. Wang, Y.X., Catlett, N.L. & Weisman, L.S. Vac8p, a vacuolar protein with armadillo repeats, functions in both vacuole inheritance and protein targeting from the cytoplasm to vacuole. *J Cell Biol* **140**, 1063-74 (1998).
10. Pan, X. & Goldfarb, D.S. YEB3/VAC8 encodes a myristylated armadillo protein of the *Saccharomyces cerevisiae* vacuolar membrane that functions in vacuole fusion and inheritance. *J Cell Sci* **111 (Pt 15)**, 2137-47 (1998).
11. Lowe, M. & Barr, F.A. Inheritance and biogenesis of organelles in the secretory pathway. *Nat Rev Mol Cell Biol* **8**, 429-39 (2007).
12. Fagarasanu, M., Fagarasanu, A. & Rachubinski, R.A. Sharing the wealth: peroxisome inheritance in budding yeast. *Biochim Biophys Acta* **1763**, 1669-77 (2006).
13. Barr, F.A. Inheritance of the endoplasmic reticulum and Golgi apparatus. *Curr Opin Cell Biol* **14**, 496-9 (2002).
14. Weisman, L.S. Organelles on the move: insights from yeast vacuole inheritance. *Nat Rev Mol Cell Biol* **7**, 243-52 (2006).
15. Boldogh, I.R., Fehrenbacher, K.L., Yang, H.C. & Pon, L.A. Mitochondrial movement and inheritance in budding yeast. *Gene* **354**, 28-36 (2005).
16. Bretscher, A. Polarized growth and organelle segregation in yeast: the tracks, motors, and receptors. *J Cell Biol* **160**, 811-6 (2003).
17. Conradt, B., Shaw, J., Vida, T., Emr, S. & Wickner, W. In vitro reactions of vacuole inheritance in *Saccharomyces cerevisiae*. *J Cell Biol* **119**, 1469-79 (1992).

18. Haas, A., Conradt, B. & Wickner, W. G-protein ligands inhibit in vitro reactions of vacuole inheritance. *J Cell Biol* **126**, 87-97 (1994).
19. Haas, A. & Wickner, W. Organelle inheritance in a test tube: the yeast vacuole. *Seminars in Cell & Developmental Biology* **7**, 517-24 (1996).
20. Xu, Z. & Wickner, W. Thioredoxin is required for vacuole inheritance in *Saccharomyces cerevisiae*. *J Cell Biol* **132**, 787-94 (1996).
21. LaGrassa, T.J. & Ungermann, C. The vacuolar kinase Yck3 maintains organelle fragmentation by regulating the HOPS tethering complex. *J Cell Biol* **168**, 401-14 (2005).
22. Weisman, L.S. Yeast vacuole inheritance and dynamics. *Annu Rev Genet* **37**, 435-60 (2003).
23. Moseley, J.B. & Goode, B.L. The yeast actin cytoskeleton: from cellular function to biochemical mechanism. *Microbiol Mol Biol Rev* **70**, 605-45 (2006).
24. Park, H.O. & Bi, E. Central roles of small GTPases in the development of cell polarity in yeast and beyond. *Microbiol Mol Biol Rev* **71**, 48-96 (2007).
25. Zheng, Y., Bender, A. & Cerione, R.A. Interactions among proteins involved in bud-site selection and bud-site assembly in *Saccharomyces cerevisiae*. *J Biol Chem* **270**, 626-30 (1995).
26. Toenjes, K.A., Sawyer, M.M. & Johnson, D.I. The guanine-nucleotide-exchange factor Cdc24p is targeted to the nucleus and polarized growth sites. *Curr Biol* **9**, 1183-6 (1999).
27. Leeuw, T. et al. Interaction of a G-protein beta-subunit with a conserved sequence in Ste20/PAK family protein kinases. *Nature* **391**, 191-5 (1998).
28. Winters, M.J. & Pryciak, P.M. Interaction with the SH3 domain protein Bem1 regulates signaling by the *Saccharomyces cerevisiae* p21-activated kinase Ste20. *Mol Cell Biol* **25**, 2177-90 (2005).
29. Gulli, M.P. et al. Phosphorylation of the Cdc42 exchange factor Cdc24 by the PAK-like kinase Cla4 may regulate polarized growth in yeast. *Mol Cell* **6**, 1155-67 (2000).
30. Bose, I. et al. Assembly of scaffold-mediated complexes containing Cdc42p, the exchange factor Cdc24p, and the effector Cla4p required for cell cycle-regulated phosphorylation of Cdc24p. *J Biol Chem* **276**, 7176-86 (2001).
31. Cvrckova, F., De Virgilio, C., Manser, E., Pringle, J.R. & Nasmyth, K. Ste20-like protein kinases are required for normal localization of cell growth and for cytokinesis in budding yeast. *Genes Dev* **9**, 1817-30 (1995).
32. Butty, A.C. et al. A positive feedback loop stabilizes the guanine-nucleotide exchange factor Cdc24 at sites of polarization. *Embo J* **21**, 1565-76 (2002).
33. Simon, M.N. et al. Role for the Rho-family GTPase Cdc42 in yeast mating-pheromone signal pathway. *Nature* **376**, 702-5 (1995).
34. Zhao, Z.S., Leung, T., Manser, E. & Lim, L. Pheromone signalling in *Saccharomyces cerevisiae* requires the small GTP-binding protein Cdc42p and its activator CDC24. *Mol Cell Biol* **15**, 5246-57 (1995).

35. Chirolì, E. et al. Budding yeast PAK kinases regulate mitotic exit by two different mechanisms. *J Cell Biol* **160**, 857-74 (2003).
36. Weiss, E.L., Bishop, A.C., Shokat, K.M. & Drubin, D.G. Chemical genetic analysis of the budding-yeast p21-activated kinase Cla4p. *Nat Cell Biol* **2**, 677-85 (2000).
37. Schmidt, M., Varma, A., Drgon, T., Bowers, B. & Cabib, E. Septins, under Cla4p regulation, and the chitin ring are required for neck integrity in budding yeast. *Mol Biol Cell* **14**, 2128-41 (2003).
38. Matsui, Y., Matsui, R., Akada, R. & Toh-e, A. Yeast src homology region 3 domain-binding proteins involved in bud formation. *J Cell Biol* **133**, 865-78 (1996).
39. Hertveldt, K., Robben, J. & Volckaert, G. Whole genome phage display selects for proline-rich Boi polypeptides against Bem1p. *Biotechnol Lett* **28**, 1233-9 (2006).
40. Bender, L. et al. Associations among PH and SH3 domain-containing proteins and Rho-type GTPases in Yeast. *J Cell Biol* **133**, 879-94 (1996).
41. Ptacek, J. et al. Global analysis of protein phosphorylation in yeast. *Nature* **438**, 679-84 (2005).
42. Drees, B.L. et al. A protein interaction map for cell polarity development. *J Cell Biol* **154**, 549-71 (2001).
43. Norden, C. et al. The NoCut pathway links completion of cytokinesis to spindle midzone function to prevent chromosome breakage. *Cell* **125**, 85-98 (2006).
44. Burke, D., Dawson, D. & Stearns, T. Methods in yeast genetics: a Cold Spring Harbor Laboratory course manual (Cold Spring Harbor Laboratory Press, Cold Spring Harbor, 2000).
45. Cormack, B.P., Valdivia, R.H. & Falkow, S. FACS-optimized mutants of the green fluorescent protein (GFP). *Gene* **173**, 33-8 (1996).
46. Aitchison, J.D., Rout, M.P., Marelli, M., Blobel, G. & Wozniak, R.W. Two novel related yeast nucleoporins Nup170p and Nup157p: complementation with the vertebrate homologue Nup155p and functional interactions with the yeast nuclear pore-membrane protein Pom152p. *J Cell Biol* **131**, 1133-48 (1995).
47. Sambrook, J. & Russell, D.W. Molecular Cloning: a laboratory manual (Cold Spring Harbor Laboratory Press, Cold Spring Harbor, 2001).
48. Waddle, J.A., Karpova, T.S., Waterston, R.H. & Cooper, J.A. Movement of cortical actin patches in yeast. *J Cell Biol* **132**, 861-70 (1996).
49. Saito, T.L. et al. SCMD: Saccharomyces cerevisiae Morphological Database. *Nucleic Acids Res* **32**, D319-22 (2004).
50. Brachmann, C.B. et al. Designer deletion strains derived from Saccharomyces cerevisiae S288C: a useful set of strains and plasmids for PCR-mediated gene disruption and other applications. *Yeast* **14**, 115-32 (1998).
51. Winzeler, E.A. et al. Functional characterization of the S. cerevisiae genome by gene deletion and parallel analysis. *Science* **285**, 901-6 (1999).

52. Bender, A. & Pringle, J.R. Use of a screen for synthetic lethal and multicopy suppressor mutants to identify two new genes involved in morphogenesis in *Saccharomyces cerevisiae*. *Mol Cell Biol* **11**, 1295-305 (1991).
53. Sikorski, R.S. & Hieter, P. A system of shuttle vectors and yeast host strains designed for efficient manipulation of DNA in *Saccharomyces cerevisiae*. *Genetics* **122**, 19-27 (1989).
54. Vida, T.A. & Emr, S.D. A new vital stain for visualizing vacuolar membrane dynamics and endocytosis in yeast. *J Cell Biol* **128**, 779-92 (1995).
55. Hallett, M.A., Lo, H.S. & Bender, A. Probing the importance and potential roles of the binding of the PH-domain protein Boi1 to acidic phospholipids. *BMC Cell Biol* **3**, 16 (2002).
56. Gomes De Mesquita, D.S. et al. Vacuole segregation in the *Saccharomyces cerevisiae* vac2-1 mutant: structural and biochemical quantification of the segregation defect and formation of new vacuoles. *Yeast* **13**, 999-1008 (1997).
57. Boldogh, I.R., Ramcharan, S.L., Yang, H.C. & Pon, L.A. A type V myosin (Myo2p) and a Rab-like G-protein (Ypt11p) are required for retention of newly inherited mitochondria in yeast cells during cell division. *Mol Biol Cell* **15**, 3994-4002 (2004).
58. Fagarasanu, M., Fagarasanu, A., Tam, Y.Y., Aitchison, J.D. & Rachubinski, R.A. Inp1p is a peroxisomal membrane protein required for peroxisome inheritance in *Saccharomyces cerevisiae*. *J Cell Biol* **169**, 765-75 (2005).
59. Lamson, R.E., Winters, M.J. & Pryciak, P.M. Cdc42 regulation of kinase activity and signaling by the yeast p21-activated kinase Ste20. *Mol Cell Biol* **22**, 2939-51 (2002).
60. Benton, B.K., Tinkelenberg, A., Gonzalez, I. & Cross, F.R. Cla4p, a *Saccharomyces cerevisiae* Cdc42p-activated kinase involved in cytokinesis, is activated at mitosis. *Mol Cell Biol* **17**, 5067-76 (1997).
61. Bokoch, G.M. Biology of the p21-Activated Kinases. *Annu Rev Biochem* (2003).
62. Leeuw, T. et al. Pheromone response in yeast: association of Bem1p with proteins of the MAP kinase cascade and actin. *Science* **270**, 1210-3 (1995).
63. Peterson, J. et al. Interactions between the bud emergence proteins Bem1p and Bem2p and Rho-type GTPases in yeast. *J Cell Biol* **127**, 1395-406 (1994).
64. Ito, T., Matsui, Y., Ago, T., Ota, K. & Sumimoto, H. Novel modular domain PB1 recognizes PC motif to mediate functional protein-protein interactions. *Embo J* **20**, 3938-46 (2001).
65. Yamaguchi, Y., Ota, K. & Ito, T. A novel Cdc42-interacting domain of the yeast polarity establishment protein Bem1. Implications for modulation of mating pheromone signaling. *J Biol Chem* **282**, 29-38 (2007).
66. Yu, J.W. et al. Genome-wide analysis of membrane targeting by *S. cerevisiae* pleckstrin homology domains. *Mol Cell* **13**, 677-88 (2004).

67. Lemmon, M.A. Pleckstrin homology domains: not just for phosphoinositides. *Biochem Soc Trans* **32**, 707-11 (2004).
68. Lemmon, M.A. Pleckstrin homology (PH) domains and phosphoinositides. *Biochem Soc Symp*, 81-93 (2007).
69. Rossman, K.L. et al. A crystallographic view of interactions between Dbs and Cdc42: PH domain-assisted guanine nucleotide exchange. *Embo J* **21**, 1315-26 (2002).
70. Rossman, K.L. et al. Functional analysis of cdc42 residues required for Guanine nucleotide exchange. *J Biol Chem* **277**, 50893-8 (2002).
71. Kim, O., Yang, J. & Qiu, Y. Selective activation of small GTPase RhoA by tyrosine kinase Etk through its pleckstrin homology domain. *J Biol Chem* **277**, 30066-71 (2002).
72. Jaffe, A.B., Aspenstrom, P. & Hall, A. Human CNK1 acts as a scaffold protein, linking Rho and Ras signal transduction pathways. *Mol Cell Biol* **24**, 1736-46 (2004).
73. Yamamoto, A. et al. Novel PI(4)P 5-kinase homologue, Fab1p, essential for normal vacuole function and morphology in yeast. *Mol Biol Cell* **6**, 525-39 (1995).
74. Xu, H. & Wickner, W. Bem1p is a positive regulator of the homotypic fusion of yeast vacuoles. *J Biol Chem* **281**, 27158-66 (2006).
75. Han, B.K. et al. Bem1p, a scaffold signaling protein, mediates cyclin-dependent control of vacuolar homeostasis in *Saccharomyces cerevisiae*. *Genes Dev* **19**, 2606-18 (2005).
76. Eitzen, G., Thorngren, N. & Wickner, W. Rho1p and Cdc42p act after Ypt7p to regulate vacuole docking. *Embo J* **20**, 5650-6 (2001).
77. Muller, O., Johnson, D.I. & Mayer, A. Cdc42p functions at the docking stage of yeast vacuole membrane fusion. *Embo J* **20**, 5657-65 (2001).
78. Eitzen, G., Wang, L., Thorngren, N. & Wickner, W. Remodeling of organelle-bound actin is required for yeast vacuole fusion. *J Cell Biol* **158**, 669-79 (2002).

CHAPTER III

THE P21-ACTIVATED KINASES CLA4 AND STE20 REGULATE THE DESTRUCTION OF THE VACUOLE SPECIFIC MYOSIN RECEPTOR VAC17

Abstract

The budding yeast *S. cerevisiae* vacuole (lysosome) is transported along actin cables by the myosin V motor, Myo2, bound to the vacuole-specific myosin receptor Vac17^{1, 2}. Directionality in vacuole transport is ensured by the bud-specific degradation of Vac17. It has been proposed that bud-specific degradation of Vac17 is promoted by proteins localized to and/or activated solely in the bud³. However, these factors have not been identified. The p21-activated kinases (PAKs) Cla4 and Ste20 are localized to and are activated in the bud, and overexpression of either inhibited vacuole inheritance. Inhibition of vacuole inheritance by *CLA4* or *STE20* overexpression was suppressed by the expression of non-degradable *VAC17*. Additionally, PAK activity was required for Vac17 degradation in late-M and *CLA4* overexpression promoted Vac17 degradation. I conclude that Cla4 and Ste20 are the bud-specific proteins that promote the bud-specific degradation of Vac17.

Introduction

Directionality in vacuole transport is achieved by spatial degradation of Vac17 in a bud-specific manner. The vacuole inheritance mutants *vac8* and *myo2-2* (a point mutant within Myo2 which specifically disrupt the Myo2-Vac17 interaction) fail to transport Vac17 into the bud and Vac17 accumulates to high levels. Bud-specific degradation of Vac17 requires a PEST sequence within Vac17. Cells expressing *VAC17* without the PEST sequence (*vac17 Δ PEST*) accumulate Vac17 to high levels and the vacuole is transported back to the mother bud neck prior to cytokinesis when the actin cytoskeleton is polarized to the mother bud neck ^{1,2}.

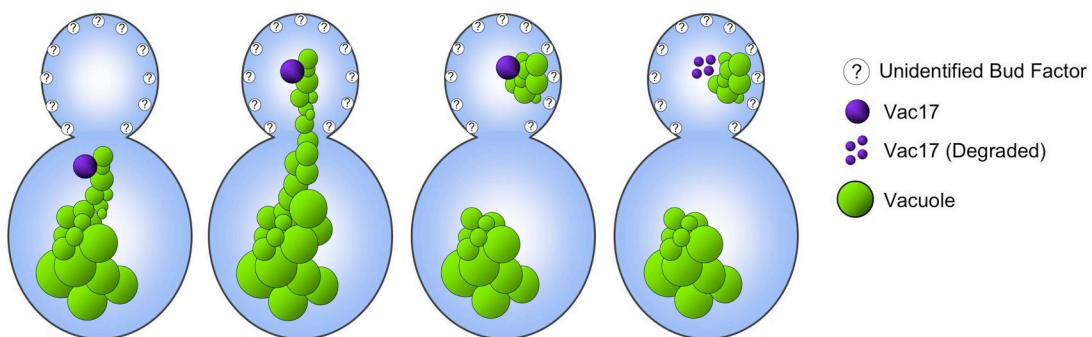


Figure 3-1. Proposed model for bud-specific degradation of Vac17.

Vac17 acts within the mother cell to transport the segregation structure into the bud. After entering the bud Vac17 comes into contact with unidentified factors localized to and/or activated specifically in the bud that prime Vac17 for degradation prior to cytoskeletal rearrangements towards the mother bud neck in preparation for cytokinesis.

It has been proposed that the spatial degradation of Vac17 solely in the bud is promoted by factors specifically localized to and/or activated in the bud (Figure 3-1) ³. However, these factors have not yet been identified. In the previous chapter, I described four factors (Boi1, Boi2, Cla4, and Ste20) that localize specifically to the bud and that regulate vacuole inheritance (Chapter 2)

⁴⁻⁸. Here, I provide evidence that the p21-activated kinases Cla4 and Ste20 are bud-localized factors promoting Vac17 degradation.

Materials and Methods

Table 3-1. Strains

Strain	Genotype	Source
W303-1A	<i>MATa ade2-1 his3-11,15 leu2-3,112 trp1-1 ura3-1</i> (W303)	⁹
Y _{CH} 4774	<i>MATa VAC17-ProA-HIS3-URA3</i> (W303)	This Study
Y _{CH} 4826	<i>MATa boi1::LEU2 boi2::URA3 vac17::kanMX4 pRS313-pVAC17-VAC17</i> (W303)	This Study
Y _{CH} 4827	<i>MATa boi1::LEU2 boi2::URA3 vac17::kanMX4 pRS313-pVAC17-vac17DPEST</i> (W303)	This Study
Y _{CH} 4837	<i>MATa pRS314-GAL-GST-STE20</i> (W303)	This Study
Y _{CH} 4843	<i>MATa pRS314-GAL-GST-STE20 VAC17-ProA-HIS3-URA3</i> (W303)	This Study
Y _{CH} 4852	<i>MATa cdc14-1 VAC17-ProA-HIS3-URA3</i> (W303)	This Study
Y _{CH} 4862	<i>MATa cdc15-2 VAC17-ProA-HIS3-URA3</i> (W303)	This Study
Y _{CH} 4869	<i>MATa dbf2-2 VAC17-ProA-HIS3-URA3</i> (W303)	This Study
Y _{CH} 4882	<i>MATa his3::GAL-CLA4-HIS3 VAC17-ProA-HIS3-URA3</i> (W303)	This Study
Y _{CH} 4893	<i>MATa ura3::4X URA3::GAL1-CLA4t swe1::LEU2 VAC17-ProA-HIS3-URA3</i> (W303)	This Study
Y _{CH} 4894	<i>MATa ura3::4X URA3::GAL1-CLA4t VAC17-ProA-HIS3-URA3</i> (W303)	This Study
Y _{CH} 4912	<i>MATa his3::GAL-CLA4-HIS3 ura3::GFP-PTS1-URA3</i> (W303)	This Study
Y _{CH} 4914	<i>MATa ura3::GFP-PTS1-URA3</i> (W303)	This Study
Y _{CH} 4974	<i>MATa his3::GAL-CLA4-HIS3 vac17::kanMX4 pRS414-pVAC17-VAC17</i> (W303)	This Study
Y _{CH} 4975	<i>MATa his3::GAL-CLA4-HIS3 vac17::kanxMX4 pRS414-pVAC17-vac17ΔPEST</i> (W303)	This Study
Y _{CH} 4978	<i>MATa SEC7-GFP-HIS3 pRS316</i> (S288c)	This Study
Y _{CH} 4980	<i>MATa SEC7-GFP-HIS3 pRS31-GAL-GST-STE20</i> (S288c)	This Study
Y _{CH} 4992	<i>MATa pRS316-GST-STE20 vac17::kanMX4 pRS414-pVAC17-VAC17</i> (W303)	This Study
Y _{CH} 4993	<i>MATa pRS316-GST-STE20 vac17::kanMX4 pRS414-pVAC17-vac17ΔPEST</i> (W303)	This Study
Y _{CH} 5162	<i>MATa PDS1-HA-LEU2::leu2 VAC17-ProA-HIS3</i> (W303)	This Study
YMG694	<i>MATa bar1-1 his3::GAL-CLA4-HIS3</i> (W303)	¹⁰

Plasmid and strain construction

Yeast strains and sources are listed in Table 3-1. Yeast strains were constructed by genetic crosses followed by tetrad dissection or by transformation using the lithium acetate method ¹¹. *ProA* and the adjacent *HIS3* and *URA3* marker were amplified by PCR and integrated to generate *VAC17-ProA* as described ¹². Plasmid sources and construction methods are listed in Table 3-2 and DNA manipulations were performed as described ¹³.

Table 3-2. Plasmids

Plasmid	Description	Source
pCH1915	<i>pRS414-pVAC17-VAC17</i> . Made by insertion of 1.94 kB <i>BamHI-Sall</i> fragment of pVAC17 ¹ into the <i>BamHI-Sall</i> site of pRS414 ¹⁴ .	This Study
pCH1916	<i>pRS414-pVAC17-vac17ΔPEST</i> Made by insertion of 1.75 kB <i>BamHI-Sall</i> fragment of pVAC17(Δ97-259) ¹ into the <i>BamHI-Sall</i> site of pRS414 ¹⁴ .	This Study
pCH1924	<i>pRS313-pVAC17-VAC17</i> Made by insertion of 1.94 kB <i>BamHI-Sall</i> fragment of pVAC17 ¹ into the <i>BamHI-Sall</i> site of pRS313 ¹⁴ .	This Study
pCH1925	<i>pRS313-pVAC17-vac17ΔPEST</i> . Made by insertion of 1.75 kB <i>BamHI-Sall</i> fragment of pVAC17(Δ97-259) ¹ into the <i>BamHI-Sall</i> site of pRS414 ¹⁴ .	This Study
pCH1926	<i>pRS314-GAL-GST-STE20</i> . Made by insertion of a 4.53 kB <i>SacII-KpnI</i> fragment of pRD20-STE20-ATG ⁸ into the <i>SacII-KpnI</i> site of pRS314 ¹⁴ .	This Study
pRD20-STE20-ATG	<i>pRS316-GST-STE20</i> .	8
pRS316	<i>pRS316</i>	14

Microscopy

Digital images were taken with a 100X objective on an Olympus microscope. NIH image 1.62 (written by Wayne Rasband) was used for image acquisition. Cells were visualized by fluorescence and differential interference contrast microscopy (DIC). Within each experiment, all images were collected and scaled identically. Images were processed with Photoshop 9.0 software (Adobe). Video microscopy was performed with mid-log phase cells placed on a drop of 2% agarose in YPD was flattened by an uncoated glass slide as described¹⁵. Cells were visualized every three to five minutes. Scale bar = 2.5 μm throughout all figures.

In vivo labeling of vacuoles and nuclei staining

To visualize vacuoles, yeast cells were concentrated and incubated for 1 hour with N-(3-triethylammoniumpropyl)-4(6(4(diethylamino)phenyl)hexatrienyl)

pyridium dibromide (FM 4-64; Molecular Probes) at a final concentration of 16.5 μM ¹⁶. Cells were then washed with appropriate media and grown for ≥ 3 hours before being viewed by fluorescence microscopy. Nuclei were visualized by fixation in 70% ethanol followed by staining with DAPI at 0.1 mg/ml.

Sizing cells and quantification of organelle inheritance

Small, medium, and large budded cells were grouped into size categories as described¹⁷. Peroxisomes and late Golgi inheritance were determined by fluorescence microscopy and bud sizes were determined by measuring the cross sectional area of mothers and buds using NIH-Image 1.62. Each cell was grouped into a category according to bud cross-sectional area expressed as a percentage of mother cell cross-sectional area. Bud size categories for late Golgi inheritance were: category I 4.0 -7.4%, II, 7.5–10.9%; category III, 11.0–14.4%; category IV, 14.5–17.9%; and category V, 18.0–21.4% as previously described¹⁸. Bud size categories for peroxisome inheritance were: category I, 0–24%; category II, 24–39%; category III, 39–50%; category IV, 50–61%, and category V 61-100% as previously described¹⁹. Six different focal planes were examined for each bud to quantify organelle inheritance.

SDS-PAGE and western blot analysis

Yeast protein levels and gel mobility were assayed by TCA precipitation followed by SDS-PAGE (7.5%) and western blot analysis using Rabbit-a-Mouse

IgG 1:1000 (Promega), Mouse- α -HA 16B12 1:1000 (Covance), and Goat- α -Actin antibodies 1:2000.

Vac17-ProA immunoprecipitation and phosphatase treatment

Pelleted cells were resuspended in lysis buffer (20mM Tris-HCl (pH 6.5), 5mM MgCl₂, 2% Triton X-100, 150 mM NaCl, 1x protease inhibitor (Roche), 1mM PMSF, 5mM EDTA, 50 mM NaF, 10 mM Na₄P₂O₇, 0.5mM NaVO₄, and 1X phosphatase inhibitor (Calbiochem)). Cells were lysed using a French Press, lysates were incubated with 300 μ l of IgG sepharose beads (Amersham Biosciences), and washed with wash buffer (20mM Tris-HCl (pH6.8), 5mM MgCl₂, 2% Triton X-100, 150 mM NaCl). Immunoprecipitates were then split and treated with 1-protein phosphatase (NEB) and phosphatase inhibitor (Calbiochem) as indicated.

Cell cycle arrests

Cell cycle arrests were performed by the addition α -factor (ZymoResearch) or nocodazole (Sigma) at the final concentration of 3 μ M and 15 μ g/ml respectively as described or by shifting temperature sensitive mutants from the permissive temperature (23°C) to the nonpermissive temperature (37°C) for three hours. Conditions for growth and release of synchronous cultures from arrest by α -factor were as described²⁰.

Other methods

YP media containing 1% yeast extract and 2% Bacto Peptone was used with addition of glucose (YPD), raffinose (YPR), and/or galactose (YPG) as carbon sources at 2% final concentration. Alternately, strains with plasmids were grown on synthetic media (SC) lacking tryptophan, uracil, or histidine to maintain plasmids.

Results

Cells overexpressing *CLA4* have a daughter-specific budding delay and a vacuole inheritance defect

I have previously shown that *boi1 boi2* and *vac8* mutant cells had a daughter-specific budding delay (Figure 2-2) and *boi1 boi2* cells had a vacuole inheritance defect suppressed by *CLA4* (Figure 2-4). In light of those results, I hypothesized that Cla4 regulates vacuole inheritance. To test this hypothesis I determined if cells overexpressing *CLA4* had a daughter-specific budding delay and/or a vacuole inheritance defect like *boi1 boi2* and *vac8* cells.

CLA4 overexpression from a *MET* promoter causes defects in growth and actin polymerization¹⁰. However, overexpression of *CLA4* from the *GAL* promoter integrated at the *HIS3* locus was not lethal and cells grew well on YP+2%Galactose plates (data not shown). I used this strain to determine if *CLA4* overexpressing cells had a daughter-specific budding delay like *boi1 boi2* and *vac8* (Figure 2-2).

Wild type and *GAL-CLA4* cells were observed by time lapse video microscopy with cells grown on agar pads containing YP+2% glucose or YP+2% galactose to induce *CLA4* overexpression. Cell division led to the production of a larger mother and a smaller daughter cell. After cell separation, wild type mother cells, grown on media containing either glucose or galactose quickly rebudded (Figure 3-2A). Smaller daughter cells grown on either glucose or galactose budded with similar kinetics but were delayed for bud emergence an average of 48 and 65 minutes respectively while they grew to a critical size (Figure 3-2A).

GAL-CLA4 mother cells grown on either glucose or galactose budded with similar kinetics to wild type mother cells. In contrast the *GAL-CLA4* daughter cells grown on either glucose or galactose did not bud with similar kinetics and daughter cells overexpressing *CLA4* were delayed on average 135 minutes longer than *GAL-CLA4* daughter cells grown on glucose (Figure 3-2).

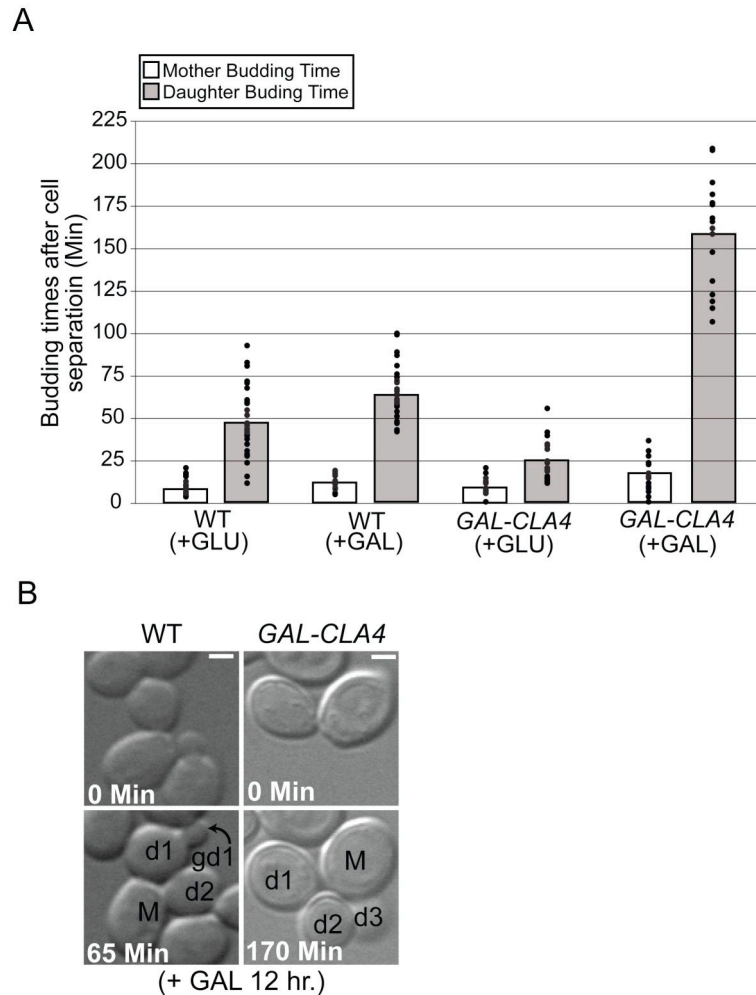


Figure 3-2. Cells overexpressing *CLA4* have a daughter-specific budding delay.

(A-B) Wild type (W303-1A) and *GAL-CLA4* (YMG694) cells were grown to early log phase in either YP+2% Glucose or YP+2% Galactose and were examined by video microscopy. The budding time, defined as the interval in minutes between cell separation and subsequent bud emergence for mother (light bar) and daughter (dark bar) cells, was determined. Black dots represent independent bud emergence events. Pedigree analysis was performed. Pedigree analysis: M (mother), d1-3 (primary - tertiary daughters) and gd1 (primary granddaughter).

Video microscopy of FM 4-64 stained wild type and *GAL-CLA4* cells was performed to determine if *CLA4* overexpression inhibited vacuole inheritance. Wild type (data not shown) and *GAL-CLA4* cells were grown on YP+2% galactose media. Unlike wild type cells in which segregation structures were frequently observed and 100% of cells inherited a vacuole (data not shown), segregation structures were formed in cells overexpressing *CLA4* (Figure 3-3A).

To further explore the ability of *CLA4* to inhibit vacuole inheritance, FM 4-64 stained wild type and *GAL-CLA4* cells were grown in YP+2% raffinose to mid-log phase at which time the cultures were split and 2% galactose was added to half the sample, and samples were examined every two hours. The presence of a segregation structure in small and medium budded cells and the presence of a daughter vacuole in large budded cells was scored for each sample. Segregation structures were present in ~30% of all wild type small and medium budded cells and 100% of all large budded cells contained a daughter vacuole in the presence or absence of galactose throughout the time course of the experiment (data not shown). *GAL-CLA4* cells grown in non-inducing conditions had similar vacuole inheritance percentages as wild type cells. In contrast, *GAL-CLA4* cells grown under inducing conditions exhibited a decrease in vacuole inheritance as early as 2 hours, rapidly decreasing vacuole inheritance between 2 and 4 hours, and by 6 hours post induction 0% of small and medium budded cells had segregation structures, and only 2% of large budded cells contained a daughter vacuole (Figure 3-3B,C).

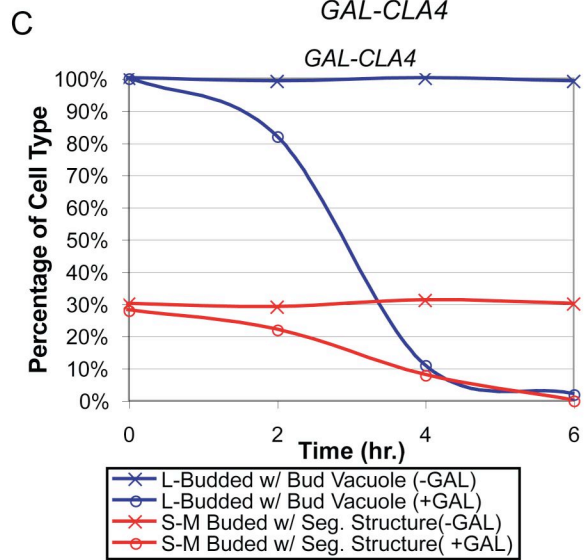
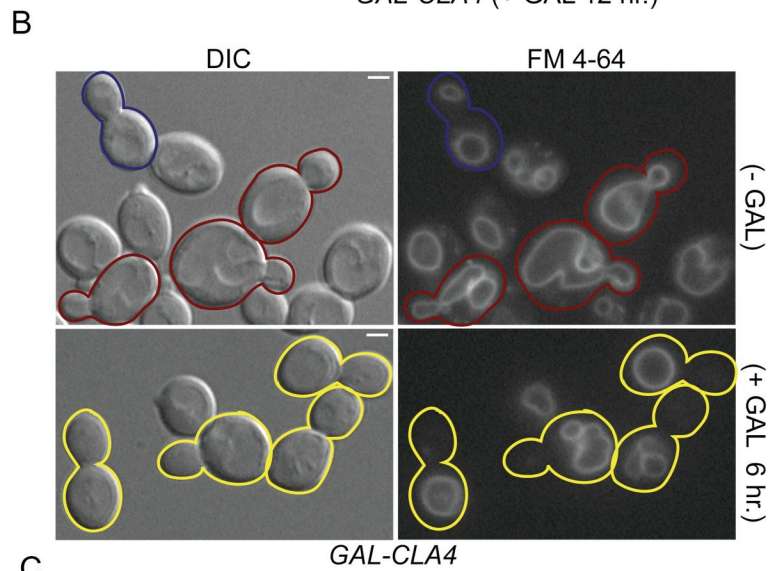
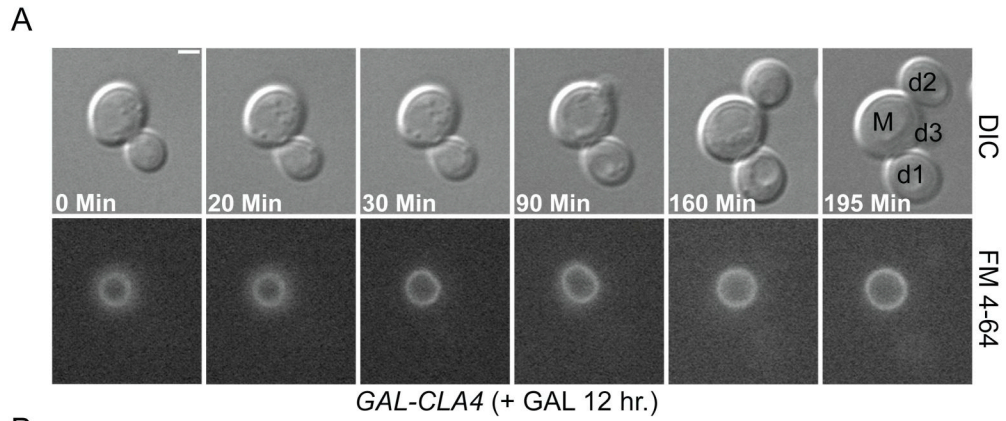


Figure 3-3. Cells overexpressing *CLA4* have a vacuole inheritance defect.

(A) Video microscopy and pedigree analysis of FM 4-64 stained *GAL-CLA4* (YMG694) cells was performed on cells grown in YP+2%Galactose. (B-C) FM 4-64 strained *GAL-CLA4* (YMG694) cells were grown in YP+2% raffinose to mid-logarithmic stage. At time 0 2% galactose was added to half the culture and the presence of segregation structures in small and medium budded cells and of daughter vacuoles in large budded cells was quantified by fluorescence microscopy. Representative pictures at the 6 hour time point are shown. Cell Outline Color Code, Red: bud contains segregation structure; Blue: bud has inherited vacuole material from mother cell; Yellow: medium or large bud lacking inherited vacuole material from mother cell. Pedigree analysis: M (mother), d1-3 (primary - tertiary daughters).

Cells overexpressing *STE20* have a vacuole inheritance defect

Cla4 and *Ste20* play many unique and overlapping roles in the cell ^{21, 22}.

Since deletion of either *CLA4* or *STE20* suppressed the *boi1 boi2* daughter-specific budding and vacuole inheritance defects (Figure 2-4). I therefore hypothesized that *STE20* overexpressing cells might also have a daughter-specific budding delay and vacuole inheritance defect.

When examined, *GAL-STE20* cells grown under either inducing or noninducing conditions did not display a daughter-specific budding delay (data not shown). However, because not all vacuole inheritance mutants have a daughter-specific budding delay ³, I proceeded to test for a vacuole inheritance defect. A culture of FM 4-64 stained *GAL-STE20* cells was grown to mid-log phase at which time the culture was split and 2% galactose was added to one 100% of all large budded cells contained a daughter vacuole throughout the time course of the experiment (Figure 3-4). *GAL-STE20* cells grown under inducing conditions had decreasing amounts of vacuole inheritance as early as 2 hours, rapidly decreasing vacuole inheritance between 2 and 4 hours, and by 6 hours post induction only 4% of small and medium budded cells had a segregation

structure and only 18% of large-budded cells had a discrete daughter vacuole (Figure 3-4).

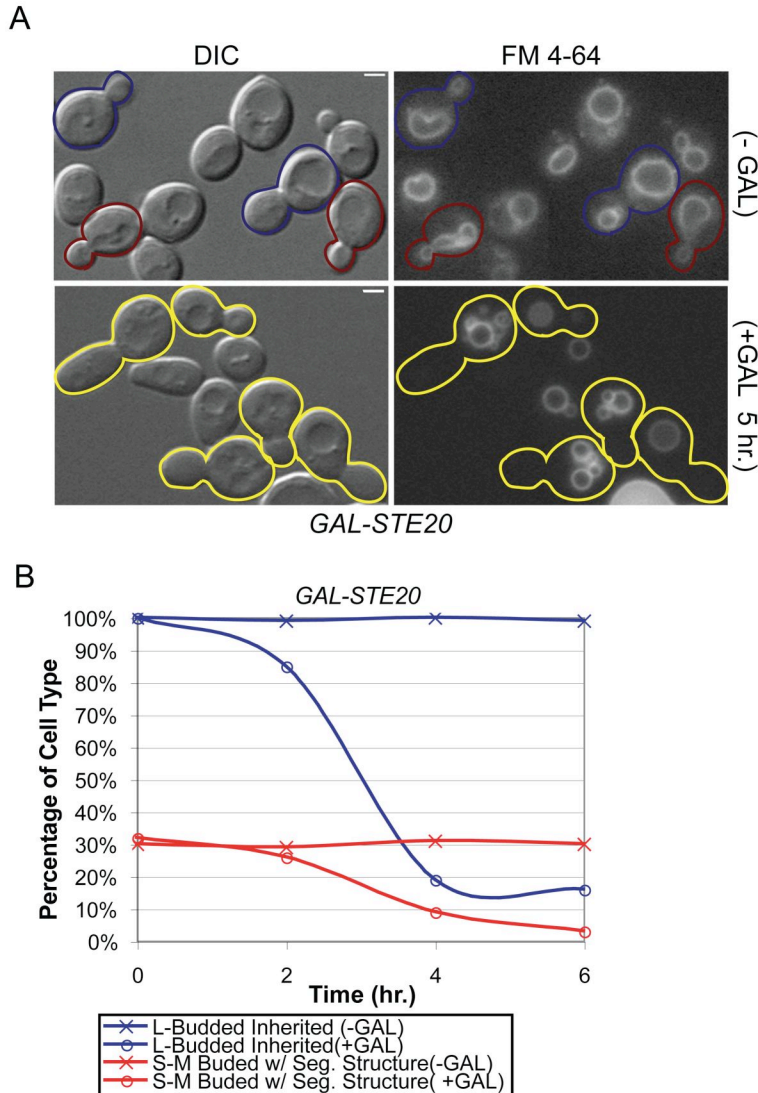


Figure 3-4. Cells overexpressing *STE20* have a vacuole inheritance defect. (A-B) FM 4-64 strained *GAL-STE20* (Y_{CH4837}) cells were grown in SC-TRP+2% raffinose to mid-logarithmic stage. At time 0 2% galactose was added to half the culture and the presence of segregation structures in small and medium budded cells and of daughter vacuoles in large budded cells was quantified by fluorescence microscopy. Representative pictures at the 6 hour time point are shown. Cell Outline Color Code, Red: bud contains segregation structure; Blue: bud has inherited vacuole material from mother cell; Yellow: medium or large bud lacking inherited vacuole material from the mother cell.

***vac17 Δ PEST* expression suppresses the vacuole inheritance defect of *CLA4* or *STE20* overexpressing and *boi1 boi2* cells**

One possible explanation for the vacuole inheritance defect exhibited in cells overexpressing *CLA4* or *STE20* was that the PAKs are the bud-specific factors that promote Vac17 degradation. I hypothesized that *CLA4* or *STE20* overexpression caused a vacuole inheritance defect by promoting the premature degradation of Vac17. If this model was correct then I would have expected that expression of the non-degradable *VAC17* (*vac17 Δ PEST*) should suppress the vacuole inheritance defect caused by *CLA4* or *STE20* overexpression.

FM 4-64 stained *GAL-CLA4 vac17* and *GAL-STE20 vac17* cells covered by a plasmid containing *VAC17* or *vac17 Δ PEST* were examined for vacuole inheritance. As expected 100% of all *GAL-CLA4* and *GAL-STE20* large budded cells contained a daughter vacuole in the presence of *VAC17* or *vac17 Δ PEST* under noninducing conditions. Under inducing conditions *GAL-CLA4* and *GAL-STE20* cells containing *VAC17* exhibited vacuole inheritance defects after 6 hours of overexpression. However expression of *vac17 Δ PEST* fully suppressed the vacuole inheritance defect in *GAL-CLA4* and *GAL-STE20* cells under inducing conditions (Table 3-3).

I have previously shown that *boi1 boi2* exhibited a vacuole inheritance defect suppressible by *CLA4* or *STE20* deletion (Table 2-3). To further test my hypothesis I determined if the *boi1 boi2* vacuole inheritance defect was suppressible by *vac17 Δ PEST* expression. FM 4-64 stained *boi1 boi2 vac17* covered by a *VAC17* containing plasmid displayed vacuole inheritance defects as

expected (Table 3-3). Expression of *vac17ΔPEST* in the *boi1 boi2 vac17* cells fully suppressed the *boi1 boi2* vacuole inheritance defect (Table 3-3).

Table 3-3. *vac17ΔPEST* expression suppresses the vacuole inheritance defect of *CLA4* or *STE20* overexpressing or *boi1 boi2* cells.

Genotype	Vacuole Inheritance of Large Budded Cells
<i>GAL-CLA4 vac17 pVAC17 (-GAL)</i>	100%
<i>GAL-CLA4 vac17 pvac17ΔPEST (-GAL)</i>	100%
<i>GAL-CLA4 vac17 pVAC17 (+GAL)</i>	2%
<i>GAL-CLA4 vac17 pvac17ΔPEST (+GAL)</i>	100%
<i>GAL-STE20 vac17 pVAC17 (-GAL)</i>	100%
<i>GAL-STE20 vac17 pvac17ΔPEST (-GAL)</i>	100%
<i>GAL-STE20 vac17 pVAC17 (+GAL)</i>	19%
<i>GAL-STE20 vac17 pvac17ΔPEST (+GAL)</i>	100%
<i>boi1 boi2 vac17 pVAC17</i>	15%
<i>boi1 boi2 vac17 pvac17ΔPEST</i>	100%

The ability of *vac17ΔPEST* expression to suppress the vacuole inheritance defect of *CLA4* or *STE20* overexpressing and *boi1 boi2* cells provided me with support for a model that PAKs are the bud specific factors that promote Vac17 degradation. I then set out to test two predictions of this model. (1) If PAKs are required for Vac17 degradation then cells lacking PAK activity should not degrade Vac17. (2) Cells overexpressing *CLA4* or *STE20* should degrade Vac17. However, to perform these experiments further information was required concerning the timing of Vac17 degradation.

Vac17 is a phosphoprotein degraded in late-M phase

Vac17 levels oscillate during the cell cycle. Vac17 levels increase as cells bud and decrease prior to cytokinesis¹. I examined Vac17 levels throughout the cell cycle to further characterize when Vac17 was degraded.

I tagged Vac17 with a ProA tag. Vacuole inheritance was assayed in *VAC17-ProA* cells and the kinetics of vacuole inheritance were identical to wild type cells suggesting that Vac17-ProA was functional (data not shown). Vac17-ProA levels were then examined in asynchronous cells by SDS-PAGE followed by western-blot analysis. I found that Vac17 ran as multiple bands suggesting the possibility that Vac17-ProA was a phosphoprotein (Figure 3-5A). Vac17-ProA was immunoprecipitated and treated with λ -phosphatase or λ -phosphatase plus phosphatase inhibitor. Vac17-ProA treated with λ -phosphatase collapsed down to a single band and phosphatase inhibitors blocked this collapse (Figure 3-5B).

The timing of Vac17 degradation was further examined during the cell cycle. *VAC17-ProA PDS1-HA* cells were arrested in G1 with α -factor and released. Samples were taken every 10 minutes, and Vac17 and Pds1 protein levels were examined throughout a single cell cycle. Pds1 is degraded as cells enter anaphase²³ and Vac17 degradation occurred after this point (Figure 3-5C). Additionally, phosphorylated Vac17 appeared common in G2/M cells arrested with nocodazole (Figure 3-5D). Together these data suggested that Vac17 destruction did not occur until after entry into anaphase.

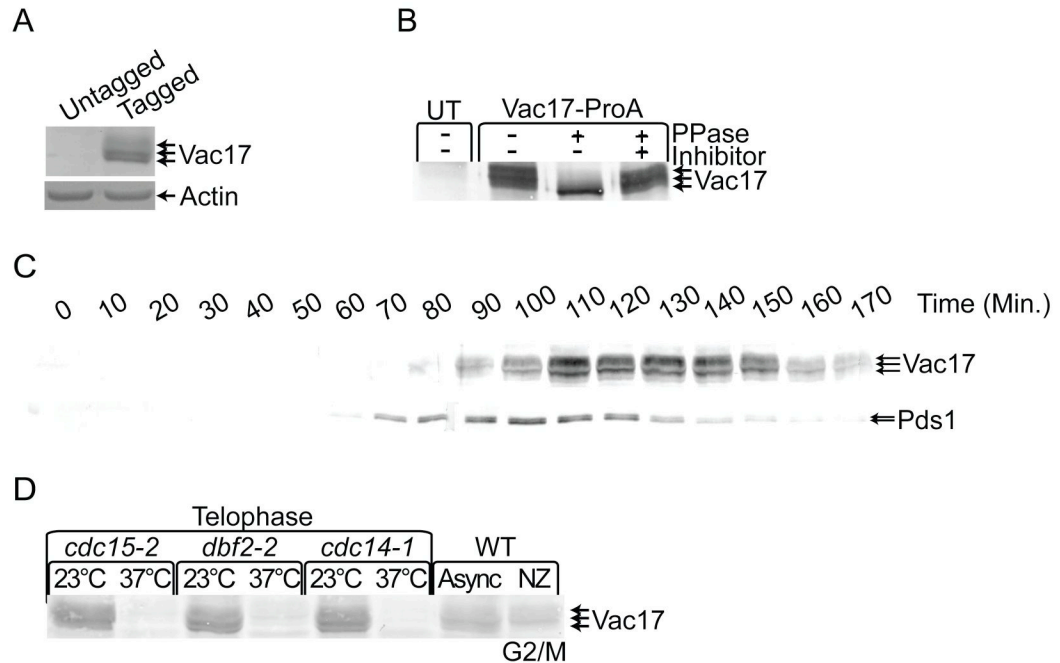


Figure 3-5. Vac17 is a phosphoprotein and is degraded in late-M phase.

(A) Vac17-ProA and actin proteins were examined by western blot analysis in untagged (W303-1A) and *VAC17-ProA* (Y_{CH4774}) cells. (B) Vac17-ProA was immunoprecipitated from protein extracts of *4X GAL-CLA4t swe1Δ VAC17-ProA* (Y_{CH4893}) or untagged (UT) *4X GAL-CLA4t swe1Δ* (Piatti2711) strains grown on YP+2%galactose media for 6 hours. Immunoprecipitated material was split and treated with buffer alone, λ -phosphatase, or λ -phosphatase plus phosphatase inhibitors. (B) Vac17-ProA and actin proteins were examined by western blot analysis in untagged (W303-1A) and *VAC17-ProA* (Y_{CH4774}) cells. (C) *VAC17-ProA PDS1-HA* (Y_{CH5162}) cells were arrested in G1 with a-factor, released, samples were taken every 10 minutes, and Vac17-ProA and Pds1-HA were examined by western blot analysis. (D) Vac17-ProA levels were assayed by western blot in *cdc15-2* (Y_{CH4862}), *dbf2-2* (Y_{CH4869}), and *cdc14-1* (Y_{CH4852}) cells grown at 23°C or arrested at telophase in 37°C media. Additionally, Vac17-ProA levels were examined in asynchronous and nocodazole arrested cells (Y_{CH4774}).

Because Vac17 degradation occurred after anaphase onset I examined if mitotic exit was required for Vac17 degradation. *CDC15*, *DBF2*, and *CDC14* are required for mitotic exit and temperature sensitive mutants in these genes arrest prior to mitotic exit^{24, 25}. Vac17-ProA levels were examined in *cdc15-2*, *dbf2-2*, and *cdc14-1* cells grown at the permissive and non-permissive temperature to arrest cells at mitotic exit. Phosphorylated Vac17-ProA was common in cells grown at the non-permissive temperature. However, cells arrested at mitotic exit only contained a small amount of what appeared to be unphosphorylated Vac17

(Figure 3-5D). This suggested that Vac17 was destroyed after anaphase entry and before mitotic exit during Late-M phase.

PAK function is required for Vac17-ProA degradation in late-M

If PAKs are required for Vac17 degradation, then in the absence of Cla4 and Ste20 activity Vac17-ProA should not be degraded. A *CLA4* allele with a truncated C-terminus (*CLA4t*) when overexpressed causes Cla4 and Ste20 to delocalize from the bud cortex and cells display similar defect as seen in cells lacking PAKs ²⁶. *4X GAL-CLA4t VAC17-ProA* cells were arrested in G1 and released, and Vac17 levels and mitotic progression were examined. As in wild type cells (Figure 3-5C), Vac17-ProA is phosphorylated and cells arrest at G2/M in a *SWE1* dependent manner (Figure 3-6A). Since Vac17 is stable at G2/M, the same experiment was performed in the absence of *SWE1*, a situation in which cells progress to Late-M when Vac17 protein levels were low (Figure 3-5D). I observed that even though cells progressed to late-M, Vac17-ProA levels remained high with large amounts of phosphorylated Vac17 present (Figure 3-6B). Thus I concluded that active PAKs were required for Vac17 degradation in late-M.

***CLA4* overexpression promotes Vac17-ProA degradation**

After examining the requirement for PAKs in Vac17 degradation I determined if PAK overexpression caused Vac17 degradation. Asynchronous cultures of wild type and *GAL-CLA4* cells were grown to mid-log phase, 2%

galactose was added at the zero time point, and samples were taken every hour for examination of Vac17-ProA levels. Over the 6 hour time course of the experiment, Vac17 remained constant in wild type cells (Figure 3-6D). However, Vac17-ProA levels decreased in *GAL-CLA4* cells over the 6 hours time course. A reduction in Vac17-ProA levels was observed as early as 2 hours with the phosphorylated Vac17-ProA disappearing quickest and Vac17-ProA levels reached very low levels at the six hour time point (Figure 3-6C). Importantly the decrease in Vac17-ProA levels occurred with similar kinetics to vacuole inheritance defects (Figure 3-3C). Therefore, *CLA4* overexpressing cells have a severe vacuole inheritance defect like the Class I vacuole inheritance mutants *vac8* and *myo2-2* which fail to inherit vacuoles. However, unlike *vac8* and *myo2-2* cells, *CLA4* overexpressing cells do not accumulate Vac17 to high levels like other Class I vacuole inheritance mutants¹, but instead Vac17 levels drop after *CLA4* overexpression is initiated. Thus I concluded that *CLA4* promotes Vac17 degradation.

Additionally the ability of *STE20* to promote Vac17-ProA degradation was examined. Asynchronous cultures of *GAL-STE20* were grown under inducing conditions, and while vacuole inheritance defects were seen as in Figure 3-4B (data not shown), Vac17-ProA levels remained constant throughout the six hour time course of the experiment (Figure 3-6E).

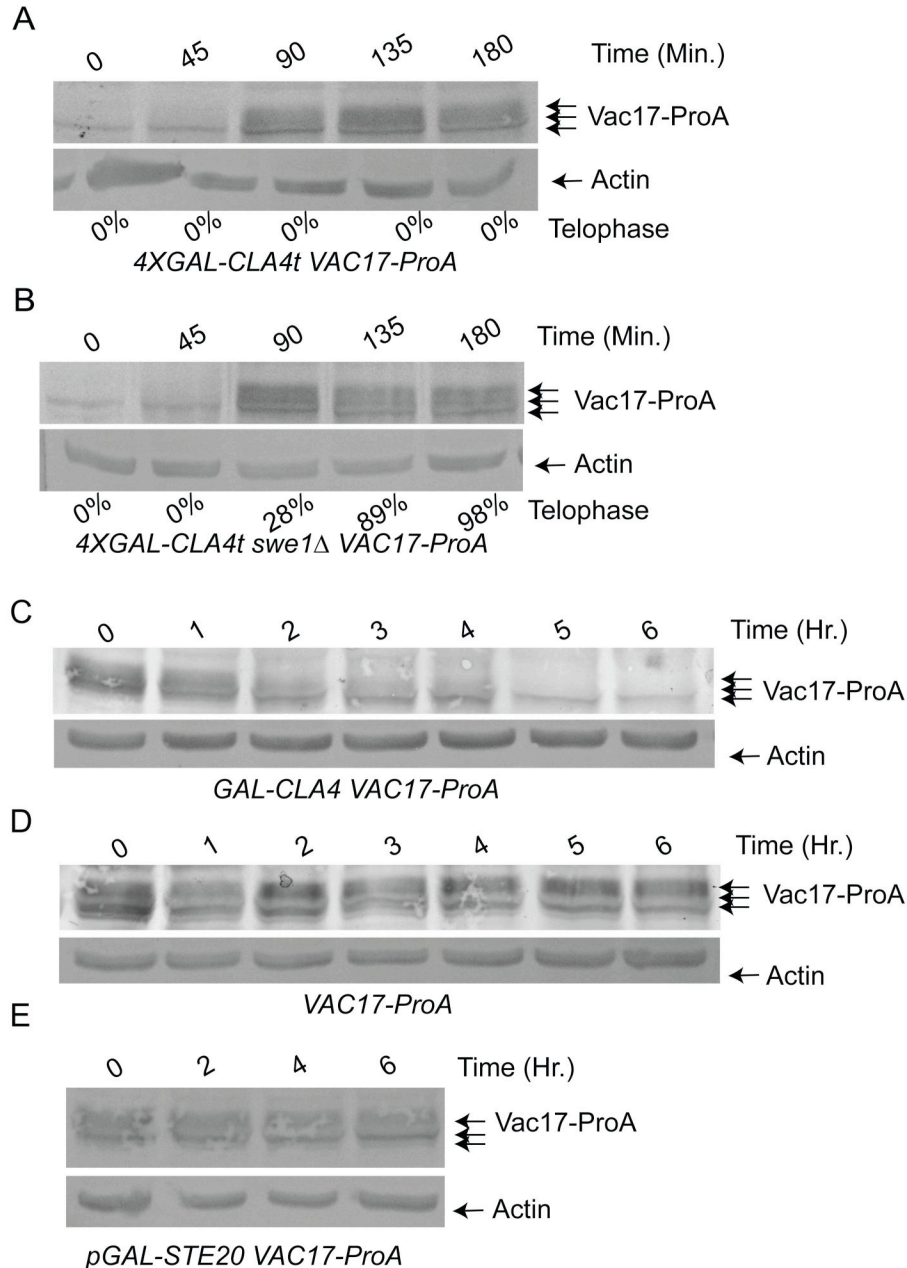


Figure 3-6. PAK function is required for Vac17-ProA degradation in late-M and *CLA4* overexpression promotes Vac17-ProA degradation.

(A-B) 4X *GAL-CLA4t VAC17-ProA* (Y_{CH}4894) and 4X *GAL-CLA4t swe1Δ VAC17-ProA* (Y_{CH}4893) were α -factor arrested, released, samples taken at the indicated times, and subjected to western blot analysis. Additionally the percentage of telophase cells was determined by DAPI staining and scoring the number of cells with mother and bud nuclei staining. (C-D) Mid-logarithmic phase *GAL-CLA4 VAC17-ProA* (Y_{CH}4882) and *VAC17-ProA* (Y_{CH}4774) were grown in YP+2% raffinose. At the 0 time point 2% galactose was added to induce *CLA4* overexpression, samples were taken every hour, and western blot analysis was performed. (E) Mid-logarithmic phase *GAL-STE20 VAC17-ProA* (Y_{CH}4843) was grown in SC-TRP+2% raffinose. At the 0 time point 2% galactose was added to induce *STE20* overexpression, samples were taken every hour, and western blot analysis was performed.

***CLA4* or *STE20* overexpression inhibits peroxisome but not late Golgi inheritance**

In addition to the yeast vacuole, Myo2 transports the late Golgi and peroxisomes along actin cables into the bud ^{18, 27}. I therefore investigated if *CLA4* or *STE20* overexpression perturbed either late Golgi or peroxisome inheritance as they had vacuole inheritance.

Inheritance of the late Golgi was investigated by examination of *SEC7-GFP* cells. The *SEC7* gene codes for a guanine nucleotide exchange factor (GEF) for ADP ribosylation factors and is found on Golgi associated vesicles and serves a marker for the late Golgi ¹⁸. Inheritance of the late Golgi is not an essential process, and in the absence of transport into the bud late Golgi is made *de novo*. Therefore, I used standard criteria for assaying late Golgi inheritance relying on the examination of small buds of various sizes ¹⁸. Overexpression of either *CLA4* or *STE20* had no effects on the inheritance of the late Golgi in comparison to wild type cells (Figure 3-7A,C).

Inheritance of peroxisomes was examined using *GFP* fused in frame with the peroxisome localization signal, *PTS1* ¹⁹. Cultures of wild type, *GAL-CLA4*, and *GAL-STE20* cells were grown under inducing conditions and peroxisome inheritance was examined by fluorescence microscopy. Peroxisome transport into buds of different sizes was quantified using established criteria ^{19, 27}. While wild type cells inherit peroxisomes, *GAL-CLA4* cells showed a severe peroxisome inheritance defect with only 25% of large budded cells having peroxisomes (Figure 3-7B,D). By comparison 30% of type IV cells lacking the peroxisome-specific Myo2 receptor Inp2 inherit a peroxisome ²⁷.

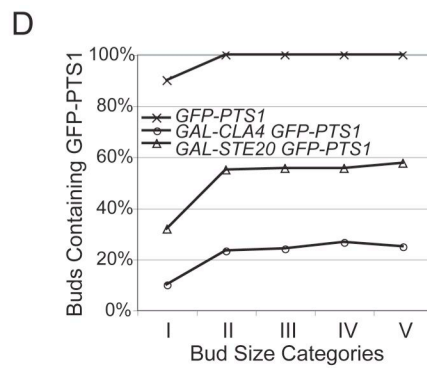
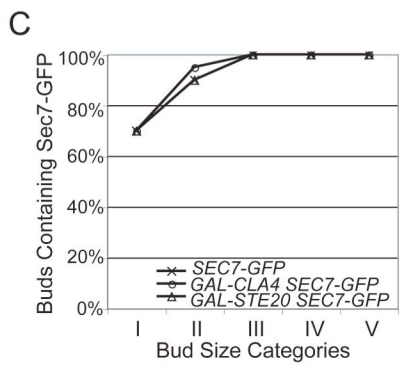
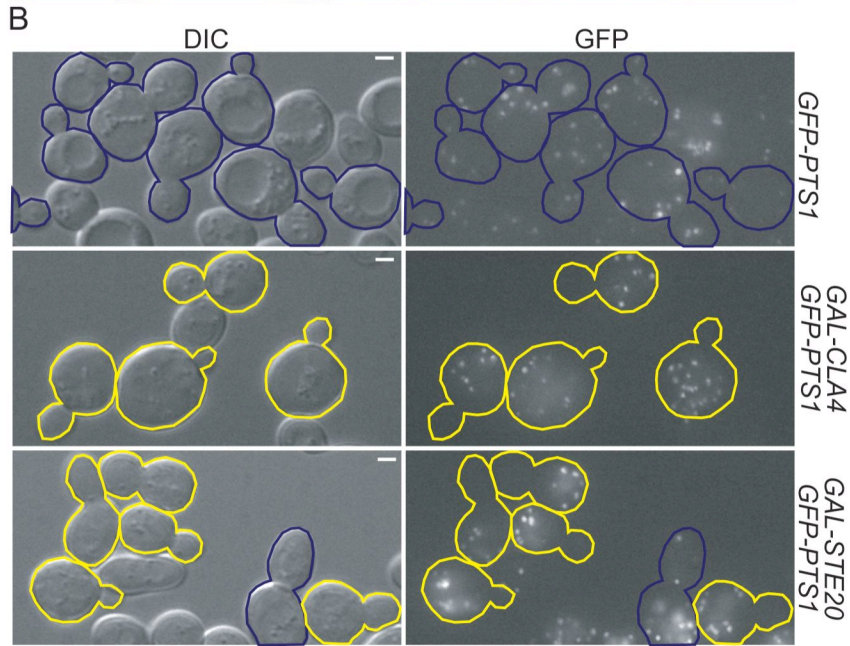
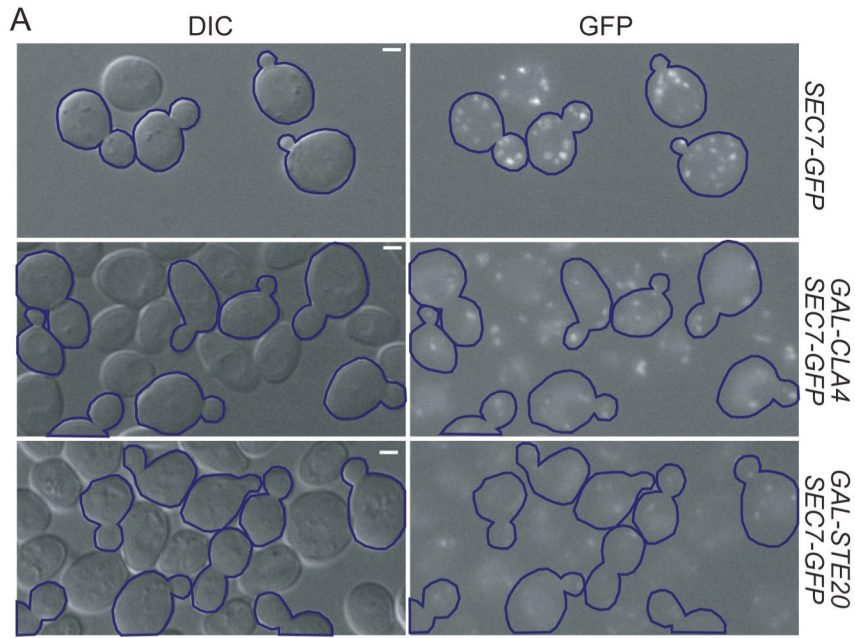


Figure 3-7. PAK overexpression inhibits peroxisome but not late Golgi inheritance.

(A) *SEC7-GFP* (Y_{CH}4978), *GAL-CLA4 SEC7-GFP* (Y_{CH}4979), *GAL-STE20 SEC7-GFP* (Y_{CH}4980), (B) *GFP-PTS1* (Y_{CH}4914), *GAL-CLA4 GFP-PTS1* (Y_{CH}4912), and *GAL-STE20 GFP-PTS1* (Y_{CH}4913) were grown in SC or SC-URA +2% raffinose/ 2% galactose for 6 hours for wild type and *GAL-STE20* and 12 hours for *GAL-CLA4* cells. Sec7-GFP and GFP-PTS1 were visualized by fluorescence microscopy. (C-D) Quantization of Sec7-GFP and GFP-PTS1 inheritance was done as described in Materials and Methods.

GAL-STE20 overexpressing cells also have a peroxisome inheritance defect with only 58% of large budded cells having peroxisomes in the bud (Figure 3-7B,D). Thus *STE20* overexpression caused a substantial, but lesser, inhibition of peroxisome inheritance in comparison to *CLA4* overexpression.

Discussion

Organelles are often localized to specific areas of the cell, placing them in the correct locale to perform their function and in correct spatial relation to other organelles. In order to be localized correctly, many organelles are actively transported along the actin or microtubule cytoskeletons by motor proteins. While many aspects of organelle transport are understood, there are still many unanswered questions about the delivery process. (1) How does the organelle ensure that once it has reached its destination that it is not subsequently transported to an incorrect location when it comes in contact with other motor proteins or when the cytoskeleton rearranges? (2) How does the transport complex and organelle know that they have arrived at the correct destination?

Studies in budding yeast focusing on vacuole transport during cell division have provided insights into these questions. Transport of vacuoles occurs during a short span of time from the time of budding to mitosis. Transportation is restricted to this brief period of time in part by carefully controlling the production and destruction of the vacuole specific myosin receptor Vac17. Transcription of *VAC17* oscillates with the cell cycle increasing very early in the cell cycle and subsequently decreasing^{28, 29}. Vac17 protein level parallel its RNA level and increase as cells begin budding (Figure 3-5C)¹. Once Vac17 accumulates, the vacuole transport complex consisting of Myo2, Vac17, and Vac8 assembles, the segregation structure forms, and it is transported into the bud.

Once it has arrived in the bud the segregation structure is resolved possibly by fusion of tubules and vesicles making up the segregation structure to

found the daughter vacuole. The cell ensures that the vacuole, which has already arrived at its correct destination, is not incorrectly repositioned after mitotic exit, when the actin cytoskeleton rearranges at the mother bud neck, by degrading Vac17 during late-M phase (Figure 3-5) ¹. The degradation of Vac17 requires transport of Vac17 into the bud as *vac8* and *myo2-2* accumulate high levels of Vac17.

However, how does the vacuole know it has arrived at its destination in the first place? This question may be answered by answering another question about Vac17. How is bud-specific degradation of Vac17 achieved? It has been proposed that factors specifically localized to or activated in the bud promote the bud-specific degradation of Vac17 thus acting as destination markers ³.

I have shown here that the p21-activated kinases *CLA4* and *STE20* regulate vacuole inheritance (Figure 3-3,4). Both *CLA4* and *Ste20* are localized to the bud thus spatially separating them from the forming segregation structure ^{4-6, 8}. Additionally, *Cla4* and *Ste20* are normally kept inactive by autoinhibition relieved by binding the activated Rho-GTPase *Cdc42* ³⁰⁻³⁵. I propose a model in which *Cla4* and *Ste20* localization and activation in the bud marks the bud as the destination for the transported vacuole. Upon entry of the segregation structure into the bud, the vacuole transport complex comes into contact with activated *Cla4* and *Ste20*, or proteins activated by *Cla4* and *Ste20* phosphorylation, that prime Vac17 for degradation (Figure 3-8). In this study I have provided multiple experimental lines of evidence supporting this model.

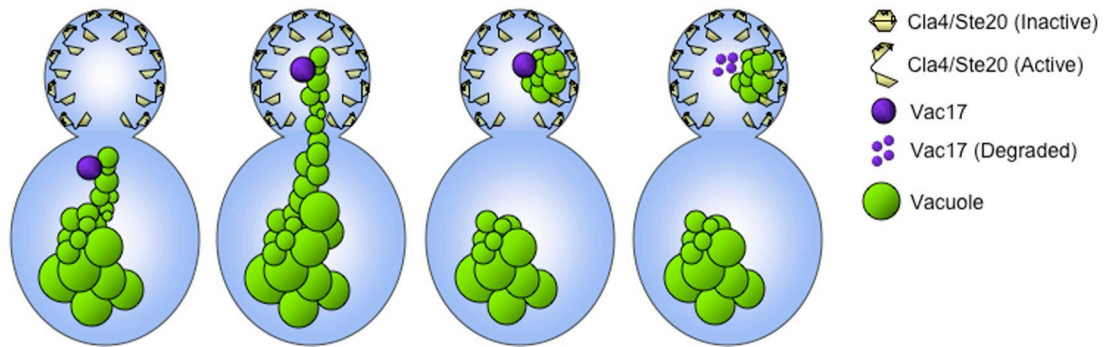


Figure 3-8. Model for PAK priming of Vac17 for degradation.

Vac17 acts within the mother cell to transport the segregation structure into the bud. After entering the bud Vac17 comes into contact with Cla4 and Ste20 localized to and activated specifically in the bud that prime Vac17 for degradation prior to cytoskeletal rearrangements towards the mother bud neck in preparation for cytokinesis.

Overexpression of either *CLA4* or *STE20* led to vacuole inheritance defects (Figure 3-3,4). Overexpression of the PAKs may have led to Cla4 and Ste20 localizing in the mother. In support of this I found that *GFP-CLA4* when overexpressed was easily seen in both the mother and daughter cytoplasm (data not shown). Additionally Cla4 and Ste20 could potentially be activated at the mother vacuole where Cdc42 is constitutively localized³⁶⁻³⁸. In further support of this possibility, the scaffolding protein Bem1 that brings together Cdc42 with its guanine nucleotide exchange factor (GEF) Cdc24^{39, 40} is localized to the vacuole where it plays a role with Cdc42 to promote homotypic vacuole fusion^{41, 42}. Cla4 and Ste20 bind directly to the second SH3 domain of Bem1^{10, 43-45} therefore bringing it into the proximity of the Cdc42 allowing potential PAK activation. Thus overexpression of PAKs disrupts the spatial separation necessary for the bud-specific degradation of Vac17.

Overexpression of *CLA4* led to the enhanced degradation of Vac17 (Figure 3-6C) and the timing of this degradation coincides temporally with the

vacuole inheritance defect (Figure 3-3C). However, *STE20* overexpression did not cause a decrease in Vac17 levels (Figure 3-6E). Several explanations can be given for this phenomenon. I noticed throughout my experiments that *CLA4* overexpression had more pronounced effect than *STE20* overexpression on either vacuole or peroxisome inheritance. *STE20* overexpressing cells must still have some Vac17 around since 18% of the cells still inherit vacuoles (Figure 3-4B). The remaining 82% of cells may have some Vac17 but not enough to inherit a vacuole. Thus one explanation of the difference between *CLA4* and *STE20* overexpression to degrade Vac17 may simply be that Cla4 is much more effective at promoting Vac17 degradation. Additionally the unaltered levels of Vac17 in *STE20* overexpressing cells do not preclude the possibility that *STE20* overexpression promotes Vac17 destruction as these cells have a vacuole inheritance defect but still do not accumulate Vac17 to high levels as in *myo2-2* and *vac8* cells ¹. Alternatively *STE20* overexpression may abrogate vacuole inheritance through a different mechanism, possibly by promoting homotypic vacuole fusion.

Despite the possibility that PAKs may regulate vacuole inheritance through vacuole fusion, the data suggests a more direct connection between PAKs and Vac17 degradation. I found that expression of *vac17 Δ PEST* suppressed the vacuole inheritance defects of cells overexpressing *CLA4* or *STE20* (Table 3-3). This data combined with my finding that PAK deficient cells do not degrade Vac17 during Late-M (Figure 3-6B), a time in which Vac17 is

usually degraded, argue for a model in which PAKs are the daughter-specific factors that promote Vac17 degradation.

How might Cla4 and Ste20 promote Vac17 degradation? The kinase activity of Ste20 is required for the vacuole inheritance defect seen in *STE20* overexpressing cells (data not shown). Therefore Cla4 and Ste20 might directly phosphorylate Vac17 priming it for destruction. Vac17 is phosphorylated in cells overexpressing *CLA4t*, suggesting that PAKs regulation may be indirect. Further research is therefore required to understand how PAKs regulate vacuole inheritance and Vac17 degradation.

During the course of my studies I found evidence that Cla4 and Ste20 might also regulate the inheritance of other organelles. Overexpression of Cla4 and Ste20 did not inhibit late Golgi inheritance. The finding that late Golgi was inherited with a normal efficiency suggested that PAK overexpression does not generally affect the transport of all Myo2 cargo. Interestingly, PAK overexpression did inhibit inheritance of peroxisomes. Therefore the mechanisms that regulate vacuole inheritance may provide useful information on the regulation of organelle inheritance more generally. Peroxisomes are transported along actin cables by Myo2 bound to the peroxisome-specific Myo2 receptor Inp2. Similar to Vac17, Inp2 production is cell cycle regulated and Inp2 destruction occurs prior to cytokinesis. Further research is required to determine if Inp2 degradation is regulated by Cla4 and Ste20 in a similar fashion to Vac17.

References

1. Tang, F. et al. Regulated degradation of a class V myosin receptor directs movement of the yeast vacuole. *Nature* (2003).
2. Ishikawa, K. et al. Identification of an organelle-specific myosin V receptor. *J Cell Biol* **160**, 887-97 (2003).
3. Weisman, L.S. Yeast vacuole inheritance and dynamics. *Annu Rev Genet* **37**, 435-60 (2003).
4. Holly, S.P. & Blumer, K.J. PAK-family kinases regulate cell and actin polarization throughout the cell cycle of *Saccharomyces cerevisiae*. *J Cell Biol* **147**, 845-56 (1999).
5. Huh, W.K. et al. Global analysis of protein localization in budding yeast. *Nature* **425**, 686-91 (2003).
6. Richman, T.J. & Johnson, D.I. *Saccharomyces cerevisiae* cdc42p GTPase is involved in preventing the recurrence of bud emergence during the cell cycle. *Mol Cell Biol* **20**, 8548-59 (2000).
7. Hallett, M.A., Lo, H.S. & Bender, A. Probing the importance and potential roles of the binding of the PH-domain protein Boi1 to acidic phospholipids. *BMC Cell Biol* **3**, 16 (2002).
8. Peter, M., Neiman, A.M., Park, H.O., van Lohuizen, M. & Herskowitz, I. Functional analysis of the interaction between the small GTP binding protein Cdc42 and the Ste20 protein kinase in yeast. *Embo J* **15**, 7046-59 (1996).
9. Thomas, B.J. & Rothstein, R. Elevated recombination rates in transcriptionally active DNA. *Cell* **56**, 619-30 (1989).
10. Gulli, M.P. et al. Phosphorylation of the Cdc42 exchange factor Cdc24 by the PAK-like kinase Cla4 may regulate polarized growth in yeast. *Mol Cell* **6**, 1155-67 (2000).
11. Burke, D., Dawson, D. & Stearns, T. Methods in yeast genetics: a Cold Spring Harbor Laboratory course manual (Cold Spring Harbor Laboratory Press, Cold Spring Harbor, 2000).
12. Aitchison, J.D., Rout, M.P., Marelli, M., Blobel, G. & Wozniak, R.W. Two novel related yeast nucleoporins Nup170p and Nup157p: complementation with the vertebrate homologue Nup155p and functional interactions with the yeast nuclear pore-membrane protein Pom152p. *J Cell Biol* **131**, 1133-48 (1995).
13. Sambrook, J. & Russell, D.W. Molecular Cloning: a laboratory manual (Cold Spring Harbor Laboratory Press, Cold Spring Harbor, 2001).
14. Sikorski, R.S. & Hieter, P. A system of shuttle vectors and yeast host strains designed for efficient manipulation of DNA in *Saccharomyces cerevisiae*. *Genetics* **122**, 19-27 (1989).
15. Waddle, J.A., Karpova, T.S., Waterston, R.H. & Cooper, J.A. Movement of cortical actin patches in yeast. *J Cell Biol* **132**, 861-70 (1996).
16. Vida, T.A. & Emr, S.D. A new vital stain for visualizing vacuolar membrane dynamics and endocytosis in yeast. *J Cell Biol* **128**, 779-92 (1995).

17. Saito, T.L. et al. SCMD: Saccharomyces cerevisiae Morphological Database. *Nucleic Acids Res* **32**, D319-22 (2004).
18. Rossanese, O.W. et al. A role for actin, Cdc1p, and Myo2p in the inheritance of late Golgi elements in Saccharomyces cerevisiae. *J Cell Biol* **153**, 47-62 (2001).
19. Fagarasanu, M., Fagarasanu, A., Tam, Y.Y., Aitchison, J.D. & Rachubinski, R.A. Inp1p is a peroxisomal membrane protein required for peroxisome inheritance in Saccharomyces cerevisiae. *J Cell Biol* **169**, 765-75 (2005).
20. Cheng, L., Hunke, L. & Hardy, C.F. Cell cycle regulation of the Saccharomyces cerevisiae polo-like kinase cdc5p. *Mol Cell Biol* **18**, 7360-70 (1998).
21. Heinrich, M., Kohler, T. & Mosch, H.U. Role of Cdc42-Cla4 interaction in the pheromone response of Saccharomyces cerevisiae. *Eukaryot Cell* **6**, 317-27 (2007).
22. Keniry, M.E. & Sprague, G.F., Jr. Identification of p21-activated kinase specificity determinants in budding yeast: a single amino acid substitution imparts Ste20 specificity to Cla4. *Mol Cell Biol* **23**, 1569-80 (2003).
23. Cohen-Fix, O., Peters, J.M., Kirschner, M.W. & Koshland, D. Anaphase initiation in Saccharomyces cerevisiae is controlled by the APC-dependent degradation of the anaphase inhibitor Pds1p. *Genes Dev* **10**, 3081-93 (1996).
24. de Bettignies, G. & Johnston, L.H. The mitotic exit network. *Curr Biol* **13**, R301 (2003).
25. McCollum, D. & Gould, K.L. Timing is everything: regulation of mitotic exit and cytokinesis by the MEN and SIN. *Trends Cell Biol* **11**, 89-95 (2001).
26. Chirolì, E. et al. Budding yeast PAK kinases regulate mitotic exit by two different mechanisms. *J Cell Biol* **160**, 857-74 (2003).
27. Fagarasanu, A., Fagarasanu, M., Eitzen, G.A., Aitchison, J.D. & Rachubinski, R.A. The peroxisomal membrane protein Inp2p is the peroxisome-specific receptor for the myosin V motor Myo2p of Saccharomyces cerevisiae. *Dev Cell* **10**, 587-600 (2006).
28. Zhu, G. et al. Two yeast forkhead genes regulate the cell cycle and pseudohyphal growth. *Nature* **406**, 90-4 (2000).
29. Spellman, P.T. et al. Comprehensive identification of cell cycle-regulated genes of the yeast Saccharomyces cerevisiae by microarray hybridization. *Mol Biol Cell* **9**, 3273-97 (1998).
30. Ramer, S.W. & Davis, R.W. A dominant truncation allele identifies a gene, STE20, that encodes a putative protein kinase necessary for mating in Saccharomyces cerevisiae. *Proc Natl Acad Sci U S A* **90**, 452-6 (1993).
31. Leberer, E., Dignard, D., Harcus, D., Thomas, D.Y. & Whiteway, M. The protein kinase homologue Ste20p is required to link the yeast pheromone response G-protein beta gamma subunits to downstream signalling components. *Embo J* **11**, 4815-24 (1992).

32. Lamson, R.E., Winters, M.J. & Pryciak, P.M. Cdc42 regulation of kinase activity and signaling by the yeast p21-activated kinase Ste20. *Mol Cell Biol* **22**, 2939-51 (2002).
33. Benton, B.K., Tinkelenberg, A., Gonzalez, I. & Cross, F.R. Cla4p, a *Saccharomyces cerevisiae* Cdc42p-activated kinase involved in cytokinesis, is activated at mitosis. *Mol Cell Biol* **17**, 5067-76 (1997).
34. Lei, M. et al. Structure of PAK1 in an autoinhibited conformation reveals a multistage activation switch. *Cell* **102**, 387-97 (2000).
35. Tu, H. & Wigler, M. Genetic evidence for Pak1 autoinhibition and its release by Cdc42. *Mol Cell Biol* **19**, 602-11 (1999).
36. Richman, T.J., Sawyer, M.M. & Johnson, D.I. *Saccharomyces cerevisiae* Cdc42p localizes to cellular membranes and clusters at sites of polarized growth. *Eukaryot Cell* **1**, 458-68 (2002).
37. Muller, O., Johnson, D.I. & Mayer, A. Cdc42p functions at the docking stage of yeast vacuole membrane fusion. *Embo J* **20**, 5657-65 (2001).
38. Eitzen, G., Wang, L., Thorngren, N. & Wickner, W. Remodeling of organelle-bound actin is required for yeast vacuole fusion. *J Cell Biol* **158**, 669-79 (2002).
39. Zheng, Y., Bender, A. & Cerione, R.A. Interactions among proteins involved in bud-site selection and bud-site assembly in *Saccharomyces cerevisiae*. *J Biol Chem* **270**, 626-30 (1995).
40. Toenjes, K.A., Sawyer, M.M. & Johnson, D.I. The guanine-nucleotide-exchange factor Cdc24p is targeted to the nucleus and polarized growth sites. *Curr Biol* **9**, 1183-6 (1999).
41. Han, B.K. et al. Bem1p, a scaffold signaling protein, mediates cyclin-dependent control of vacuolar homeostasis in *Saccharomyces cerevisiae*. *Genes Dev* **19**, 2606-18 (2005).
42. Xu, H. & Wickner, W. Bem1p is a positive regulator of the homotypic fusion of yeast vacuoles. *J Biol Chem* **281**, 27158-66 (2006).
43. Leeuw, T. et al. Interaction of a G-protein beta-subunit with a conserved sequence in Ste20/PAK family protein kinases. *Nature* **391**, 191-5 (1998).
44. Winters, M.J. & Pryciak, P.M. Interaction with the SH3 domain protein Bem1 regulates signaling by the *Saccharomyces cerevisiae* p21-activated kinase Ste20. *Mol Cell Biol* **25**, 2177-90 (2005).
45. Bose, I. et al. Assembly of scaffold-mediated complexes containing Cdc42p, the exchange factor Cdc24p, and the effector Cla4p required for cell cycle-regulated phosphorylation of Cdc24p. *J Biol Chem* **276**, 7176-86 (2001).

CHAPTER IV

THE P21-ACTIVATED KINASES CLA4 AND STE20 ARE REQUIRED FOR RESOLUTION OF THE VACUOLE SEGREGATION STRUCTURE

Abstract

Each time budding yeast divide they ensure that both the mother and daughter cell inherit a vacuole. Because budding yeast divide asymmetrically by budding, the vacuole must be actively transported into the bud. As the mother cell begins budding, a tubular and vesicular segregation structure forms which is transported into the bud^{1, 2}. Formation of the segregation requires the inhibition of vacuole fusion and production of PtdIns(3,5)P₂, which usually promotes vacuole fission³⁻⁵. The segregation structure is transported into the bud along actin cables by the myosin V motor, Myo2. Upon arriving in the bud the segregation structure is resolved to form the daughter vacuole. How the segregation structure is resolved in a spatially dependent manner after entering the bud is unknown. During my investigation I found the p21-activated kinase (PAK) Cla4 localized to the segregation structure just prior to segregation structure resolution. In addition I showed that cells lacking active PAKs failed to resolve the segregation structure. I propose that Cla4 and Ste20 localize to the bud where they promote segregation structure resolution.

Introduction

The yeast vacuole is partitioned into the bud along polarized actin cables⁶. Partitioning begins late in G1, continues through S phase, and is finished by the onset of mitosis⁷. Vacuole movement is mediated by the myosin V receptor, Vac17, which interacts with both Myo2 and the vacuole membrane protein, Vac8^{8, 9}. This complex of three proteins transports the segregation structure into the bud. Upon entry into the bud the tubules and vesicles making up the segregation structure are resolved in what likely involves fusion to form the daughter vacuole¹⁰⁻¹⁴. The mechanisms that promote the fusion of the tubules and vesicles in a spatially dependent manner specifically in the bud are not known.

The p21-activated kinases (PAKs) Cla4 and Ste20 localize specifically to the bud. Cla4 has been shown to localize to isolated vacuoles and *cla4* mutants have a fragmented vacuole, a hallmark of mutants defective for vacuole fusion¹⁵,¹⁶. Vacuole fusion requires actin polymerization and Cla4 and Ste20 promote actin polymerization through phosphorylation of Myo3 and Myo5¹⁷⁻²⁰. Ste20 and Cla4 have overlapping functions and double mutants lacking both functions are delayed in metaphase and are synthetically lethal^{21, 22}. I here report that Cla4 localized to the segregation structure after it enters the bud and just prior to resolution of the segregation structure, placing it at the right place at the right time to promote segregation structure resolution. Additionally, I have shown that in the absence of PAK function that the segregation structure was formed, was transported into the bud, but the segregation structure failed to resolve.

Materials and Methods

Strains, plasmids, and media

Details of yeast strains and plasmids used in this study can be found in Table 4-1. The yeast strains used in this study are all derivatives of W303 except for the *CLA4-GFP* strains (BY4741 derivatives). Yeast strains were grown in YPD (1% yeast extract, 2% peptone, and 2% glucose, raffinose or raffinose/galactose).

Table 4-1. Strains

Strain	Genotype	Source
FM452	<i>MATa cdc34-2</i> (W303)	23
K2944-1B	<i>MATa cdc15-2</i> (W303)	24
KN3591	<i>MATa cla4::LEU2</i> (W303)	21
KN3621	<i>MATa ste20::URA3</i> (W303)	21
KN4580	<i>MATa bar1::hisG cla4::LEU2 YCp-TRP1-cla4-75 ste20::URA3</i>	21
Piatti2625	<i>MATa ura3::4X URA3::GAL1-CLA4t</i> (W303)	22
Piatti2711	<i>MATa ura3::4X URA3::GAL1-CLA4t swe1::LEU2</i> (W303)	22
RSY136	<i>MATa ura3::GAL-SWE1-12Myc-URA3</i> (W303)	25
W303-1A	<i>MATa ade2-1 his3-11,15 leu2-3,112 trp1-1 ura3-1</i> (W303)	26
Y _{CH} 146	<i>MATa cdc14-2</i> (W303)	This Study
Y _{CH} 1028	<i>MATa cdc15-2 CLA4-GFP</i> (S88c)	This Study
Y _{CH} 1665	<i>MATa vac8::kanMX4 CLA4-GFP</i> (S88c)	This Study
Y _{CH} 1752	<i>MATa myo2-2 CLA4-GFP</i> (S88c)	This Study
Y _{CH} 3250	<i>MATa CLA4-GFP</i> (S88c)	This Study
Y _{CH} 5233	<i>MATa cdc7-4 ura3::URA3::3xGAL-CLA4t</i> (W303)	This Study
Y _{CH} 5342	<i>MATa vac8::kanMX4</i> (W303)	This Study

Synchronization and cell cycle arrests

Conditions for growth and release of synchronous cultures from arrest by α -factor were as described with α -factor (ZymoResearch) used at a final concentration of 3 μ M²⁷. Centrifugal elutriation was performed in a Beckman-Coulter type J centrifuge as recommended by Beckman-Coulter and as described²⁸. Fractions with greater than 98% unbudded cells were pooled and

used for each experiment. Cell cycle arrests were performed by addition of hydroxyurea (Sigma) or nocodazole (Sigma) at the final concentration of 200 mM or 15 $\mu\text{g/ml}$ respectively as described or by shifting temperature sensitive mutants from the permissive temperature (23°C) to the nonpermissive temperature (37°C) for three hours.

Microscopy

Images were acquired using two microscopes. All images, with the exception of those for Figure 2A and Figure 4, were taken using a microscope (BX60; Olympus) with a UPlanApo 100x NA 1.30 oil immersion objective (Olympus) and a camera (DAGE ISIT-68) using NIH image 1.62 (Wayne Rasband). Images for Figure 2A and Figure 4 were acquired using a microscope (BX50; Olympus) with a UPlanF1 100x NA 1.30 oil immersion objective (Olympus) and a camera (CoolSNAP HQ; Photometrics). Images were collected using MetaVue version 4.6 (Molecular Devices). GFP was visualized using an X-cite 120-UV lamp and a Chroma filter set. Within each experiment, all images were collected and scaled identically. Images were processed with Photoshop 9.0 software (Adobe). Small, medium and large budded cells were grouped into size categories as described²⁹. Scale bar = 2.5 μm throughout all figures.

In vivo labeling of vacuoles

To visualize vacuoles, yeast cells were concentrated and incubated for 1 hour with N-(3-triethylammoniumpropyl)-4(6(4(diethylamino)phenyl)hexatrienyl)

pyridium dibromide (FM 4-64; Molecular Probes) at a final concentration of 16.5 mM. Cells were then washed with appropriate media and grown for ≥ 3 hours before being viewed by fluorescence microscopy³⁰.

***In vivo* fusion assay**

In vivo fusion assays were performed as described³¹. In brief flow cells were prepared by treating coverslips and slides with concanavalin-A (1mg/ml in 50 mM HEPES, pH 7.5, 20mM calcium acetate, and 1 mM MnSO₄) that were then allowed to air-dry. Coverslips were attached to slides using double-sided tape. FM 4-64 stained cells grown in YPD as described were harvested in a microcentrifuge at 10,000 rpm for 15 seconds. Cells were introduced into the flow cell and incubated for 5 minutes. A hypertonic solution of 25% yeast extract/peptone/dextrose, 75% H₂O was flushed through the flow cell and images were taken at the indicated times.

Results

Cell cycle progression is not required for segregation structure resolution

Prior studies reported that the vacuole segregation structure is resolved to form the daughter vacuole prior to nuclear division ⁷. I found that cells arrested in late G1 uniformly inherited and formed a daughter vacuole (Figure 4-1). Additionally cells arrested in S-Phase by HU, at G2/M by either overexpression of *SWE1* or NZ treatment, or at telophase using the temperature sensitive MEN mutants *cdc15-2* or *cdc14-2* formed daughter vacuoles. Thus, the determinants for daughter vacuole formation are set up early in the cell cycle.

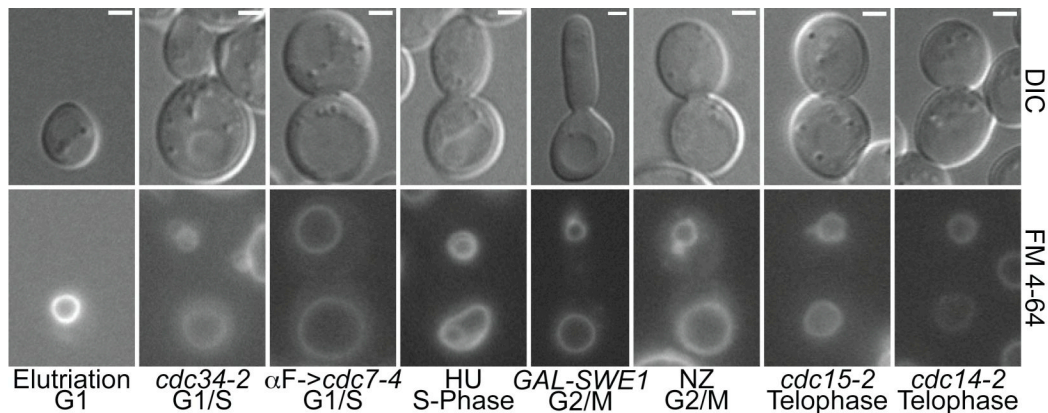


Figure 4-1. Cell cycle progression is not required for segregation structure resolution. Cells were stained with FM 4-64 to visualize vacuoles. G1/S cells were obtained by growth of *cdc34-2* (FM452) cells at 37°C or α -factor arrest release of *cdc7-4* cells ($Y_{CH}5233$) into 37°C media. S-phase arrested cells were obtained by hydroxyurea (HU) (W303-1A) treatment. G2/M cells were obtained by either nocodazole (NZ) (W303-1A) treatment or by α -factor arrest of *GAL-SWE1* (RSY136), followed by induction of *SWE1* overexpression by the addition of 2% galactose for 60 minutes, and released into YP+2% galactose media for 120 minutes. Telophase arrested cells were obtained by arresting *cdc15-2* (K2944-1B) and *cdc14-2* ($Y_{CH}146$) strains at 37°C.

Cla4 localizes to the vacuole segregation structure

In addition to its reported localization at the bud cortex, I found that Cla4 localized to a non cortex localized punctate structure within the buds of small,

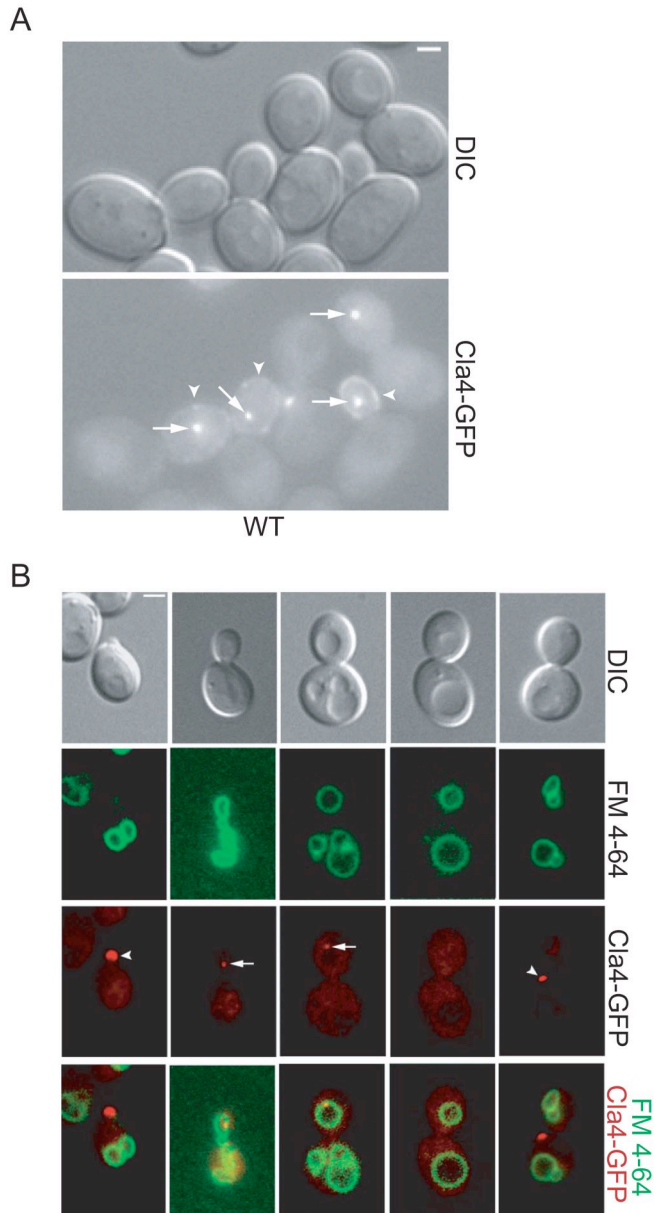


Figure 4-2. Cla4 localizes with the vacuole.

(A) Cla4-GFP was visualized in asynchronous Wild type (Y_{CH3250}) cells. Arrows indicate perivacuolar Cla4-GFP localization and arrowheads indicate cortex localization. (B) *CLA4-GFP* (Y_{CH3250}) cells were FM 4-64 stained and examined by fluorescent microscopy

medium, and some large budded cells (Figure 4-2A). Biochemical studies indicate that Cla4 is enriched on isolated vacuoles¹⁵. Therefore, I postulated that the Cla4 punctate structure might colocalize with the vacuole. To determine if Cla4 colocalized with the vacuole, *CLA4-GFP* strains were FM 4-64 stained. I

found that in 100% of cells in which the punctate Cla4-GFP structure was visualized that it colocalized with the segregation structure or the daughter vacuole (Figure 4-2B).

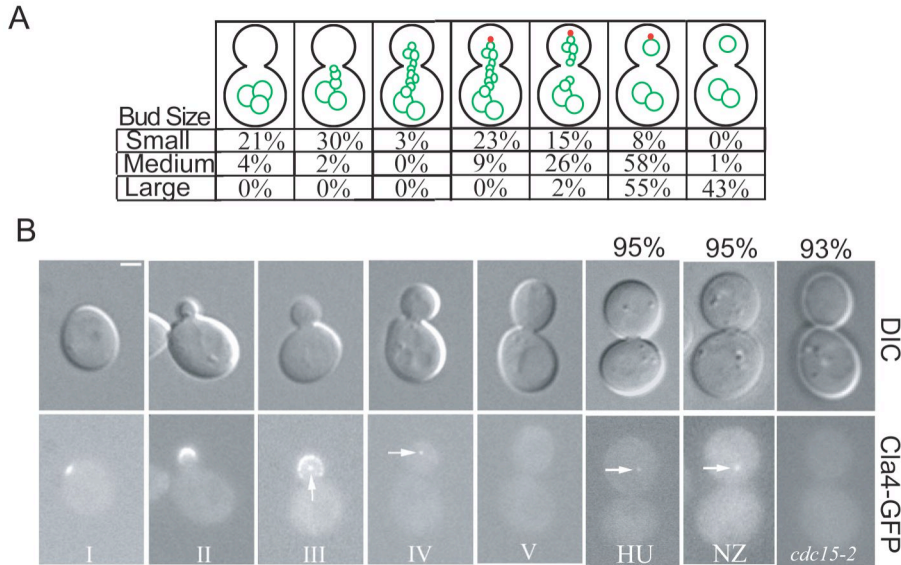


Figure 4-3. Cla4 remains on the daughter vacuole until late-M phase.

(A) Cla4-GFP (Y_{CH3250}) and FM 4-64 stained vacuole localization was quantified in small, medium, and large budded cells (>200 cells were counted for each bud size). (B) *CLA4-GFP* (Y_{CH3250}) localization was visualized in cells of various bud sizes and cells arrested in S-phase with hydroxyurea (HU), at G2/M with nocodazole (NZ), or at mitotic exit by arresting *cdc15-2* (Y_{CH1028}). Percentages indicate the percentage cells with the displayed Cla4-GFP localization.

Further quantification of the vacuole morphology and Cla4 localization to the vacuole showed that Cla4 localized to the vacuole almost immediately upon entry of segregation structure into the bud as only a very small percentage of cells with a segregation structure in the bud did not colocalize with Cla4 (Figure 4-3A). Most cells with Cla4 colocalizing with the vacuole had resolved the segregation structure and formed a daughter vacuole (Figure 4-3A). Cla4 persisted on the vacuole until late-M and cells arrested in S-phase or G2/M, but not at mitotic exit, had Cla4 spots in the bud (Figure 4-3B).

The machinery required to form and transport the segregation structure to the bud consists of a myosin V motor, Myo2, a vacuole receptor, Vac17, and a vacuole-associated protein, Vac8. I observed that cells that did not form vacuole segregation structures, including *vac8* and *myo2-2* mutants, lacked a Cla4 spot in the mother or bud (Figure 4-4). Thus, Cla4 localization at the vacuole was dependent on vacuole partitioning. Cla4 leaves the vacuole late in mitosis and localizes to the mother bud neck prior to cell separation (data not shown).

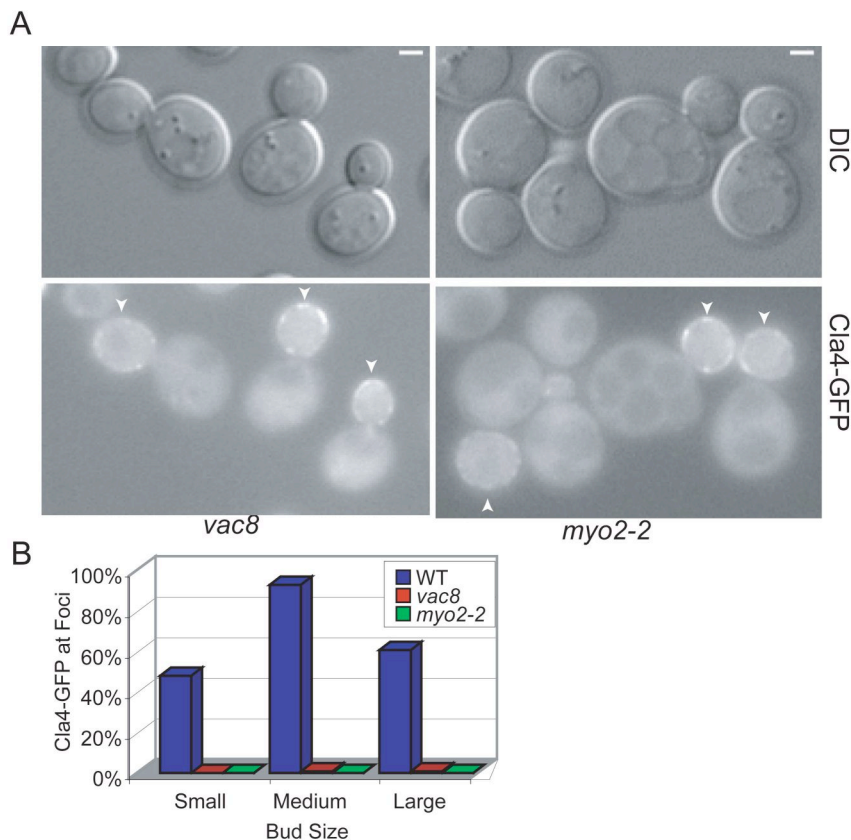


Figure 4-4. Cla4-GFP requires vacuole inheritance for vacuole associated punctate structure localization.

(A) Cla4-GFP was visualized in *vac8* (Y_{CH}1665) and *myo2-2* (Y_{CH}1752) cells. Arrowheads indicate Cla4-GFP localization at the cortex. (B) Cla4-GFP and FM 4-64 stained vacuole localization was quantified in small, medium, and large budded wild type (Y_{CH}3250), *vac8* (Y_{CH}1665), and *myo2-2* (Y_{CH}1752) cells (>200 cells were counted for each bud size).

Cla4 accumulation at the incipient bud site early in the cell cycle and its localization at the vacuole segregation structure prior to daughter vacuole

formation places Cla4 in right place at the right time to play a role in resolving the segregation structure.

PAKs are required for resolution of the vacuole segregation structure

Cla4 is proposed to have overlapping functions with the PAK, Ste20, as *cla4* and *ste20* single mutants are viable but the *cla4 ste20* double mutant is synthetically lethal ²¹. Consistent with these observations I found that *cla4* and *ste20* single mutants formed daughter vacuoles (Figure 4-5A). In order to characterize cells lacking both Cla4 and Ste20 function I used a *cla4-75 ste20* strain with mutant *cla4* and *ste20* kept alive by plasmid based expression of a temperature sensitive *cla4-75* allele ²¹. When grown at the permissive temperature, vacuoles in the *cla4-75 ste20* cells were similar to vacuoles in *ste20* cells (data not shown). After cells were synchronized by centrifugal elutriation in G1 and released at the restrictive temperature, the *cla4-75 ste20* double mutant cells initially were similar to wild type cells and formed a segregation structure that was directed toward the bud tip (Figure 4-5B,C). Strikingly, after 120 minutes, 98% of the *cla4-75 ste20* cells maintained the segregation structure (Figure 4-5C). After 240 minutes 95% of the cells arrested with an intact segregation structure (Figure 4-5D). This was in sharp contrast to wild type cells that resolve their segregation structures soon after they enter the bud (Figure 4-5B). The failure of the *cla4-75 ste20* cells to resolve the segregation structure is a novel phenotype.

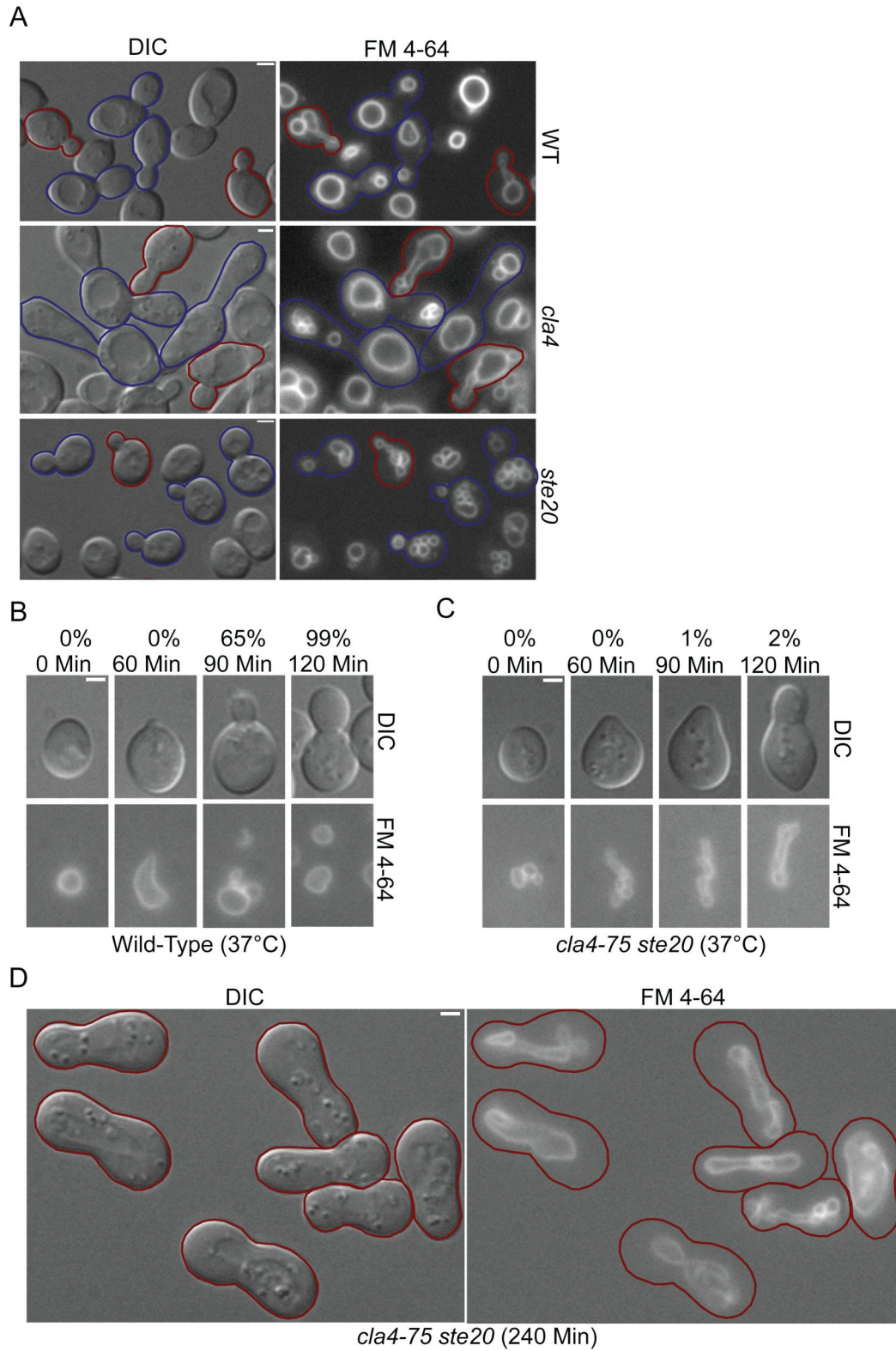


Figure 4-5. Cells lacking PAK function form but do not resolve segregation structures.

(A) Mid-logarithmic phase FM 4-64 stained wild type (W303-1A), *cla4* (KN3591), and *ste20* (KN3621) strains were examined by fluorescence microscopy. (B-D) Asynchronous FM 4-64 stained wild type (W303-1A) and *cla4-75 ste20* (KN4580) cells were elutriated to obtain a uniform population of G1 cells, grown at 37°C, and examined at the indicated times by fluorescence microscopy. Percentage in (B-C) are the percentage of cells with a daughter vacuole. Cell Outline Color Code, Red: bud contains segregation structure; Blue: bud has inherited vacuole material from mother cell; Yellow: medium or large bud lacking inherited vacuole material from mother cell.

Cells overexpressing *CLA4t* fail to form a daughter vacuole and have a partial *in vivo* vacuole fusion defect

Overexpression of truncated *CLA4* missing the final C-terminal 67 amino acids (*CLA4t*) causes mislocalization of both *Cla4* and *Ste20* and *CLA4t* overexpression likely inhibits both endogenous *Cla4* and *Ste20*²². Because *cla4-75 ste20* cells fail to form a daughter vacuole, I hypothesized that cells overexpressing *CLA4t* may also fail to form a daughter vacuole. In support of this hypothesis I found that FM 4-64 strained *4X GAL-CLA4* and *4X GAL-CLA4t swe1* cells arrested in G1 by the addition of α -factor and released into YP + 2% galactose media to induce the overexpression of *CLA4t* failed to form a daughter vacuole (data not shown and Figure 4-6).

It has previously been shown that vacuole fusion promotes the formation of the daughter vacuole^{5, 10-13}. In response to hyposmotic conditions vacuole lobes fuse to form a single large vacuole. Using an *in vivo* vacuole fusion assay the vacuole of *vac8* cells do not fuse under hypotonic conditions³¹. In support of these experiments I found that the vacuoles of wild type but not *vac8* cells fuses under hyposmotic conditions (Figure 4-6). However, the vacuoles in *4X GAL-CLA4t* and *4X GAL-CLA4t swe1* cells overexpressing *CLA4t* have a partial vacuole fusion defect in comparison to wild type cells (Figure 4-6). Therefore

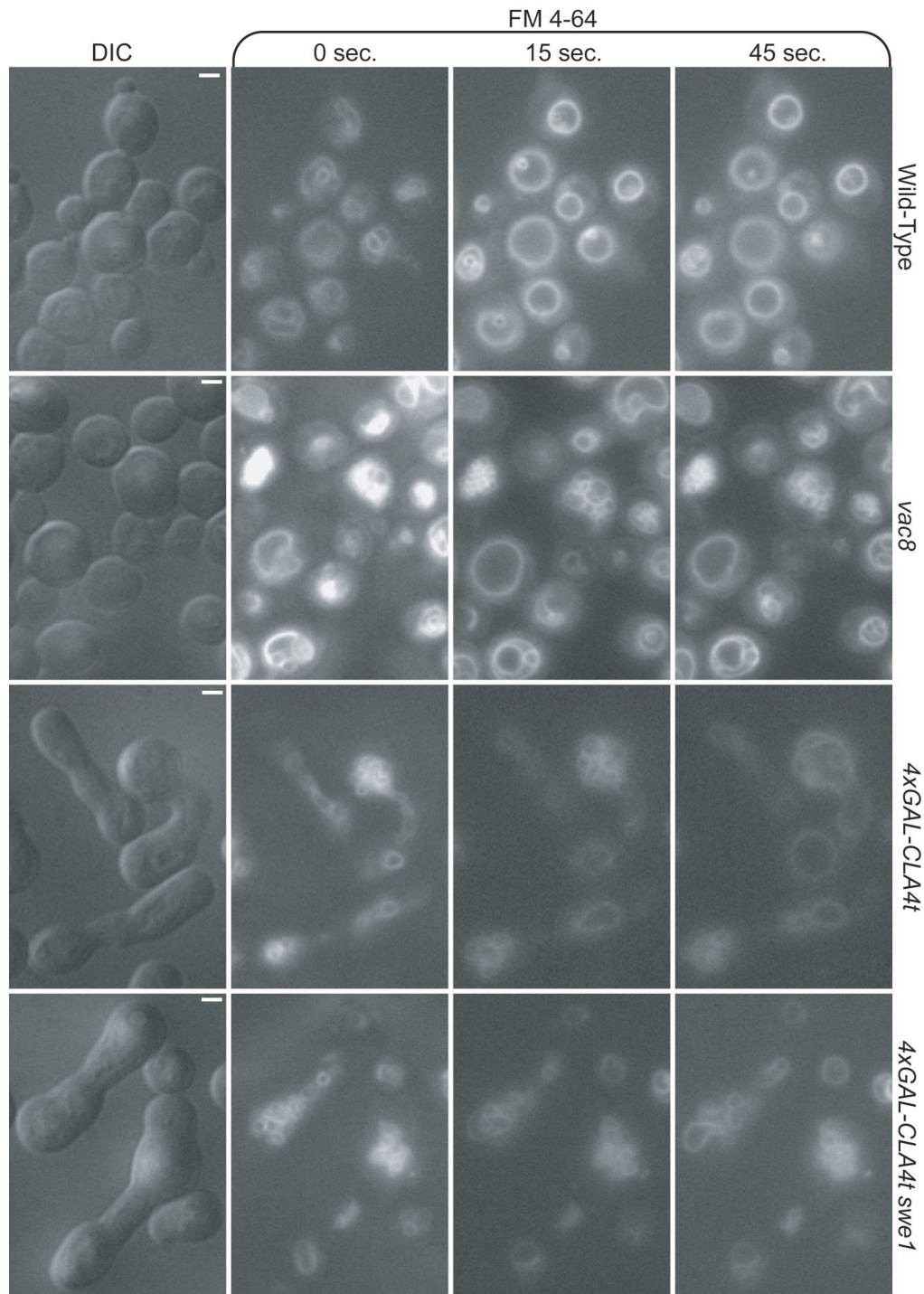


Figure 4-6. Cells overexpressing *CLA4t* fail to form a daughter vacuole and have a partial *in vivo* vacuole fusion defect.

Wild type (W303-1A), *vac8* (Y_{CH}5342), 4X *GAL-CLA4t* (Piatti2625), and 4X *GAL-CLA4t swe1* (Piatti2711) cells were grown in YP+ 2% raffinose and FM 4-64 stained. After staining 4X *GAL-CLA4t* and 4X *GAL-CLA4t swe1* were α -factor arrested and all strains were grown in YP+2% galactose for 4 hours and *in vivo* fusion assays were performed.

Cla4 and Ste20 may promote daughter vacuole formation by promoting vacuole fusion in the bud to promote segregation structure resolution.

Discussion

Over the last years various strides have been made in forming a model for how the segregation structure is resolved. Together the experimental data suggests that the segregation structure is resolved by the fusion of tubular and vesicular structures in the bud. The data that support this model are reviewed below. (1) Formation of the vacuole segregation structure requires PtdIns(3,5)P₂ production on the vacuole which promotes fission of the vacuole^{4, 32-36}. Since the production of the segregation structure requires the fission machinery, it has been postulated that upregulation of fusion or down regulating fission by decreasing the levels of PtdIns(3,5)P₂ promotes resolution of the segregation structure³⁷. (2) Examination of labeled vacuoles by microscopy showed transport of vesicular structures from the mother into the daughter and fusion of these vesicles to form a larger daughter vacuole¹⁰. (3) Studies of isolated vacuoles from semi-permeabilized cells show the formation of tubular and vesicular structures followed by vacuole fusion¹⁰⁻¹³. (4) Resolution of segregation structures in zygotes involves vacuole fusion and merging of vacuole contents¹⁴. (5) Formation of the segregation structure is promoted by Yck3 maintaining fragmentation through inhibition of homotypic vacuole fusion⁵.

Together these data suggest a model in which the segregation structure is formed by fission of the yeast vacuole. Fission is promoted by both production of

PtdIns(3,5)P₂ and the inhibition of fusion by Yck3. After the tubular and vesicular segregation structure is formed, the segregation structure is transported into the bud along actin cables. Finally, fusion of the tubules and vesicles in the bud leads to the resolution of the segregation structure and the founding of the bud daughter vacuole. Missing from this model of segregation structure formation and resolution, however, is a mechanism for not only promoting, but insuring, that the segregation structure is only resolved after arriving in the bud. Several potential models could exist to explain this spatial regulation of vacuole inheritance.

First, cell cycle progression could be responsible for regulating vacuole inheritance. In this model, fusion would be inhibited during S phase when vacuole inheritance takes place and is promoted during either G2 or M to resolve segregation structures. However, my results make this model unlikely because segregation structure resolution and fusion occurs in *cdc34-2* and *cdc7-4* arrested cells that fail to enter S-phase (Figure 4-1).

Second, segregation structure resolution could be caused by actin cable rearrangements. In budding yeast actin is polarized at the tip of the emerging bud but undergoes an apical-isotropic switch in G2 leading to depolarization of the actin cables caused by the accumulation of active Clb/CDK during G2. However, my results suggest this model is unlikely because cells overexpressing the Wee1 kinase in yeast (*Swe1*) arrest at G2 with elongated buds due to a failure to undergo the apical-isotropic switch³⁸⁻⁴⁰ but still have resolved segregation structures (Figure 4-1). Additionally, some common strain backgrounds of

budding yeast such as the S288c strain do not undergo an apical-isotropic switch yet still resolve segregation structures normally ⁴¹.

Third, degradation of Vac17 (the vacuole specific myosin-receptor necessary for vacuole inheritance) in the bud may also promote segregation structure resolution. However, this model is also unlikely since segregation structures are resolved prior to Vac17 degradation (Figure 4-1 and Figure 3-5)⁴².

Fourth, as has been proposed for Vac17 degradation ⁶, there may be factors specifically localized and/or activated in the bud that promote segregation resolution. Thus segregation structure resolution could be spatially controlled with resolution by vacuole fusion only taking place when the segregation structure enters the bud. Here I provide evidence supporting this model and propose that Cla4 and Ste20, which are specifically partitioned to and activated in the bud, promote the spatial regulation of segregation structure resolution.

I reported that Cla4 colocalized with the vacuole (Figure 4-2B). This, however, is not the first report of Cla4 localization to vacuole as others have previously identified Cla4 on isolated vacuoles ¹⁵. However, my findings add substantially to our understanding of the timing of Cla4 localization to the vacuole. I did see Cla4-GFP localized to the cortex of small, medium, and some large budded cells as previously reported ⁴³⁻⁴⁵. I additionally found that Cla4-GFP localized to segregation structures when they entered the bud. Almost every segregation structure that entered the bud and no segregation structures that had not entered the bud had Cla4-GFP localized to them (Figure 4-3A). I found that Cla4-GFP localization to the vacuole is dependent on the vacuole transport

machinery Vac8 and Myo2 (Figure 4-4A,B), further suggesting that Cla4-GFP localization to the vacuole is dependent on transport of vacuoles into the bud. Together these data demonstrate that Cla4 is at the right place at the right time to promote segregation structure resolution in a spatially dependent manner.

So how does Cla4 promote the resolution of the segregation structure? The current model for segregation structure resolution proposes that the segregation structure is resolved by homotypic vacuole fusion of tubules and vesicles. Intriguingly Cla4 has been implicated both directly and indirectly in vacuole fusion. Mutant cells lacking *CLA4* have fragmented vacuoles, a key indicator of a vacuole fusion defect^{15, 16}. Cdc42, the upstream regulator of both Cla4 and Ste20, is also required for vacuole fusion^{15, 46-48}. The adaptor protein Bem1, to which Boi1, Boi2, Cla4, and Ste20 bind, also promotes homotypic vacuole fusion^{47, 49}. Finally, vacuole fusion requires actin polymerization and Cla4 and Ste20 promote actin polymerization through phosphorylation of Myo3 and Myo5¹⁷⁻²⁰. I propose that Cla4 localizes to the segregation structure where it promotes homotypic vacuole fusion leading to resolution of the segregation structure. Ste20 may promote vacuole fusion when the segregation structure comes into contact with the bud cortex or is just localized to the vacuole at low levels below the detection limit by fluorescence microscopy.

In support of this model I found that a G1 population of *cla4-75 ste20* cells grown at the non-permissive temperature form and transport segregation structures into the bud but failed to resolve the segregation structure (Figure 4-5C,D). Additionally, the overexpression of a dominant negative Cla4t which is

thought to eliminate Cla4 and Ste20²² function also shows a similar phenotype further strengthening the model that PAK function is required for segregation structure resolution. Finally, the finding that cells overexpressing *CLA4t* have little vacuole fusion when placed in hypotonic conditions suggests that PAK function promotes fusion (Figure 4-6). However, this experiment must be interpreted with caution because the segregation structure could potentially be resistant to vacuole fusion. However, while hyposmotic conditions caused a regression or resolution of segregation structure in WT cells (data not shown), this was not the case for cells overexpressing *CLA4t* (Figure 4-6).

Study of segregation structures in yeast has been a daunting task due to this transient existence. Based on the rate of vacuole movement and the distance of travel, segregation structures can be around for as little as 30 seconds during the cell cycle⁶. During this 30 seconds a complex set of reactions has been proposed to occur, including the production of PtdIns(3,5)P₂⁶, the recruitment of PtdIns(3,5)P₂ binding proteins⁵⁰⁻⁵³, formation of the segregation structure, transport of the segregation structure into the bud, and fusion to resolve the segregation structure. The very transient nature of the segregation structure and the impossibility of reliably synchronizing a population with intact segregation structures have made further analysis of the segregation structure difficult if not impossible. The identification of vacuole segregation structure resolution mutants *cla4-75 ste20* and *4X GAL-CLA4t* may provide much the needed tool to further study these steps in vacuole inheritance.

References

1. Weisman, L.S., Bacallao, R. & Wickner, W. Multiple methods of visualizing the yeast vacuole permit evaluation of its morphology and inheritance during the cell cycle. *J Cell Biol* **105**, 1539-47 (1987).
2. Raymond, C.K., O'Hara, P.J., Eichinger, G., Rothman, J.H. & Stevens, T.H. Molecular analysis of the yeast VPS3 gene and the role of its product in vacuolar protein sorting and vacuolar segregation during the cell cycle. *J Cell Biol* **111**, 877-92 (1990).
3. Yamamoto, A. et al. Novel PI(4)P 5-kinase homologue, Fab1p, essential for normal vacuole function and morphology in yeast. *Mol Biol Cell* **6**, 525-39 (1995).
4. Bonangelino, C.J., Catlett, N.L. & Weisman, L.S. Vac7p, a novel vacuolar protein, is required for normal vacuole inheritance and morphology. *Mol Cell Biol* **17**, 6847-58 (1997).
5. LaGrassa, T.J. & Ungermann, C. The vacuolar kinase Yck3 maintains organelle fragmentation by regulating the HOPS tethering complex. *J Cell Biol* **168**, 401-14 (2005).
6. Weisman, L.S. Yeast vacuole inheritance and dynamics. *Annu Rev Genet* **37**, 435-60 (2003).
7. Gomes de Mesquita, D.S., ten Hoopen, R. & Woldringh, C.L. Vacuolar segregation to the bud of *Saccharomyces cerevisiae*: an analysis of morphology and timing in the cell cycle. *J Gen Microbiol* **137 (Pt 10)**, 2447-54 (1991).
8. Tang, F. et al. Regulated degradation of a class V myosin receptor directs movement of the yeast vacuole. *Nature* **422**, 87-92 (2003).
9. Ishikawa, K. et al. Identification of an organelle-specific myosin V receptor. *J Cell Biol* **160**, 887-97 (2003).
10. Conradt, B., Shaw, J., Vida, T., Emr, S. & Wickner, W. In vitro reactions of vacuole inheritance in *Saccharomyces cerevisiae*. *J Cell Biol* **119**, 1469-79 (1992).
11. Haas, A., Conradt, B. & Wickner, W. G-protein ligands inhibit in vitro reactions of vacuole inheritance. *J Cell Biol* **126**, 87-97 (1994).
12. Haas, A. & Wickner, W. Organelle inheritance in a test tube: the yeast vacuole. *Seminars in Cell & Developmental Biology* **7**, 517-24 (1996).
13. Xu, Z. & Wickner, W. Thioredoxin is required for vacuole inheritance in *Saccharomyces cerevisiae*. *J Cell Biol* **132**, 787-94 (1996).
14. Weisman, L.S. & Wickner, W. Intervacuole exchange in the yeast zygote: a new pathway in organelle communication. *Science* **241**, 589-91 (1988).
15. Eitzen, G., Wang, L., Thorngren, N. & Wickner, W. Remodeling of organelle-bound actin is required for yeast vacuole fusion. *J Cell Biol* **158**, 669-79 (2002).
16. Seeley, E.S., Kato, M., Margolis, N., Wickner, W. & Eitzen, G. Genomic analysis of homotypic vacuole fusion. *Mol Biol Cell* **13**, 782-94 (2002).

17. Lechler, T., Shevchenko, A. & Li, R. Direct involvement of yeast type I myosins in Cdc42-dependent actin polymerization. *J Cell Biol* **148**, 363-73 (2000).
18. Wu, C. et al. Activation of myosin-I by members of the Ste20p protein kinase family. *J Biol Chem* **271**, 31787-90 (1996).
19. Wu, C., Lytvyn, V., Thomas, D.Y. & Leberer, E. The phosphorylation site for Ste20p-like protein kinases is essential for the function of myosin-I in yeast. *J Biol Chem* **272**, 30623-6 (1997).
20. Evangelista, M. et al. A role for myosin-I in actin assembly through interactions with Vrp1p, Bee1p, and the Arp2/3 complex. *J Cell Biol* **148**, 353-62 (2000).
21. Cvrckova, F., De Virgilio, C., Manser, E., Pringle, J.R. & Nasmyth, K. Ste20-like protein kinases are required for normal localization of cell growth and for cytokinesis in budding yeast. *Genes Dev* **9**, 1817-30 (1995).
22. Chiroli, E. et al. Budding yeast PAK kinases regulate mitotic exit by two different mechanisms. *J Cell Biol* **160**, 857-74 (2003).
23. Kim, J.H., Brachet, V., Moriya, H. & Johnston, M. Integration of transcriptional and posttranslational regulation in a glucose signal transduction pathway in *Saccharomyces cerevisiae*. *Eukaryot Cell* **5**, 167-73 (2006).
24. Benton, B.K., Tinkelenberg, A., Gonzalez, I. & Cross, F.R. Cla4p, a *Saccharomyces cerevisiae* Cdc42p-activated kinase involved in cytokinesis, is activated at mitosis. *Mol Cell Biol* **17**, 5067-76 (1997).
25. Sia, R.A., Bardes, E.S. & Lew, D.J. Control of Swe1p degradation by the morphogenesis checkpoint. *Embo J* **17**, 6678-88 (1998).
26. Thomas, B.J. & Rothstein, R. Elevated recombination rates in transcriptionally active DNA. *Cell* **56**, 619-30 (1989).
27. Cheng, L., Hunke, L. & Hardy, C.F. Cell cycle regulation of the *Saccharomyces cerevisiae* polo-like kinase cdc5p. *Mol Cell Biol* **18**, 7360-70 (1998).
28. Johnston, L.H. & Johnson, A.L. Elutriation of budding yeast. *Methods Enzymol* **283**, 342-50 (1997).
29. Saito, T.L. et al. SCMD: *Saccharomyces cerevisiae* Morphological Database. *Nucleic Acids Res* **32**, D319-22 (2004).
30. Vida, T.A. & Emr, S.D. A new vital stain for visualizing vacuolar membrane dynamics and endocytosis in yeast. *J Cell Biol* **128**, 779-92 (1995).
31. Wang, Y.X., Kauffman, E.J., Duex, J.E. & Weisman, L.S. Fusion of docked membranes requires the armadillo repeat protein Vac8p. *J Biol Chem* **276**, 35133-40 (2001).
32. Efe, J.A., Botelho, R.J. & Emr, S.D. The Fab1 phosphatidylinositol kinase pathway in the regulation of vacuole morphology. *Curr Opin Cell Biol* **17**, 402-8 (2005).
33. Rudge, S.A., Anderson, D.M. & Emr, S.D. Vacuole size control: regulation of PtdIns(3,5)P₂ levels by the vacuole-associated Vac14-Fig4 complex, a PtdIns(3,5)P₂-specific phosphatase. *Mol Biol Cell* **15**, 24-36 (2004).

34. Bonangelino, C.J. et al. Osmotic stress-induced increase of phosphatidylinositol 3,5-bisphosphate requires Vac14p, an activator of the lipid kinase Fab1p. *J Cell Biol* **156**, 1015-28 (2002).
35. Gary, J.D. et al. Regulation of Fab1 phosphatidylinositol 3-phosphate 5-kinase pathway by Vac7 protein and Fig4, a polyphosphoinositide phosphatase family member. *Mol Biol Cell* **13**, 1238-51 (2002).
36. Gary, J.D., Wurmser, A.E., Bonangelino, C.J., Weisman, L.S. & Emr, S.D. Fab1p is essential for PtdIns(3)P 5-kinase activity and the maintenance of vacuolar size and membrane homeostasis. *J Cell Biol* **143**, 65-79 (1998).
37. Weisman, L.S. Organelles on the move: insights from yeast vacuole inheritance. *Nat Rev Mol Cell Biol* **7**, 243-52 (2006).
38. Booher, R.N., Deshaies, R.J. & Kirschner, M.W. Properties of *Saccharomyces cerevisiae* wee1 and its differential regulation of p34CDC28 in response to G1 and G2 cyclins. *Embo J* **12**, 3417-26 (1993).
39. Richman, T.J., Sawyer, M.M. & Johnson, D.I. The Cdc42p GTPase is involved in a G2/M morphogenetic checkpoint regulating the apical-isotropic switch and nuclear division in yeast. *J Biol Chem* **274**, 16861-70 (1999).
40. Lew, D.J. & Reed, S.I. Morphogenesis in the yeast cell cycle: regulation by Cdc28 and cyclins. *J Cell Biol* **120**, 1305-20 (1993).
41. Amberg, D.C. Three-dimensional imaging of the yeast actin cytoskeleton through the budding cell cycle. *Mol Biol Cell* **9**, 3259-62 (1998).
42. Tang, F. et al. Regulated degradation of a class V myosin receptor directs movement of the yeast vacuole. *Nature* (2003).
43. Holly, S.P. & Blumer, K.J. PAK-family kinases regulate cell and actin polarization throughout the cell cycle of *Saccharomyces cerevisiae*. *J Cell Biol* **147**, 845-56 (1999).
44. Huh, W.K. et al. Global analysis of protein localization in budding yeast. *Nature* **425**, 686-91 (2003).
45. Richman, T.J. & Johnson, D.I. *Saccharomyces cerevisiae* cdc42p GTPase is involved in preventing the recurrence of bud emergence during the cell cycle. *Mol Cell Biol* **20**, 8548-59 (2000).
46. Eitzen, G., Thorngren, N. & Wickner, W. Rho1p and Cdc42p act after Ypt7p to regulate vacuole docking. *Embo J* **20**, 5650-6 (2001).
47. Han, B.K. et al. Bem1p, a scaffold signaling protein, mediates cyclin-dependent control of vacuolar homeostasis in *Saccharomyces cerevisiae*. *Genes Dev* **19**, 2606-18 (2005).
48. Muller, O., Johnson, D.I. & Mayer, A. Cdc42p functions at the docking stage of yeast vacuole membrane fusion. *Embo J* **20**, 5657-65 (2001).
49. Xu, H. & Wickner, W. Bem1p is a positive regulator of the homotypic fusion of yeast vacuoles. *J Biol Chem* **281**, 27158-66 (2006).
50. Efe, J.A., Botelho, R.J. & Emr, S.D. Atg18 regulates organelle morphology and fab1 kinase activity independent of its membrane recruitment by phosphatidylinositol 3,5-bisphosphate. *Mol Biol Cell* **18**, 4232-44 (2007).
51. Ito, T. et al. A comprehensive two-hybrid analysis to explore the yeast protein interactome. *Proc Natl Acad Sci U S A* **98**, 4569-74 (2001).

52. Georgakopoulos, T. et al. Functional analysis of the *Saccharomyces cerevisiae* YFR021w/YGR223c/YPL100w ORF family suggests relations to mitochondrial/peroxisomal functions and amino acid signalling pathways. *Yeast* **18**, 1155-71 (2001).
53. Dove, S.K. et al. Svp1p defines a family of phosphatidylinositol 3,5-bisphosphate effectors. *Embo J* **23**, 1922-33 (2004).

CHAPTER V

THE VACUOLE SEGREGATION STRUCTURE IS A SENSOR FOR REGULATING ENTRY INTO MITOSIS.

Abstract

The vacuole of budding yeast is partitioned along actin cables into the bud via a tubular and vesicular segregation structure. Prior to nuclear division the segregation structure is resolved to form the daughter vacuole. Here I have reported the identification of a novel checkpoint that monitors the inheritance of the yeast vacuole and prevents nuclear division in cells that failed to resolve their vacuole segregation structure. My results indicate that the vacuole segregation structure acts as a sensor for regulating entry into mitosis through inhibition of a key promoter of mitosis, the polo kinase Cdc5. The p21-activated kinases (PAKs) play roles in relieving this inhibition by binding to the segregation structure after it enters the bud and promoting formation of the daughter vacuole.

Introduction

Checkpoints delay cell cycle progression in response to a failure to complete earlier events through transduction of a negative signal to the cell cycle machinery^{1,2}. The signaling mechanisms used to delay cell cycle progression in response to chromosome segregation defects have been well characterized³. In contrast the mechanisms used to delay cell cycle progression in response to defects in organelle distribution have not been identified⁴. To better understand how organelle distribution is coordinated with the cell cycle I am studying organelle inheritance in the budding yeast *S. cerevisiae* and focusing on vacuole inheritance.

Most Ste20 group kinases are activators of mitogen-activated protein kinase (MAPK) cascades and have been divided into two main groups the p21-activated kinases (PAKs) and the germinal center kinases (GCKs)⁵. Budding yeast contain two main p21-activated kinases, the founding member of the family Ste20 and Cla4. Ste20 and Cla4 accumulate in the bud at sites of polarized bud growth where they are effectors of the small GTPase, Cdc42⁶. My findings suggest that Cla4, which localizes to both the segregation structure and cortex of the bud, and Ste20, which localizes to the bud cortex, act as spatial markers to promote segregation structure resolution in the bud (Chapter 4).

Ste20 and Cla4 have overlapping functions and double mutants lacking both functions are delayed in metaphase and are synthetically lethal^{7,8}. The metaphase arrest of PAK deficient cells is dependent on Swe1⁸. Swe1, the homologue of the mitotic Cdk inhibitor Wee1, inhibits the G2/M transition by

phosphorylation of the Clb(B-type cyclin)-bound Cdc28. The polo kinase Cdc5 is a key promoter of mitosis⁹ including a role as a negative regulator of Swe1¹⁰⁻¹². Additionally, Cla4 phosphorylates Swe1 and Cla4 and Ste20 indirectly negative regulate Swe1 by promoting septin formation where Swe1 is negatively regulated^{7, 13-15}.

In this chapter I provide evidence for a vacuole segregation checkpoint. Cells lacking PAK arrest in G2 and fail to resolve their vacuole segregation structures. The delay in cell cycle progression is connected to resolution of the segregation structure and to inhibition of Cdc5. The PAKs relieve this inhibition by binding to the segregation structure and promoting its resolution, to form the daughter vacuole. In this manner nuclear division is dependent on the completion of an earlier event, the resolution of the vacuole segregation structure.

Materials and Methods

Strains, plasmids, and media

Table 5-1. Strains

Strain	Genotype	Source
KN4580	<i>MATa bar1::hisG cla4::LEU2 YCp-TRP1-cla4-75 ste20::URA3</i>	7
PJ69-4a	<i>MATa LYS2::GAL1-HIS3 GAL2-ADE2 met2::GAL7-lacZ gal4Δ gal80Δ trp1-901 leu2-3,112 ura3-52 his3-200</i>	16
W303-1A	<i>MATa ade2-1 his3-11,15 leu2-3,112 trp1-1 ura3-1 (W303)</i>	17
Y _{CH} 2752	<i>MATa cla4::LEU2 YCp-TRP1-cla4-75 ste20::URA3 swe1::kanMX4 (W303)</i>	This Study
Y _{CH} 5335	<i>MATa bar1::hisG cla4::LEU2 YCp-TRP1-cla4-75 ste20::URA3 vac8::kanMX4 (W303)</i>	This Study
Y _{CH} 5359	<i>MATa bar1::hisG cla4::LEU2 YCp-TRP1-cla4-75 ste20::URA3 vac17::kanMX4 (W303)</i>	This Study
Y _{CH} 5361	<i>MATa atg11::kanMX4 (W303)</i>	This Study
Y _{CH} 5363	<i>MATa atg11::kanMX4 bar1::hisG cla4::LEU2 YCp-TRP1-cla4-75 ste20::URA3 (W303)</i>	This Study
Y _{CH} 5414	<i>MATa ura3::3X URA3::GAL-CDC5-HAx3 cla4::LEU2 YCp-TRP1-cla4-75 ste20::URA3 (W303)</i>	This Study
Y _{CH} 5521	<i>MATa atg11::kanMX4 cdc5-DG-URA3 cla4::LEU2 YCp-TRP1-cla4-75 ste20::URA3 GAL-UBR1-HIS3 (W303)</i>	This Study
Y _{CH} 5518	<i>MATa atg11::kanMX4 cdc5-dg-URA3 cla4::LEU2 YCp-TRP1-cla4-75 ste20::URA3 (W303)</i>	This Study

Details of yeast strains and plasmids used in this study can be found in Table 5-1 and 5-2 respectively. The yeast strains used in this study are all derivatives of W303. Plasmid cloning was performed according to standard molecular biology strategies. Yeast strains were grown in YPD (1% yeast extract, 2% peptone, and 2% glucose, raffinose or raffinose/galactose) or in synthetic complete (SC) media with 2% glucose, raffinose or raffinose/galactose and lacking appropriate amino acids. Centrifugal elutriation was performed in a Beckman-Coulter type J centrifuge as recommended by Beckman-Coulter and as described¹⁸. Fractions with greater than 98% unbudded cells were pooled and used for each experiment. Two-hybrid analysis was performed in strain PJ69-4a

and as described ¹⁶. Nuclei were visualized by fixation in 70% ethanol followed by staining with DAPI at 0.1 mg/ml.

Table 5-2. Plasmids

Plasmid	Description	Source
pCH441	<i>GAD-DBf4 (LEU2)</i>	¹⁹
pCH608	<i>GBD-CDC5 (URA3)</i>	¹⁰
pCH1775	<i>GAD-atg11Δ1-686</i>	This Study

Microscopy

Images were acquired using two microscopes. All images, with the exception of those for Figure 5-4, were taken using a microscope (BX60; Olympus) with a UPlanApo 100x NA 1.30 oil immersion objective (Olympus) and a camera (DAGE ISIT-68) using NIH image 1.62 (Wayne Rasband). Images for Figure 5-4 were acquired using a microscope (BX50; Olympus) with a UPlanF1 100x NA 1.30 oil immersion objective (Olympus) and a camera (CoolSNAP HQ; Photometrics). Images were collected using MetaVue version 4.6 (Molecular Devices). GFP images were visualized using an X-cite 120-UV lamp and Chroma filter sets. Within each experiment, all images were collected and scaled identically. Images were processed with Photoshop 9.0 software (Adobe). Small, medium and large budded cells were grouped into size categories as described ²⁰. Scale bar = 2.5 μm throughout all figures.

***In vivo* labeling of vacuoles**

To visualize vacuoles, yeast cells were concentrated and incubated for 1 hour with N-(3-triethylammoniumpropyl)-4(6(4(diethylamino)phenyl)hexatrienyl)pyridium dibromide (FM 4-64; Molecular Probes) at a final concentration of 16.5 mM. Cells were then washed with appropriate media and grown for ≥ 3 hours before being viewed by fluorescence microscopy²¹.

Results

***cla4-75 ste20* cells fail to form a daughter vacuole and arrest at G2/M**

Cla4 has overlapping functions with the PAK, Ste20, as *cla4* and *ste20* single mutants are viable but the *cla4 ste20* double mutant is synthetically lethal⁷. After cells were synchronized by centrifugal elutriation in G1 and released for growth at the restrictive temperature, the *cla4-75 ste20* double mutant cells formed a segregation structure that was directed toward the bud tip but strikingly, after 240 minutes, 95% of the *cla4-75 ste20* cells maintained the segregation structure and 98% arrested with a single nucleus (Chapter 4-5 and Figure 5-1).

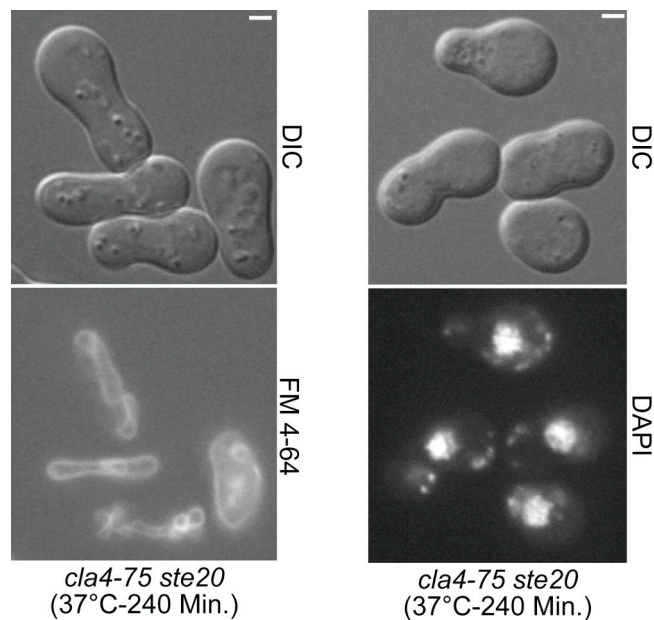


Figure 5-1. *cla4-75 ste20* cells fail to form a daughter vacuole and arrest at G2/M.

(A-B) FM 4-64 stained *cla4-75 ste20* (KN4580) G1 cells were obtained by elutriation, shifted to 37°C for 240 minutes, and viewed by fluorescence microscopy to image vacuoles or DAPI stained to image nuclei.

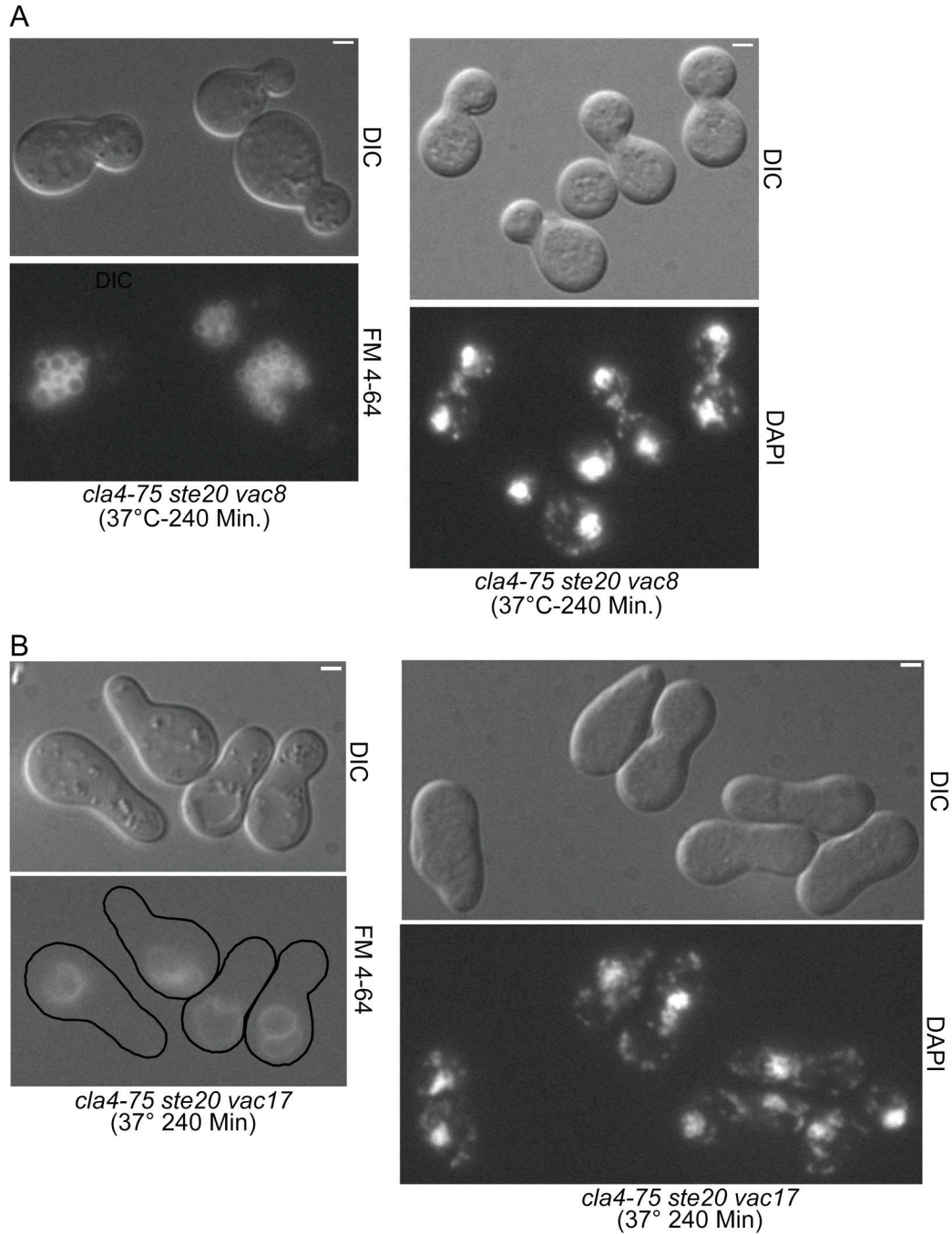


Figure 5-2. *cla4-75 ste20 vac8* and *cla4-75 ste20 vac17* cells do not arrest at G2/M.

(A-B) FM 4-64 stained *cla4-75 ste20 vac17* (YCH 5359) and *cla4-75 ste20 vac8* (YCH5335) G1 cells were obtained by elutriation, shifted to 37°C for 240 minutes, and viewed by fluorescence microscopy to image vacuoles or DAPI stained to image nuclei.

Metaphase arrest of *cla4-75 ste20* is linked to the vacuole segregation structure

The persistence of the segregation structure in metaphase arrested *cla4-75 ste20* cells suggested that the segregation structure itself might act as a sensor for regulating entry into mitosis. To test this model, I constructed *cla4-75 ste20 vac8* and *cla4-75 ste20 vac17* triple mutants. The *cla4-75 ste20 vac8* and *cla4-75 ste20 vac17* cells were synchronized in G1 by centrifugal elutriation and then shifted to the restrictive temperature. After 4 hours, 40% of all cells and 80% of all large budded cells had 2 nuclei indicating that the cells were no longer arrested in metaphase (Figure 5-2, 5-3B). These results suggest that the cell cycle arrest of *cla4-75 ste20* cells is linked to the vacuole segregation structure.

Deletion of *SWE1* uncouples daughter vacuole formation and mitotic progression

Related studies have reported that G1 cells from the *cla4-75 ste20* strain arrest in metaphase at the restrictive temperature ⁷ and that the metaphase arrest of PAK-deficient cells is dependent on Swe1, the homolog of the Cdk inhibitor, Wee1 ⁸. To test for the role of Swe1, I shifted a population of G1 synchronized *cla4-75 ste20 swe1* cells to the restrictive temperature for 4 hours. 53% of the cells entered mitosis and yet 95% of all cells in the population failed to form a daughter vacuole (Figure 5-3A). Because the cytoskeleton is depolarized when cells enter anaphase ²² the segregation structure is dissolved and no longer stretched toward the bud tip in *cla4-75 ste20 swe1* cells that enter anaphase. These results are consistent with a requirement for PAKs to form the

daughter vacuole and suggest a possible role for Swe1 in ensuring that daughter vacuole formation is completed before nuclear division initiates.

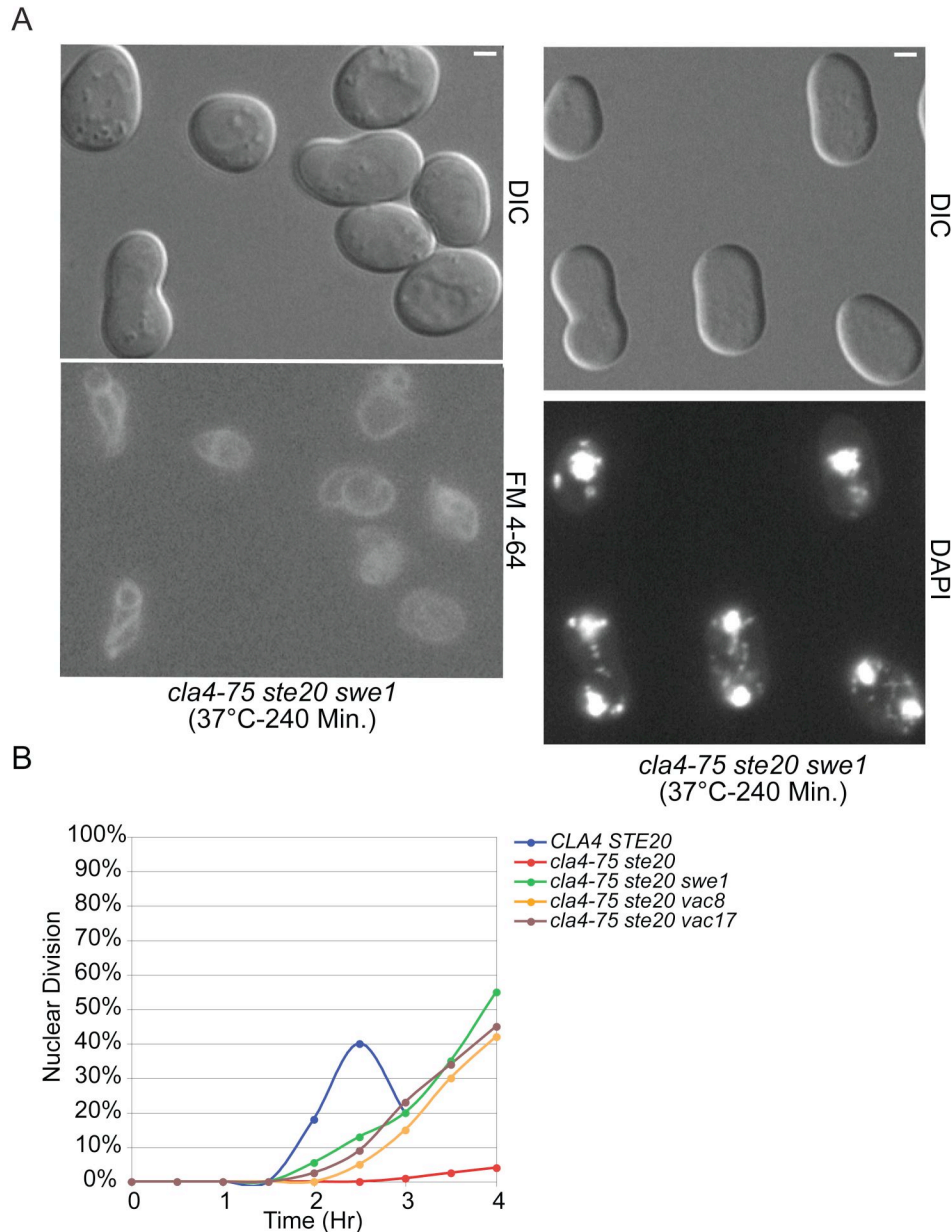


Figure 5-3. Deletion of *SWE1* partially suppresses the *cla4-75 ste20* G2/M arrest but not the failure to resolve segregation structures.

(A) FM 4-64 stained *cla4-75 ste20 swe1* (Y_{CH2752}) G1 cells were obtained by elutriation, shifted to 37°C for 240 minutes, and viewed by fluorescence microscopy to image vacuoles or DAPI stained to image nuclei. (B) Wild type (W303-1A), *cla4-75 ste20* (KN4580), *cla4-75 ste20 swe1* (Y_{CH2752}), *cla4-75 ste20 vac17* (Y_{CH5359}), and *cla4-75 ste20 vac8* (Y_{CH5535}) G1 cells grown at the permissive temperature were obtained by elutriation, shifted to 37°C, and samples were DAPI stained to determine the percentage of cells having undergone nuclear division at the indicated times.

Hsl1 was mislocalized in *cla4-75 ste20* and *cla4-75 ste20 vac8* cells

Microscopic observation of the *cla4-75 ste20*, *cla4-75 ste20 vac17*, and *cla4-75 ste20 vac8* strains showed that they all failed to form a normal mother bud neck when grown at the restrictive temperature (Figure 5-2). Hsl1 is localized to the bud neck and it is required for localization and negative regulation of Swe1 at the bud neck. As a further test of the state of the mother bud neck I decided to examine the localization of Hsl1 in these strains. The different strains were synchronized in G1 by centrifugal elutriation then shifted to the restrictive temperature and examined after four hours. Strikingly, I found that the pattern of Hsl1 in *cla4-75 ste20* and *cla4-75 ste20 vac8* cells was similar (Figure 5-4). Hsl1 localized exclusively to the bud neck at permissive temperatures in these strains but at the restrictive temperature the Hsl1 was very weak in the majority of the cells (greater than 74% in all strains), and in those cells where it was detectable it was delocalized over the entire cortex or at the bud tip. Therefore, the maintenance of the segregation structure in the mother bud neck of the *cla4-75 ste20* cells was not responsible for the defective morphology of the mother bud neck. These results suggest that the segregation structure is functioning independent of the bud neck to restrict cell cycle progression in the *cla4-75 ste20* cells.

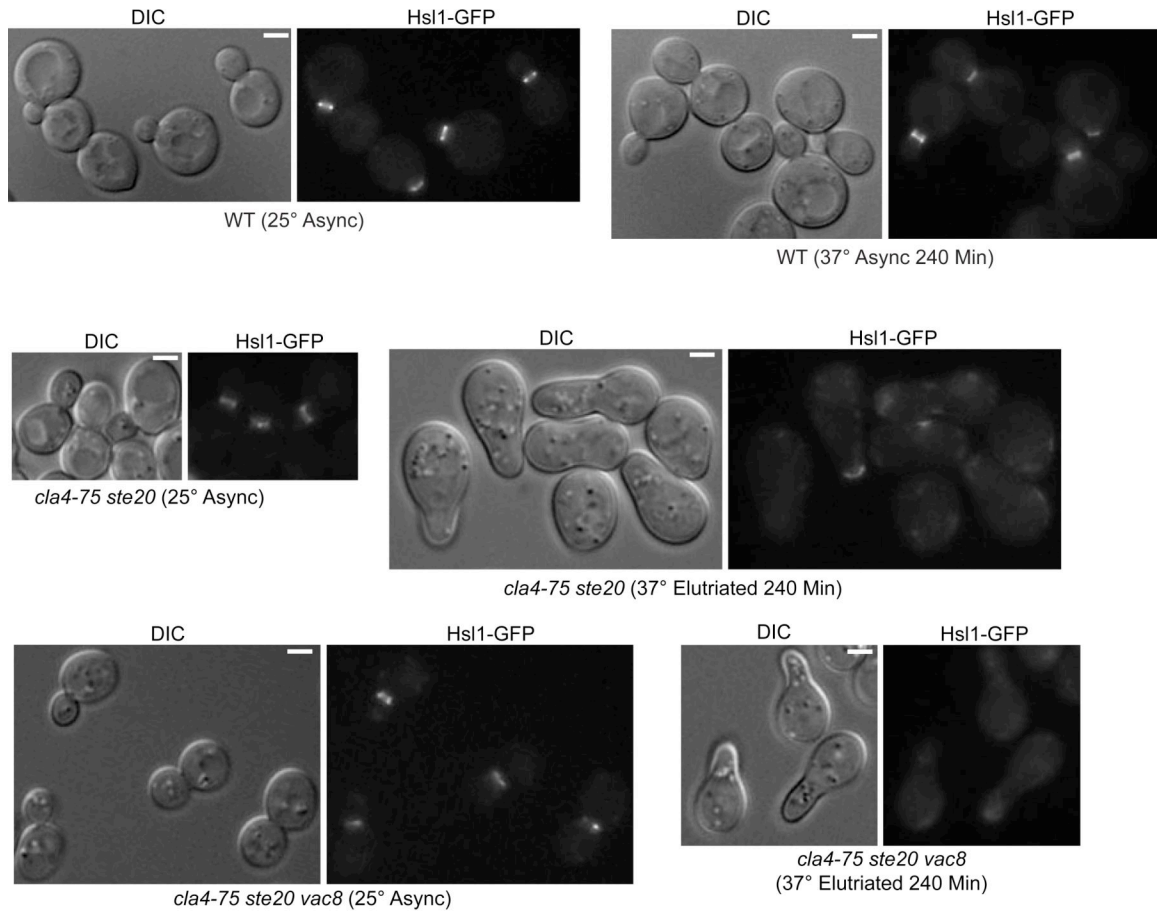


Figure 5-4. Hsl1 is mislocalized in *cla4-75 ste20* and *cla4-75 ste20 vac8* cells. *HSL1-GFP* ($Y_{CH}5352$), *cla4-75 ste20 HSL1-GFP* ($Y_{CH}5340$) and *cla4-75 ste20 vac8 HSL1-GFP* ($Y_{CH}5341$) cells were synchronized by centrifugal elutriation in G1 then shifted to 37° for the indicated period of time.

Cdc5 through interaction with Atg11 is a target of the vacuole segregation checkpoint

To determine how the segregation structure communicates with the cell cycle machinery to prevent cell cycle progression, I focused on the polo kinase, Cdc5, which is a negative regulator of Swe1^{10, 11}, as a potential target of a vacuole segregation checkpoint. Strikingly, in a two-hybrid screen using Cdc5 as bait the cytosol to vacuole transport (Cvt) pathway component, Atg11^{23, 24} was identified as a Cdc5 interactor (Figure 5-5A). Atg11 localizes to a structure on the

vacuole, called the pre-autophagic structure (PAS), thus suggesting that Cdc5 may be regulated at the vacuole.

Deletion of *ATG11* suppresses the metaphase arrest of *cla4-75 ste20* cells in a Cdc5 dependent manner

To directly test if Atg11 was acting in the vacuole inheritance checkpoint, *cla4-75 ste20 atg11* cells were examined to determine if nuclear division occurred with similar kinetics to the *cla4-75 ste20 swe1* cells. G1 cells for each strain were isolated by centrifugal elutriation and then grown at 37°. Interestingly, in response to inactivation of Cla4, the *cla4-75 ste20 atg11* cells underwent nuclear division with similar kinetics to the *cla4-75 ste20 swe1* cells (Fig 5-5B). In addition, I found that the *cla4-75 ste20 atg11* cells failed to form a daughter vacuole like *cla4-75 ste20 swe1* cells (Figure 5-5B). This suppression of the *cla4-75 ste20* arrest is *ATG11* dependent as reintroduction of *ATG11* on a plasmid, but not an empty plasmid, restored the G2/M arrest (data not shown). One model to explain the above results is that when a segregation structure is present that Atg11 acts to negatively regulate Cdc5 thus allowing active Swe1 to arrest the cell cycle. One prediction of this model is that *cla4-75 ste20 atg11* cells containing a temperature sensitive version of Cdc5 that is degraded at 37° (*cdc5-DG*)²⁵ should arrest at G2/M. If Cdc5 activity is rate limiting for mitotic progression in the *cla4-75 ste20* cells, then a second prediction of my model is that overexpression of *CDC5* in *GAL-CDC5 cla4-75 ste20* cells should override the metaphase arrest of these cells. To test the first prediction, G1 *cla4-75 ste20*

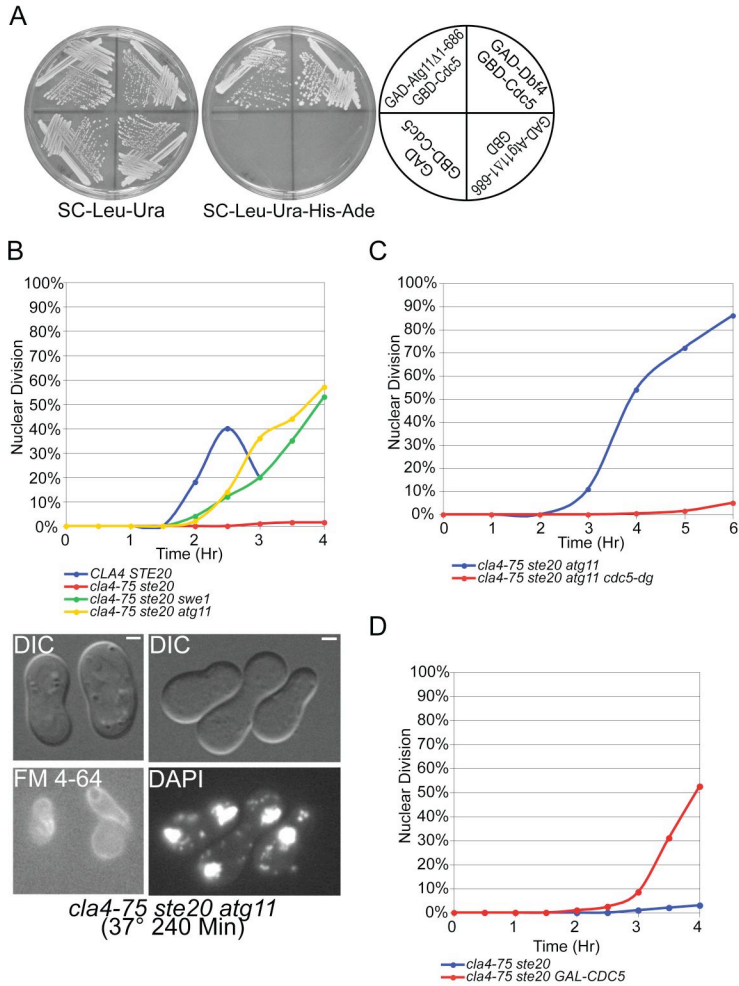


Figure 5-5. Cdc5 is a target of the vacuole segregation checkpoint. (A) Two-hybrid analysis between *pGAD-Cdc5* and *pGBD-Atg11Δ1-686* or *pGBD-Dbf4* (positive control). Growth on Sc-Leu-Ura indicates protein-protein interactions. (B) *Wild type* (W303-1a), *cla4-75 ste20* (KN4580), *cla4-75 ste20 swe1* (Y_{CH}2752) and *cla4-75 ste20 atg11* (Y_{CH}5363) cells in YP+2% glucose at 23° were synchronized in G1 and then shifted to 37°. (C) *cla4-75 ste20 atg11* (Y_{CH}5363) and *cla4-75 ste20 atg11 cdc5-dg* (Y_{CH}5518) cells in YP+2% galactose were synchronized in G1 and then shifted to 37° in YP+2% galactose. (D) *GAL-CDC5 cla4-75 ste20* (Y_{CH}5414) cells in YP+2% raffinose at 23° were synchronized in G1 then shifted to 37° for 2 hours when galactose was added to 2%. Nuclear division assayed by DAPI staining and synchronization by centrifugal elutriation B-D.

atg11 and *cla4-75 ste20 atg11 cdc5-DG* cells were isolated by centrifugal elutriation and then grown at 37°. Interestingly, in response to inactivation of Cla4, *cla4-75 ste20 atg11 cdc5-DG* cells arrested at G2/M with a single nuclei while *cla4-75 ste20 atg11* cells grown under the same conditions underwent

nuclear division with similar kinetics as seen previously (Figure 5-5C). As further support for the checkpoint model, *CDC5* overproduction overrode the *cla4-75 ste20* metaphase arrest, suggesting that Cdc5 activity in the arrested cells is indeed rate limiting for cell cycle progression (Figure 5-5D).

Discussion

Cells must coordinate organelle inheritance with nuclear inheritance. Previously research shows that cells lacking PAK function arrest at G2/M in a *SWE1* dependent manner^{8, 13}. In this report I provide evidence for a vacuole segregation checkpoint. My results indicate that nuclear division is delayed in cells that have not resolved their vacuole segregation structure (Figure 5-2). The delay in cell cycle progression is linked to inhibition of Cdc5 (Figure 5-5C,D). The PAKs relieve this inhibition by binding to the segregation structure and promoting its resolution to form the daughter vacuole. In this manner nuclear division is dependent on the completion of an earlier event, the resolution of the vacuole segregation structure (Figure 5-6).

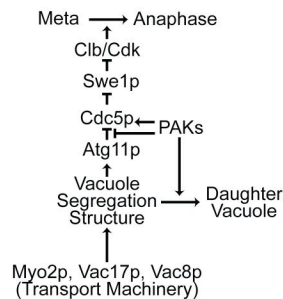


Figure 5-6. Model of the vacuole segregation checkpoint.

How might Atg11 inhibit Cdc5 function? Atg11 is a peripheral membrane protein and contains multiple coiled coil domains²⁶. Through these coiled coils Atg11 functions as a scaffold that coordinates the formation of the protein complexes that make up the core of the Cvt pathway²⁶. I propose that Atg11 takes on a Cdc5 inhibitory function in the presence of the segregation structure. The formation of the segregation structure may release Atg11 from its Cvt

functions at the vacuole and in the process make it available for interaction with Cdc5. Furthermore, the PAK-mediated resolution of the segregation structure regulates the Cdc5-Atg11 interaction by altering the function or localization of Atg11, perhaps through mediating formation of the PAS following daughter vacuole formation. Alternatively, the PAKs might directly regulate the Atg11-Cdc5 interaction through modification of either Atg11 or Atg11-interacting proteins such as Atg1²³, which also interacts with Cla4 (data not shown). Further work is required to understand the role of Atg11 in regulation of Cdc5.

Vacuole resolution is now the third example in which the nuclear machinery delays at G2/M in response to failure to complete organelle inheritance. In yeast the cortical endoplasmic reticulum (cER) is transported along actin cables by the Myosin V motor, Myo4, into the bud where it becomes anchored at the tip of the bud and expands to fill the bud⁴. Cells lacking *SCS2* and *ICE2*, which are required for cER inheritance, have perturbed septins, activate Swe1, and delay in G2/M²⁷. Thus the organelle inheritance checkpoints for cER and vacuole inheritance show many similarities. Both *scs2 ice2* and *cla4 ste20* mutants have septin defects, delay at G2/M, and depend on Swe1 for the checkpoint to function. Intriguingly, cER is also regulated by a MAP kinase pathway²⁸, and Cla4 works synergistically with Scs2 and Ice2 to promote proper septin localization²⁷.

In mammalian cells the Golgi apparatus is composed of 4-8 cisternae anchored at pericentriolar region of the cell. During prophase this Golgi ribbon fragments into smaller vesicles and tubules that are subsequently dispersed

during metaphase ⁴. Failure to fragment the Golgi activates the Golgi mitotic checkpoint ²⁹. However, the mechanism for this checkpoint has not been elucidated. Known, however, is that inhibition of MAP kinases involved in Golgi fragmentation results in significant delays during the G2/M transition ^{30, 31}. Additionally the polo-like kinase PLK1 is also required for fragmentation of the Golgi stacks and involved in Golgi checkpoint signaling ^{32, 33}. Thus, not only do mechanisms which regulate vacuole inheritance and coordination with the cell cycle show similarities with regulation of other organelles in yeast, but the key proteins involved in this regulation, namely polo-kinases and proteins participating in MAP kinase cascades, are conserved in mammalian cells. Further study of how vacuole inheritance is coordinated with the cell cycle may shed further insights on the coordination of organelle inheritance with cell cycle more generally in both yeast and mammalian cells.

References

1. Hartwell, L.H. & Weinert, T.A. Checkpoints: Controls That Ensure the Order of Cell Cycle Events. *Science* 246, 629-634 (1989).
2. Elledge, S.J. Cell cycle checkpoints: preventing an identity crisis. *Science* 274, 1664-72 (1996).
3. Cleveland, D.W., Mao, Y. & Sullivan, K.F. Centromeres and kinetochores: from epigenetics to mitotic checkpoint signaling. *Cell* 112, 407-21 (2003).
4. Lowe, M. & Barr, F.A. Inheritance and biogenesis of organelles in the secretory pathway. *Nat Rev Mol Cell Biol* 8, 429-39 (2007).
5. Dan, I., Watanabe, N.M. & Kusumi, A. The Ste20 group kinases as regulators of MAP kinase cascades. *Trends Cell Biol* 11, 220-30 (2001).
6. Holly, S.P. & Blumer, K.J. PAK-family kinases regulate cell and actin polarization throughout the cell cycle of *Saccharomyces cerevisiae*. *J Cell Biol* 147, 845-56 (1999).
7. Cvrckova, F., De Virgilio, C., Manser, E., Pringle, J.R. & Nasmyth, K. Ste20-like protein kinases are required for normal localization of cell growth and for cytokinesis in budding yeast. *Genes Dev* 9, 1817-30 (1995).
8. Chiroli, E. et al. Budding yeast PAK kinases regulate mitotic exit by two different mechanisms. *J Cell Biol* 160, 857-74 (2003).
9. Barr, F.A., Sillje, H.H. & Nigg, E.A. Polo-like kinases and the orchestration of cell division. *Nat Rev Mol Cell Biol* 5, 429-40 (2004).
10. Bartholomew, C.R., Woo, S.H., Chung, Y.S., Jones, C. & Hardy, C.F. Cdc5 interacts with the Wee1 kinase in budding yeast. *Mol Cell Biol* 21, 4949-59 (2001).
11. Sakchaisri, K. et al. Coupling morphogenesis to mitotic entry. *Proc Natl Acad Sci U S A* 101, 4124-9 (2004).
12. Asano, S. et al. Concerted mechanism of Swe1/Wee1 regulation by multiple kinases in budding yeast. *Embo J* 24, 2194-204 (2005).
13. Weiss, E.L., Bishop, A.C., Shokat, K.M. & Drubin, D.G. Chemical genetic analysis of the budding-yeast p21-activated kinase Cla4p. *Nat Cell Biol* 2, 677-85 (2000).
14. Schmidt, M., Varma, A., Drgon, T., Bowers, B. & Cabib, E. Septins, under Cla4p regulation, and the chitin ring are required for neck integrity in budding yeast. *Mol Biol Cell* 14, 2128-41 (2003).
15. Kadota, J., Yamamoto, T., Yoshiuchi, S., Bi, E. & Tanaka, K. Septin ring assembly requires concerted action of polarisome components, a PAK kinase Cla4p, and the actin cytoskeleton in *Saccharomyces cerevisiae*. *Mol Biol Cell* 15, 5329-45 (2004).
16. James, P., Halladay, J. & Craig, E.A. Genomic libraries and a host strain designed for highly efficient two-hybrid selection in yeast. *Genetics* 144, 1425-36 (1996).

17. Thomas, B.J. & Rothstein, R. Elevated recombination rates in transcriptionally active DNA. *Cell* 56, 619-30 (1989).
18. Johnston, L.H. & Johnson, A.L. Elutriation of budding yeast. *Methods Enzymol* 283, 342-50 (1997).
19. Hardy, C.F. & Pautz, A. A novel role for Cdc5p in DNA replication. *Mol Cell Biol* 16, 6775-82 (1996).
20. Saito, T.L. et al. SCMD: *Saccharomyces cerevisiae* Morphological Database. *Nucleic Acids Res* 32, D319-22 (2004).
21. Vida, T.A. & Emr, S.D. A new vital stain for visualizing vacuolar membrane dynamics and endocytosis in yeast. *J Cell Biol* 128, 779-92 (1995).
22. Lew, D.J. & Reed, S.I. Morphogenesis in the yeast cell cycle: regulation by Cdc28 and cyclins. *J Cell Biol* 120, 1305-20 (1993).
23. Kim, J. et al. Cvt9/Gsa9 functions in sequestering selective cytosolic cargo destined for the vacuole. *J Cell Biol* 153, 381-96 (2001).
24. Yorimitsu, T. & Klionsky, D.J. Autophagy: molecular machinery for self-eating. *Cell Death Differ* 12 Suppl 2, 1542-52 (2005).
25. Hu, F. et al. Regulation of the Bub2/Bfa1 GAP complex by Cdc5 and cell cycle checkpoints. *Cell* 107, 655-65 (2001).
26. He, C. et al. Recruitment of Atg9 to the preautophagosomal structure by Atg11 is essential for selective autophagy in budding yeast. *J Cell Biol* 175, 925-35 (2006).
27. Loewen, C.J., Young, B.P., Tavassoli, S. & Levine, T.P. Inheritance of cortical ER in yeast is required for normal septin organization. *J Cell Biol* 179, 467-83 (2007).
28. Du, Y., Walker, L., Novick, P. & Ferro-Novick, S. Ptc1p regulates cortical ER inheritance via Slf2p. *Embo J* 25, 4413-22 (2006).
29. Sutterlin, C., Hsu, P., Mallabiabarrena, A. & Malhotra, V. Fragmentation and dispersal of the pericentriolar Golgi complex is required for entry into mitosis in mammalian cells. *Cell* 109, 359-69 (2002).
30. Feinstein, T.N. & Linstedt, A.D. Mitogen-activated protein kinase kinase 1-dependent Golgi unlinking occurs in G2 phase and promotes the G2/M cell cycle transition. *Mol Biol Cell* 18, 594-604 (2007).
31. Shaul, Y.D. & Seger, R. ERK1c regulates Golgi fragmentation during mitosis. *J Cell Biol* 172, 885-97 (2006).
32. Preisinger, C. et al. Plk1 docking to GRASP65 phosphorylated by Cdk1 suggests a mechanism for Golgi checkpoint signalling. *Embo J* 24, 753-65 (2005).
33. Sutterlin, C. et al. Polo-like kinase is required for the fragmentation of pericentriolar Golgi stacks during mitosis. *Proc Natl Acad Sci U S A* 98, 9128-32 (2001).

CHAPTER VI

FUTURE DIRECTIONS

The work presented in chapters two through five provides a substantial step forward in our understanding how vacuole inheritance is regulated spatially and how vacuole inheritance is coordinated with mitosis. However, these new insights about vacuole inheritance also provoke new questions and inspire new lines of research. In this concluding chapter I will discuss some remaining issues, suggest further experiments to test the various models presented, and suggest future directions based on the experimental data provided in the preceding chapters.

How do Cla4 and Ste20 promote resolution of the segregation structure?

Cla4 and Ste20 localize to and are activated specifically in the bud, thus spatially separating them from the forming segregation structure¹⁻⁴. In chapter IV I proposed that the segregation structure was resolved by Cla4 and Ste20 when it entered the bud. In support of this model I found that (1) overexpression of either *CLA4* or *STE20* suppressed vacuole inheritance (Figure 3-3,4), (2) Cla4 localized to the segregation structure when it entered the bud (Figure 4-2,3A), and that (3) *cla4-75 ste20* cells failed to resolve the segregation structure (Figure 4-5D). I then proposed that Cla4 and Ste20 promote segregation structure resolution through vacuole fusion and showed that cells overexpressing *CLA4t*

had a partial vacuole fusion defect (Figure 4-6). In further support of this model others show that Cla4 localizes to isolated vacuoles ⁵, *cla4* mutants have fragmented vacuoles ^{5, 6}, Cla4 and Ste20 phosphorylate Myo3 and Myo5 ⁷⁻⁹ which promote actin polymerization, and that actin polymerization promotes vacuole fusion ^{5, 10-12}. I propose the following experiments to further test this model.

A role in vacuole fusion for Ste20 is not as well supported by documented evidence, as is the case for Cla4. To remedy this situation I propose to look for vacuole enrichment of Ste20. To perform this experiment immunoblot analysis of isolated vacuoles and cell lysates should be performed as described ⁵. As positive controls actin, Cla4, and carboxypeptidase Y could be used. A simple and reliable *in vitro* assay for vacuole fusion also exists which is based on the maturation and activation of pro-alkaline phosphatase by proteinase A ¹³. I suggest using this assay with vacuoles isolated from *cla4* strains and determine if depletion of Ste20 using anti-Ste20 antibody inhibits vacuole fusion as has been done previously to show that Las17 and Ypt7 promote vacuole fusion ⁵. I could, furthermore, look for an *in vivo* role for Ste20 in vacuole fusion by examining the effects of *STE20* overexpression on vacuole morphology in *cla4* and *cdc42^{ts}* mutants which normally have fragmented vacuoles ^{5, 11}.

While Cla4 localizes to isolated vacuoles and has a fusion defect *in vivo*, finding that Cla4 promotes vacuole fusion *in vitro* would provide additional evidence in support of the model. In the first paper that proposes a role for Cla4 in vacuole fusion, Eitzen *et al.* propose that vacuole fusion is promoted by actin

polymerization controlled by the following cascade: Cdc42→Cla4→Las17/Vrp1→Arp2/3→actin. Eitzen *et al.* then go on to show that inhibition of Las17, Vrp1, Arp2/3, and actin inhibits vacuole fusion *in vitro*. Noticeably absent from their analysis are *in vitro* fusion assays on vacuoles from *cla4* mutant cells. I propose to look at fusion rates of vacuole derived from *cla4*, *ste20*, *cla4-75 ste20*, and cells overexpressing *CLA4t* and determine rates of vacuole fusion as compared to fusion rates for vacuoles derived from wild type and *vac8* mutants as controls. One important control would be to add back purified Cla4 or Ste20 to vacuoles isolated from *cla4-75 ste20* cells in the *in vitro* assay to determine if this promotes homotypic vacuole fusion. Additional *in vivo* evidence supporting a role for Cla4 in vacuole fusion could be found by examining the effects *CLA4* overexpression on vacuole morphology in *cdc42^{ts}* and *las17-6* cells. Together these experiments could potentially strengthen the model that Cla4 and Ste20 resolve the segregation structure by promoting vacuole fusion.

How do Boi1 and Boi2 regulate Cla4 and Ste20?

In chapter two I proposed that Boi1 and Boi2 negatively regulate residual Cla4 and Ste20 that remain in the bud by restricting PAK access to Cdc42. This hypothesis is consistent with my findings that (1) *boi1 boi2* mutants had a vacuole inheritance defect (Figure 2-3), (2) the *boi1 boi2* vacuole inheritance defect was suppressed by deletion of *CLA4* or *STE20* (Figure 2-4), and (3) the Boi1 PH domain interacts with Cdc42¹⁴, and (4) that the PH domain of Boi1 was

necessary and sufficient to suppress the *boi1 boi2* vacuole inheritance defect (Figure 2-5).

This model has a number of predictions that could be tested. First if Boi1 and Boi2 act at the vacuole then Boi1 and Boi2 should be detectable on isolated vacuoles like Bem1, Cla4, and Cdc42^{5, 15, 16}. To determine if Boi1 and Boi2 localize to the vacuole, immunoblot analysis of isolated vacuoles and cell lysates should be performed as described⁵. As positive controls actin, Cla4, and carboxypeptidase Y could be used. If found at the vacuole the domain necessary for vacuole localization could be tested with the mutants used to determine which region of Boi1 was necessary to suppress the *boi1 boi2* vacuole inheritance defect (Figure 2-5). Overexpression of *BOI1-GFP* and *BOI2-GFP* may also allow visualization of Boi1-GFP or Boi2-GFP localization at the vacuole.

The above model also predicts that Boi1 and Boi2, and specifically the PH domain, interacts with Cdc42. The Boi1-Cdc42 interaction has been previously shown only by two-hybrid. In these experiment *Bender et al.* found that PH domain interacts by 2-hybrid with the predominately GTP bound Cdc42^{Q61L} but not with the predominantly GDP bound Cdc42^{D118A} or the other the other Rho-type GTPases Rho1, Rho2, Rho3, or Rho4¹⁴. To further determine if Cdc42 interacts with Boi1 or Boi2 *in vivo* coimmunoprecipitation experiments should be performed using Bud1 or Bem1 as positive controls¹⁷⁻¹⁹. If coimmunoprecipitation detects a Boi1-Cdc42 interaction then the domain necessary for coimmunoprecipitation could also be determined. GTP-Cdc42 but not GDP-Cdc42 binds Cla4 or Ste20 *in vitro*. To further test the model I propose

testing if the *in vitro* interaction between Cdc42-Cla4 or Cdc42-Ste20 is disrupted by the addition of either Boi1 or Boi2. The above experiments could potentially strengthen our model or suggest alternative models by which Boi1 and Boi2 regulate Cla4 and Ste20.

How do Cla4 and Ste20 regulate Vac17?

In chapter III I proposed that Cla4 and Ste20 are the bud-specific proteins localized to and activated in the bud that prime Vac17 for degradation. In support of this hypothesis I found that *CLA4* overexpression causes Vac17 degradation (Figure 3-6C) and that active PAKs were required for Vac17 degradation in late-M (Figure 3-6B). The mechanism whereby Cla4 and Ste20 prime Vac17 for degradation remains unknown. I propose the general hypothesis that Cla4 and Ste20 promote Vac17 degradation directly by phosphorylating Vac17 or indirectly through proteins activated by Cla4 or Ste20.

In vitro phosphorylation assays for Cla4 and Ste20 are established²⁰⁻²². I propose using these *in vitro* assays to determine if PAKs directly phosphorylate Vac17. Cla4 overexpression had a stronger effect on Vac17 degradation than Ste20. To further test if Cla4 phosphorylates Vac17, I propose using the previously characterized analog sensitive version of Cla4 (*cla4-as3*) whose nucleotide binding specificity is altered to allow it to use a modified form of ATP²³. To perform this experiment kinase assays will be performed in *cla4-as3 VAC17-ProA* cell extracts by adding radiolabelled *N*⁶-benzyl-ATP as described²⁴. Vac17-ProA will then be immunoprecipitated and examined by SDS-PAGE for

the incorporation of the radiolabelled N^6 -benzyl-ATP. As positive controls Cdc24 or Lte1 could be used, and as a negative control cells containing wild type *CLA4* could be used. If Cla4 and Ste20 are shown to phosphorylate Vac17 then I propose mapping the phosphorylation sites then mutating the serines and/or threonine to determine their function *in vivo*.

Alternately, Cla4 and Ste20 could regulate Vac17 indirectly. In support of this possibility I have found that deletion of *LTE1* or *ATG11* partially suppressed the vacuole inheritance defects of *CLA4* overexpressing cells. The MEN mutant *cdc5-1* suppressed the vacuole inheritance defect of *STE20* overexpressing cells. Since Cla4 and Ste20 may regulate vacuole inheritance both by modulating Vac17, and through promoting vacuole inheritance, then Vac17 protein levels need to be carefully examined for each of the above cases. If PAK regulation of Vac17 is indirect, then dissecting exactly how Cla4 and Ste20 regulate Vac17 may be exceedingly difficult.

It is presently unclear if Vac17 degradation by *CLA4* overexpression (Figure 3-6C) is dependent on cell cycle progression. To further clarify this point I suggest looking at Vac17 levels in cells overexpressing *CLA4* that are arrested in S-phase using a *cdc7-4* mutant and at G2/M with nocodazole. As negative controls cells not overexpressing *CLA4* or overexpressing kinase-dead *cla4* could be used²⁵. It would also be interesting to examine the ability of *CLA4* and *STE20* overexpression to promote degradation of Vac17 in the Class I *vac* mutants *vac8* and *myo2-2*. This would provide further evidence that Cla4 and Ste20 are the daughter-specific factors that promote Vac17 degradation.

Because Vac17 accumulates to such high levels in *vac8* and *myo2-2* cells, it may be necessary to arrest cells in G1 with α -factor to see an effect. As controls I can examine vacuole inheritance in cells overexpressing neither *CLA4* nor *STE20* or that overexpress kinase dead versions of these kinases^{4,25}.

Is PAK regulation of vacuole inheritance connected to Vac17 degradation?

One of the ongoing questions that I have pursued is if Vac17 degradation by PAKS is separable from PAK resolution of the segregation structure. It is possible that segregation structure resolution causes Vac17 degradation. If correct then premature segregation structure resolution by overexpression of *Cla4* is the cause of Vac17 degradation (Figure 3-6C). The failure to degrade Vac17 in late-M phase could be caused by a failure resolve the segregation structure (Figure 3-6B). Separating these two processes has been difficult.

Initially I tried to separate the two processes by α -factor arresting *cdc7-4* *4X GAL-CLA4t swe1 bub2 VAC17-ProA* cells and releasing them at 37°C in YP+2% raffinose. Cells arrested just prior to S-phase with a resolved segregation structures (Figure 4-1). Once cells were uniformly arrested, 2% galactose was added to induce *CLA4t* overexpression. Cells were then subsequently released by shifting to 25°C. Under these conditions the cells did not exit mitosis synchronously making assaying for Vac17-ProA degradation ambiguous since cells could not be arrested in G1 with α -factor. I also FM 4-64 stained cells under the same conditions and looked for movement of vacuole back to the neck. I did not find movement back to the neck. However, cells were defective for cell

separation suggesting that actin polymerization to the mother bud neck may be defective under *CLA4t* overexpression conditions. Therefore, I have been unable to resolve this question. I do think that the process of inhibition of vacuole inheritance by promoting fusion is separable from Vac17 destruction as *boi1 boi2* cells have a vacuole inheritance defect and accumulate Vac17, though to a lesser degree than in *vac8* cells (data not shown).

Do PtdIns(3,5)P₂ levels increase during segregation structure formation?

In the absence of the machinery necessary to produce PtdIns(3,5)P₂ the tubules and vesicles that make up the segregation structure are not formed²⁶⁻²⁹. However, it remains to be shown that PtdIns(3,5)P₂ levels increase during segregation structure formation. Because the segregation structure is transient, it has been impossible to show that PtdIns(3,5)P₂ rise during this period of time. I propose to look at PtdIns(3,5)P₂ levels in *cla4-75 ste20* and *GAL-CLA4t* cells. It would be interesting to examine the timing of PtdIns(3,5)P₂ levels increase and decrease during inheritance. It could be that the enlarged vacuole morphology in the *cla4-75 ste20* vacuole could be due to a decrease in PtdIns(3,5)P₂ after prolonged stasis as a segregation structure leading to small amounts of fusion that increase the size of the vacuole.

Atg18 is a PtdIns(3,5)P₂ binding protein that is thought to localize to segregation structures³⁰. However, this hypothesis has been difficult to verify due to the transience of the segregation structure. It would be interesting to test this hypothesis by examining Atg18-GFP localization in the *cla4-75 ste20* and

GAL-CLA4t strains that have persistent segregation structures. These reagents could be used with future PtdIns(3,5)P₂ effectors to show they localize to the segregation structure.

How do PAKs regulate peroxisome inheritance?

Peroxisomes are transported along actin cables by the myosin V motor protein Myo2. Peroxisomes are attached to Myo2 through a peroxisome-specific Myo2 receptor, Inp2. Like Vac17, Inp2 production is cell cycle regulated and Inp2 is degraded prior to cytokinesis^{31, 32}. I found that overexpression of either *CLA4*, and to a lesser extent *STE20*, suppressed peroxisome inheritance (Figure 3-7B,D). I hypothesize that, like Vac17, PAK overexpression causes a degradation of Inp2 and that Inp2 destruction requires PAK activity. To test this hypothesis I propose looking at Inp2 stability in cells overexpressing *CLA4* and *STE20*. Additionally, I propose looking at Inp2 stability in cells overexpressing *GAL-CLA4t* as performed for Vac17 (Figure 3-6). If positive results are found then phosphorylation of Inp2 by Cla4 and Ste20 could be examined as described above for Vac17. Alternately, peroxisome inheritance could be regulated instead by phosphorylation of Myo2 which is phosphorylated in a cell cycle dependent manner³³.

Vacuole inheritance checkpoint

Cla4 and Ste20 both have many roles in the cell. Particularly, Cla4 and Ste20 play roles in regulating septin formation and Swe1 degradation. To show

that septin defects are not responsible for the failure to resolve the segregation structure I looked at vacuole morphology in temperature sensitive septin mutant that had been α -arrested then released at the restrictive temperature. These cells formed a bud vacuole suggesting failure to form a bud vacuole was not linked to septin defects. Additionally, it would be a good idea to perform the same experiment with elutriated cells.

To further differentiate *cla4-75 ste20* septin defects from the vacuole inheritance defect it would be a good idea to look for a *cla4* mutant that doesn't localize to the vacuole. One possible method for creating this mutant would be to mutagenize the PH domain to inactivate it or to exchange it with a domain which binds PtdIns(4)P or PtdIns(4,5)P₂ strongly. However, it may be possible for the segregation structure to be resolved even if it doesn't directly localize to the vacuole as I think is happening for Ste20. Alternately, Cla4 could be localized specifically to the mother bud neck by fusion with Hsl1 or Hsl7.

References

1. Holly, S.P. & Blumer, K.J. PAK-family kinases regulate cell and actin polarization throughout the cell cycle of *Saccharomyces cerevisiae*. *J Cell Biol* **147**, 845-56 (1999).
2. Huh, W.K. et al. Global analysis of protein localization in budding yeast. *Nature* **425**, 686-91 (2003).
3. Lamson, R.E., Winters, M.J. & Pryciak, P.M. Cdc42 regulation of kinase activity and signaling by the yeast p21-activated kinase Ste20. *Mol Cell Biol* **22**, 2939-51 (2002).
4. Peter, M., Neiman, A.M., Park, H.O., van Lohuizen, M. & Herskowitz, I. Functional analysis of the interaction between the small GTP binding protein Cdc42 and the Ste20 protein kinase in yeast. *Embo J* **15**, 7046-59 (1996).
5. Eitzen, G., Wang, L., Thorngren, N. & Wickner, W. Remodeling of organelle-bound actin is required for yeast vacuole fusion. *J Cell Biol* **158**, 669-79 (2002).
6. Seeley, E.S., Kato, M., Margolis, N., Wickner, W. & Eitzen, G. Genomic analysis of homotypic vacuole fusion. *Mol Biol Cell* **13**, 782-94 (2002).
7. Lechler, T., Shevchenko, A. & Li, R. Direct involvement of yeast type I myosins in Cdc42-dependent actin polymerization. *J Cell Biol* **148**, 363-73 (2000).
8. Wu, C. et al. Activation of myosin-I by members of the Ste20p protein kinase family. *J Biol Chem* **271**, 31787-90 (1996).
9. Wu, C., Lytvyn, V., Thomas, D.Y. & Leberer, E. The phosphorylation site for Ste20p-like protein kinases is essential for the function of myosin-I in yeast. *J Biol Chem* **272**, 30623-6 (1997).
10. Eitzen, G., Thorngren, N. & Wickner, W. Rho1p and Cdc42p act after Ypt7p to regulate vacuole docking. *Embo J* **20**, 5650-6 (2001).
11. Muller, O., Johnson, D.I. & Mayer, A. Cdc42p functions at the docking stage of yeast vacuole membrane fusion. *Embo J* **20**, 5657-65 (2001).
12. Eitzen, G. Actin remodeling to facilitate membrane fusion. *Biochim Biophys Acta* **1641**, 175-81 (2003).
13. Haas, A., Conradt, B. & Wickner, W. G-protein ligands inhibit in vitro reactions of vacuole inheritance. *J Cell Biol* **126**, 87-97 (1994).
14. Bender, L. et al. Associations among PH and SH3 domain-containing proteins and Rho-type GTPases in Yeast. *J Cell Biol* **133**, 879-94 (1996).
15. Xu, H. & Wickner, W. Bem1p is a positive regulator of the homotypic fusion of yeast vacuoles. *J Biol Chem* **281**, 27158-66 (2006).
16. Han, B.K. et al. Bem1p, a scaffold signaling protein, mediates cyclin-dependent control of vacuolar homeostasis in *Saccharomyces cerevisiae*. *Genes Dev* **19**, 2606-18 (2005).
17. Bose, I. et al. Assembly of scaffold-mediated complexes containing Cdc42p, the exchange factor Cdc24p, and the effector Cla4p required for

- cell cycle-regulated phosphorylation of Cdc24p. *J Biol Chem* **276**, 7176-86 (2001).
18. Gulli, M.P. et al. Phosphorylation of the Cdc42 exchange factor Cdc24 by the PAK-like kinase Cla4 may regulate polarized growth in yeast. *Mol Cell* **6**, 1155-67 (2000).
 19. Kozminski, K.G. et al. Interaction between a Ras and a Rho GTPase couples selection of a growth site to the development of cell polarity in yeast. *Mol Biol Cell* **14**, 4958-70 (2003).
 20. Sakchaisri, K. et al. Coupling morphogenesis to mitotic entry. *Proc Natl Acad Sci U S A* **101**, 4124-9 (2004).
 21. Versele, M. & Thorner, J. Septin collar formation in budding yeast requires GTP binding and direct phosphorylation by the PAK, Cla4. *J Cell Biol* **164**, 701-15 (2004).
 22. Drogen, F. et al. Phosphorylation of the MEKK Ste11p by the PAK-like kinase Ste20p is required for MAP kinase signaling in vivo. *Curr Biol* **10**, 630-9 (2000).
 23. Weiss, E.L., Bishop, A.C., Shokat, K.M. & Drubin, D.G. Chemical genetic analysis of the budding-yeast p21-activated kinase Cla4p. *Nat Cell Biol* **2**, 677-85 (2000).
 24. Dephoure, N., Howson, R.W., Blethrow, J.D., Shokat, K.M. & O'Shea, E.K. Combining chemical genetics and proteomics to identify protein kinase substrates. *Proc Natl Acad Sci U S A* **102**, 17940-5 (2005).
 25. Hofken, T. & Schiebel, E. A role for cell polarity proteins in mitotic exit. *Embo J* **21**, 4851-62 (2002).
 26. Gary, J.D., Wurmser, A.E., Bonangelino, C.J., Weisman, L.S. & Emr, S.D. Fab1p is essential for PtdIns(3)P 5-kinase activity and the maintenance of vacuolar size and membrane homeostasis. *J Cell Biol* **143**, 65-79 (1998).
 27. Bonangelino, C.J., Catlett, N.L. & Weisman, L.S. Vac7p, a novel vacuolar protein, is required for normal vacuole inheritance and morphology. *Mol Cell Biol* **17**, 6847-58 (1997).
 28. Cooke, F.T. et al. The stress-activated phosphatidylinositol 3-phosphate 5-kinase Fab1p is essential for vacuole function in *S. cerevisiae*. *Curr Biol* **8**, 1219-22 (1998).
 29. Yamamoto, A. et al. Novel PI(4)P 5-kinase homologue, Fab1p, essential for normal vacuole function and morphology in yeast. *Mol Biol Cell* **6**, 525-39 (1995).
 30. Efe, J.A., Botelho, R.J. & Emr, S.D. Atg18 regulates organelle morphology and fab1 kinase activity independent of its membrane recruitment by phosphatidylinositol 3,5-bisphosphate. *Mol Biol Cell* **18**, 4232-44 (2007).
 31. Fagarasanu, A., Fagarasanu, M., Eitzen, G.A., Aitchison, J.D. & Rachubinski, R.A. The peroxisomal membrane protein Inp2p is the peroxisome-specific receptor for the myosin V motor Myo2p of *Saccharomyces cerevisiae*. *Dev Cell* **10**, 587-600 (2006).
 32. Fagarasanu, M., Fagarasanu, A. & Rachubinski, R.A. Sharing the wealth: peroxisome inheritance in budding yeast. *Biochim Biophys Acta* **1763**, 1669-77 (2006).

33. Legesse-Miller, A., Zhang, S., Santiago-Tirado, F.H., Van Pelt, C.K. & Bretscher, A. Regulated phosphorylation of budding yeast's essential myosin V heavy chain, Myo2p. *Mol Biol Cell* **17**, 1812-21 (2006).